Development and modelling of compact dual membrane contactor for gas treatment

by

©Jing Jing Cai

A thesis submitted to the
School of Graduate Studies
in partial fulfilment of the
requirements for the degree of
Doctor of Philosophy

Faculty of Engineering and Applied Science
Memorial University of Newfoundland

July 2016

St. John's Newfoundland

ABSTRACT

In this work a novel dual hollow fibre membrane contactor (HFMC) has been designed and modeled for offshore gas processing when there are stringent limitations on space and weight allocated to the purification process. In the dual membrane module, the membrane core is composed of porous polypropylene fibre membrane and nonporous silicone rubber fibre membrane. The target gas component diffuses through the porous membrane and is absorbed by solvent circulated in the shell side. The dissolved gas is then stripped out of the solvent, driven by differential pressure into the nonporous membrane. As a result, the solvent is partially regenerated and the concentration driving force can be maintained.

A preliminary study of the performance of the dual HFMC has been conducted through a numerical approach. A mathematical model was developed to describe the mass transfer process in the proposed dual membrane contactor. Simulation results from the model demonstrate that the proposed novel dual HFMC could improve the gas removal efficiency by 36%, compared to a single membrane system.

The proposed model was validated through lab scale experiments. Based on the experimental results, the mass transfer resistance in the fabricated dual membrane module was evaluated and an empirical correlation was developed to predict the mass transfer coefficient in the dual membrane contactor. The experiments also showed that the dual membrane module increased the permeation flux by 12-78%, compared to conventional modules containing only one type of porous membrane. The enhancement could be

further improved by optimizing the membrane design and operational conditions. The mass transfer resistance in the dual membrane module existed mainly in the liquid phase and the membrane's contribution to the total mass transfer resistance was approximately 7%. By reducing the gas flow rates, increasing the liquid flow rates and lowering the vacuum pressure in nonporous fibers, the absorption performance of the proposed dual membrane contactor could be further enhanced.

To further reveal the fundamentals of the mass transfer process and module performance, the impact of module design (module geometry etc.) on absorption performance was investigated using computational fluid dynamics (CFD). The CFD model was first validated with experimental data. Design factors, such as the shell configuration, inlet geometry, header shape, fibre bed height and packing density, and their impact on shell-side flow and overall contactor performance were studied. The simulation results showed the shell-side flow dynamics played a critical role in determining the module performance which was strongly influenced by module geometries. Under the same operational conditions, shell-side velocity and shell-side flow uniformity were found different in modules with various configurations. Compared to the average shell-side velocity, the shell side flow distribution was proven to play a less significant role on the overall mass transfer performance.

Combined with empirical correlations derived from experiments, CFD modeling approach could potentially decrease the number of experiments required, thus reducing costs and time required. The CFD model was then expanded to study the concentration profiles within the HFMC and simulate the impact of factors such as baffled modules and

modules containing unevenly distributed fibre bundle. The research demonstrated that the CFD simulation could be used as an effective design tool in the development and optimization of cross flow membrane module.

Compared to the conventional absorption column, the lab scale dual membrane contactor designed and fabricated in this study could reduce the footprint by 80% and solvent consumption by 70%. This result was obtained by comparing the experimental results from a lab scale packed column to the modeled results of dual membrane module containing the equivalent amount of interfacial area. This difference could be further enhanced by increasing the fiber packing density in the membrane core of dual membrane module. The compatibility, capability in reducing size and solvent consumption and ease in operation makes the dual membrane contactor ideal candidate for offshore gas processing where space has stringent specifications.

Keywords: Hollow fibre membrane contactor, module design, cross-flow, shell flow dynamics, computational fluid dynamics (CFD) simulation

ACKNOWLEDGEMENT

The long journey towards pursuing the Ph. D degree finally comes to a successful end. It is a journey full of challenges, innovation, excitements, and occasional frustrations. Fortunately, I was never alone traveling through this journey. There are a number of people behind this piece of work who deserve to be both acknowledged and thanked here. It is them who made me more than who I am and I am so grateful to have them by my side.

First and foremost, I would like to thank two of my supervisors, Dr. Kelly Hawboldt and Dr. Majid Abdi, for their guidance, unrelenting support and friendship throughout this process. I am privileged to have the opportunity to work with them. Kelly, thank you for trusting me and allowing me to explore my own ideas while staying closely to steer me back to the right track when I am confused or lost; thank you for going beyond your duties to fire fight my worries, concerns, and anxieties and instilling confidence in myself and my work. I will never forget how your encouragement and humor brightened my days in times of stress. Majid, thank you for your tireless support, timely encouragement and valuable advice in the past few years. Your passion for research, diligent work ethic and frequent insight and patience are invaluable to me. I also would like to thank Dr. Faisal Khan, who is the member of my Ph.D committee. Thank you for your feedback, direction, and assistance when I needed it.

I would like to acknowledge the academic, financial and technical support from the Faculty of Engineering and Applied Science. In particular, thanks to Dr. Lesley James and Dr. Yan Zhang for their help and inspiring discussion on my study and research throughout my Ph.D. program; thanks to Frank Pippy, Caroline Koenig, William Bidgood, David Snook, Kelly Leshane for providing constant technical support to my experimental work; thanks to Dr. Leonard Lye for your valuable experience and insightful guidance on academic writing; and thanks to Moya Crocker, Colleen Mahoney, Nicole Parisi for your daily assistance.

Financial support was gratefully provided by the Faculty of Engineering and Applied Science, Memorial University (MUN), National Research Council of Canada (NSERC), Development Corporation of Newfoundland and Labrador (RDC).

I have been so lucky to make many good friends over my years living in St. John's and their friendship made my life more enjoyable and unforgettable. Particularly, I would like to thank Mr. Rick Siu, Ms. Janice Siu and Mr. Simon Tam, for all their continuous prayers and supports. A sincere thanks to my gangs, Xiaonan Wu, Lei Wang and Nan Zhang for sharing laughs and tears with me, and for simply listening to me.

Family gave me a great deal of support throughout my degree and my life in St. John’s. I would like to extend my inexpressible gratitude to my parents and parents in-law for their unconditional love, comfort and advice. Most of all, I would like to offer my deepest thanks to my husband, Liang Jing. Thank you for believing in me and holding my hands

through all the ups and downs. Your love, tolerance and patience turned this long journey into a pleasure.

TABLE OF CONTENTS

TABLE OF FIGURES

TABLE OF TABLES

LIST OF SYMBOLES

A	area m^2
A_m	membrane surface area per unit total volume m^{-1}
C	concentration mol/m^3
C_1	permeability coefficient
C_2	inertial loss coefficient
C_G	concentration in gas phase $mole/m^3$
C_L	concentration in liquid phase $mole/m^3$
C_{SNP}	concentration in the surface of nonporous membrane $mole/m^3$
D	diffusion coefficient m^2/s
d	diameter m
d_0	Membrane fiber outside diameter m
D_{eff}	effective diffusivity m^2/s
dh	hydraulic diameter m
Dw	CO_2 diffusion coefficient in water m^2/s
g	gravity force m/s^2
H	Henry's constant
h	height of membrane module m
in	inlet
ID	inner diameter m
J	Mass flux $kg/m^2/s$
k	mass transfer coefficient m/s
k_L	liquid phase mass transfer coefficient m/s

k_m	mass transfer coefficient through membrane m/s
k_{ol}	overall mass transfer coefficient through membrane m/s
k_P	shell side mass transfer coefficient m/s
k_{per}	permeability coefficient Barrer
L	Length of membrane module m
l	thickness of membrane
L	length of membrane m
N	number of hollow fibers
O	diameter of opening inlet m
OD	outer diameter m
out	outlet
P	Pressure Pascal
P_{er}	permeability coefficient Barrer
P_{out}	pressure in nonporous membrane Pascal
Q	volumetric flow rate m^3/s
R	Gas constant $m^3\,Pa\,K^{-1}\,mol^{-1}$
r	sink term
Re	Reynolds number (dimensionless)
R_g	Mass transfer resistance in gas phase(s/m)
R_l	Mass transfer resistance in liquid phase(s/m)
R_{Total}	Total mass transfer resistance (s/m)
R_m	Mass transfer resistance in porous membrane (s/m)
R_{nm}	Mass transfer resistance in nonporous membrane (s/m)

S	continuity source term
Sc	Schmidt number
Sg	source term in continuity equation kg/m^3/s)
Sh	Sherwood number
Sr	momentum source term
t	time s
T	temperature K
t	thickness of membrane m
u	shell side velocity m/s
$\vec{v}$	velocity vector m/s
v_{ave}	the average velocity m/s
$\bar{v}_{shell}$	the average shell-side velocity
V_{mag}	magnitude of the superficial velocity vector m/s
W	width of membrane module m
X	Length of membrane module m
x	length coordinate position m
y	height coordinate position m
Y	Length of membrane module m
z	width coordinate position m

Greek Letters

α	constant
β	constant
ε	void fraction
ρ	density kg/m^3

μ	dynamic viscosity P
ν	kinematic viscosity m^2/s
τ	stress tensor

Subscripts

I	location
L	liquid phase
G	gas phase
P	porous membrane
NP	nonporous membrane
in	inlet
out	outlet

CHAPTER 1

INTRODUCTION

This dissertation is an investigation of innovative gas processing systems to address the unique challenges of processing gas on offshore facilities. As conventional sources of hydrocarbons decrease, exploration has being driven further to deep water offshore locations.

On offshore production facilities, natural gas produced from wellhead can be transported onshore either by pipeline or as liquefied natural gas (LNG) if space and location permit. There is also ongoing research on compressed gas (CNG) (Lothe, 2005). The gas can also be re-injected for reservoir pressure maintenance and enhanced oil recovery, and used as a fuel. All of these processes require the partial or total removal of carbon dioxide (CO_2), hydrogen sulfide (H_2S), water and other contaminants in raw natural gas. The presence of these contaminants may increase the risk of corrosion of well bore/pipeline and gas tanks, hydrate formation, and other environmental issues. Therefore, removal of these

contaminants from gas streams before delivery and transportation is critical to meet injection and pipeline specifications and avoid potential environmental issues.

Gas separation processes can vary from simple physical techniques to complex hybrid multi-step processes, depending on the properties of impurities as well as on the treated gas specifications. The primary operation of gas purification processes can be generally classified into four types (Dindore, 2005): absorption into a liquid; adsorption on a solid; condensation; and permeation through a membrane. The first three processes are widely used in gas processing industries. In most cases, these operations require equipment with large size and heavy weight. Sour gas removal processes typically use liquid-gas extraction processes that require packed and regeneration columns which can be over 60 meters high with the weight over hundred tonnes. This hinders the application of conventional gas processing units in offshore gas processing. Further, many offshore sites are minimally or remotely operated, as such gas processing systems cannot be overly complex with respect to operation and/or maintenance. In addition, the direct contact of liquid and gas phase in conventional absorption columns may result in several operational issues such as flooding, foaming, channeling and high operation cost (Gabelman et al., 1999). The potential to reduce the equipment's footprint and the feature of indirect contact between liquid and gas phases have made membrane contactor technology a compelling solution for the removal of contaminants from natural gas and flue gas. In membrane contactors, the membrane acts as a barrier between liquid and gas phase to avoid flooding, channelling and foaming caused by direct contact between two phases (Gabelman et al., 1999). Membrane contactors also offer numerous advantages over the

conventional gas-liquid contactors, which include but are not limited to, smaller footprint, ease in set-up, and larger contact area for increased mass transfer rate in a more compact size (Gabelman et al., 1999, Jahn et al., 2012). These features make membrane contactors especially attractive for offshore application. Kvaerner Oil and Gas investigated the potential of replacing conventional absorption columns with membrane contactors for CO_2 removal on offshore platforms and the membrane gas/liquid contactor reduced equipment size by 72% and a 66% reduction in weight (Falk-Pedersen et al., 1997). Furthermore, the total separation process could be optimized with respect to energy consumption, corrosion and degradation of the solvent, if membrane contactors were used for both absorption and solvent regeneration (Falk-Pedersen et al., 1997). Figure 1.1 compares a membrane contactor and a typical absorption column in terms of size and footprint for the same processing capacity and removal.

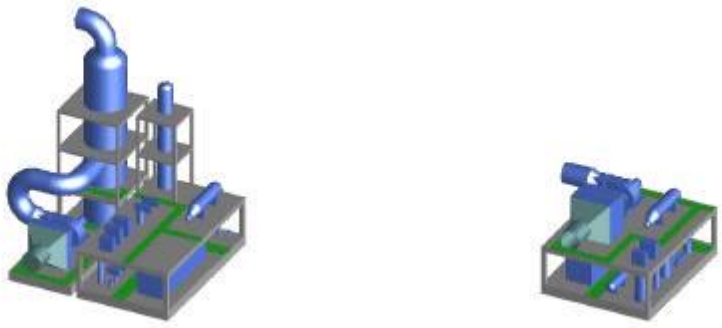

Conventional process membrane process

Figure 1.1: Comparison of sizes between membrane unit and typical absorption column (Herzog et al., 2013)

1.1 Motivation

Since the Kvaerner membrane contactor was developed and tested for CO_2 separation from gas turbine exhaust in 1997, extensive efforts have been made in designing and developing membrane contactors for offshore gas processing. Yet only few membrane gas-liquid contactors have been commercialized for CO_2 removal (Feron et al., 2002; Hoff et al., 2003). In most existing membrane systems, gas absorption and solvent regeneration take place in two separate units (Lee et al., 2001; Kosaraju et al., 2005). PETRONAS and Cameron tested the idea of packing two types of membranes into one unit to replace the multiple stages membrane based absorber for bulk removal of CO_2 in offshore gas fields (Isa et al., 2012). By combining two membrane contactors into one unit, the same absorption performance can be achieved with a 50% reduction in the equipment footprint. The possibility of achieving gas absorption and solvent regeneration in one compact unit instead of multiple modules however has never been explored.

The absorption performance of membrane contactors depends on many factors such as membrane material, selection of solvents, operation conditions and module design. Compared to extensive work carried out in the development of novel membrane material and absorbent (Khaisri et al., 2009; Wongchitphimon et al., 2011; Rajabzadeh et al., 2013), less effort has been directed towards the process engineering aspects such as transport phenomena and module design. Thus far, to our best knowledge, there are no comprehensive studies have been carried out with a focus on the optimization of the module performance by exploring novel membrane module design that suitable for offshore use.

One of the most commonly used approach to reduce the operating cost is through the optimization of the operation conditions. It can be achieved through conducting sensitivity analysis on estimated performance of membrane module. As it is essential to use unit models to accurately describe the process behavior in any new process, the prediction of module performance is important in the design of membrane contactor. The ability to experiment on the computer with alternative process setups and operating conditions reduces the costly and time-consuming laboratory and pilot plant effort. Prediction of the module performance for design purpose requires knowledge of the mixing patterns and mass transfer characteristics of the membrane contactor (Dindore et al., 2005). This is technically challenging due to the complex nature of flow through membrane module.

1.2 Objectives

The goal of this research, therefore, is to develop and optimize a novel design of membrane contactor that satisfies the challenges imposed by offshore. It also deals with the assessment and optimization of hollow fiber-based membrane module design and operation with a focus on gas absorption.

The objectives of current research include:

- To design a novel membrane contactor with a reduced footprint, more compact volume and better performance, compared to current membrane systems;
- To establish a mathematical model to approximate and evaluate absorption performance of the proposed membrane contactor;

- To fabricate a lab scale module for the proposed membrane contactor and experimentally test its performance;
- To develop a computational fluid dynamics (CFD) based model to assist decision making in terms of design optimization;
- To evaluate alternative membrane module configurations by investigating the impact of module geometry on gas absorption performance.

In order to achieve these objectives, the following areas are included in the scope of this research:

- At the pre-design stage, a novel membrane system for offshore gas processing is proposed. Modelling of mass transfer process in the proposed module is carried out to gain a better understanding of the module performance.
- At the design stage, the impact of module geometry on module performance is investigated using a customized CFD model for the optimization of module design.
- At the experimental stage, a lab scale module is fabricated with its performance tested in a lab scale flow loop. Absorption of CO_2 is carried out in the proposed module to gain a better understanding on the mass transfer process in the proposed membrane module. Furthermore, module performance is evaluated by varying operational conditions. Experimental results are used to validate the accuracy of the proposed model.

1.3 Dissertation Structure

- Chapter 1 includes a brief introduction to the background of membrane based gas absorption as well as the description of research objectives and scope.
- Chapter 2 gives a comprehensive literature review of membrane technology used for gas processing from the perspectives of transport phenomena, selection of module design, development of modelling approach that approximate module performance. It is expected that this review can provide inspiration for novel module development that serves for future offshore gas absorption.
- Chapter 3 presents a novel design of dual membrane contactor which potentially achieves gas absorption and the regeneration of solvent in the same unit. The module design and mass transfer mechanism in the proposed module is described in details. Following that, a mathematical model based on mass balance principle is subsequently proposed to describe the mass transfer phenomena in the module. The model is validated through benchmarking against published experimental results (Dindore et al., 2005).
- Chapter 4 explores the performance of the proposed membrane contactor through experimental approach. A better understanding of mass transfer mechanisms in the proposed module is obtained through experimental observations of CO_2 removal from gas mixtures. Further, the experimental results are compared with modelled results for validation. The effect of operational conditions such as flow rates and pressure control are also discussed.

- Chapter 5 proposes a modeling approach based on CFD technology to examine the effect of module design on the module performance. A series of three dimensional module geometries were built computationally and CFD simulations were carried out to investigate the impact of major design factors case studies. It is further attempted to model CO_2 absorption in modules with various design factors. Criteria based on the modelled results are established through modelling approach for future design.
- Chapter 6 developed a modelling approach to provide more accurate description of mass transfer in both tube side and shell side in the proposed dual membrane contactor. The impact of the shell side flow pattern and the fluid mixing on the module performance is discussed with details. Furthermore, by applying the proposed model on CO_2 absorption carried out under a wide range of operational conditions, a sensitivity analysis and a performance comparison with other models are performed. The proposed modelling approach takes into consideration of the impact of flow dynamics factors and it can be applied to modules with complex geometries.
- Chapter 7 summarizes the key points of this dissertation, recapitulates its main contributions and limitations, and suggests some directions for future research.

References

Alexander, S.R., Winnick, J., Removal of hydrogen sulfide from natural gas through an electrochemical membrane separator, AIChE Journal, 40 (4) (1994), 613-620

Dindor, V.Y., Gas purification using membrane gas absorption processes, Thesis, University of University of Twent, 2005

Dindore, V.Y., Brilman, G. F.,Versteeg, D. W. F., Modelling of cross-flow membrane contactors: physical mass transfer processes, Journal of Membrane Science, 251 (2005), 209-222

Dindore, V.Y., Cents, A.H.G., Brilman, D.W.F.,Versteeg, G.F., Shell-side dispersion coefficients in a rectangular cross-flow hollow fibre membrane module, Chemical Engineering Research and Design, 83(A3) (2005), 317-325

Esato, K., Eiseman, B., Experimental evaluation of Gore-Tex membrane Oxygenator, Journal of Thoracic and Cardiovascular Surgery, 69(5) (1975), 690-697

Falk-Pedersen, O., Dannström, H., Separation of carbon dioxide from offshore gas turbine exhaust, Energy Conversion and Management, 38 (1997), S81-S86

Feron, P.H.M., Jansen, A.E., CO2 separation with polyolefin membrane contactors and dedicated absorption liquids: performance and prospects, Separation and Purification Technology 27 (2002), 231-242

Gabelman, A., Hwang, S., Hollow fibre membrane contactors, Journal of Membrane Science, 159 (1999), 61-106

Herzog, H., Falk-Pedersen, O., The Kvaerner membrane contactor: Lessons from a case

study in how to reduce capture costs, 5th International Conference on Greenhouse Gas Control Technologies, Cairns, Australia, 2000

Hoff, K.A., Modeling and experimental study of carbon dioxide absorption in a membrane contactor, Ph.D. Thesis, Norwegian University of Science and Technology, Norway, 2003

Isa, F.M., Ahmad, A.S., Karim, F.A., Raham, F.H., Peters, R., Development of innovative membrane for offshore high CO_2 separation, World Gas Conference, Kuala Lumpur, 2012

Jahn, J., Bos, P.V.D, Broeke, L.J.V.D, Evaluation of membrane processes for acid gas treatment, SPE International and Operation Conference, Doha, Qatar, 2012

Khaisri, S., deMontigny, D., Tontiwachwuthikul, P. and Jiraratananon, R., Comparing membrane resistance and absorption performance of three different membranes in a gas absorption membrane contactor, Separation and Purification Technology, 65(2009), 290-297

Kosaraju, P., Kovvali, A.S., Korikov,A., Sirkar,K.K., Hollow fiber membrane contactor based CO_2 absorption-stripping using novel solvents and membranes, Industrial & Engineering Chemistry Research, 44 (2005), 1250-1258

Lee, Y., Noble, R.D., Yeom, B.Y., Park, Y.I. Lee, K.H., Analysis of CO_2 removal by hollow fiber membrane contactors, Journal of Membrane Science, 194 (2001), 57-67

Lothe, P., Pressurized natural gas: An effective and reliable gas solution for offshore gas transportation, Offshore Technology Conference, Houston, Texas, USA, 2005

Nymeijer, D.C., Folkers, B., Breebaart, I., Mulder, M.H.V., Wessling, M., Selection of top layer materials for gas-liquid membrane contactors, Journal of Applied Polymer Science, 92 (2004), 323

Rajabzadeh, S., Yoshimoto S., Teramoto, M., Al-Marzouqi, M., Ohmukai, Y., Maruyama, T., Matsuyama, H., Effect of membrane structure on gas absorption performance and long-term stability of membrane contactors, Separation and Purification Technology, 108(2013), 65-73

Tabe-Mohammadi, A., A review of the applications of membrane separation technology in natural gas treatment, Separation science and technology, 34 (1999), 2095-2111

Zhang, Z.E., Yan, Y.F., Zhang, L., Ju, S.X., Hollow fiber membrane contactor absorption of CO_2 from flue gas: Review and perspective, Global NEST Journal, 16 (2) (2014), 354-373

CHAPTER 2

LITERATURE REVIEW

This chapter reviews the current membrane technologies used for gas processing. In section 2.1, an overview of gas purification using different membrane technologies will be presented. Particularly, two possible mechanisms of mass transfer in membrane based gas processing will be briefly explained. Section 2.2 mainly discusses gas absorption using membrane contactors and further compares various absorbents used for gas absorption. Section 2.3 reviews the technical benefits and limitations of existing membrane contactors in terms of their application in gas absorption. Prior studies in membrane contactors with various configurations, process modeling and hollow fibre module design will also be summarized in this section. It is expected that this review can provide insights in developing novel module that will be suitable for offshore gas processing purpose.

2.1 Overview of Gas processing

Raw natural gas contains impurities such as H_2O, CO_2 and H_2S that may result in hydrate formation, corrosion and pose health and environmental hazards during transport. To

meet pipeline specifications and avoid potential environmental issues, removal of these contaminants from gas streams before delivery and transportation is critical. As mentioned in the previous section, the operations for gas processing can be classified into four categories, in which amine absorption system is a proven, well-accepted technology for acid gas removal in natural gas processing. In general, chemical absorption processes using amine takes up 95 % of all gas sweetening market (Baker 2008).

A typical amine absorption process is illustrated in Figure 2.1, in which two towers are used as absorber and desorber, respectively. In the first tower, the feed gas, usually at high pressure, and an absorbent liquid flows countercurrent to each other. The absorbent liquid that contains the absorbed component (CO_2, water, or heavy hydrocarbon) is removed from the bottom of the tower. The liquid is then heated and sent to a low-pressure stripper tower. The combination of heat and lower pressure liberates the absorbed component, which leaves the stripper tower as a low pressure .The regenerated absorbent liquid is then recycled to the first tower.

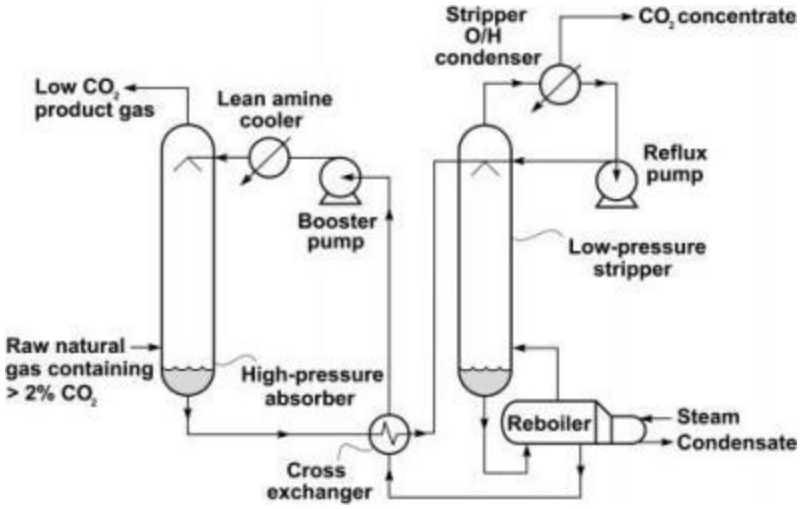

Figure 2.1 : Typical natural gas absorber-stripper treatment process using amine absorbents to remove carbon dioxide (Baker et al., 2008)

Chemical absorption using absorber-desorber is usually conducted in heavy and bulky towers. It requires large amounts of expensive amines to operate. Furthermore, corrosion is a critical maintenance issue. Take acid gas removal for example, amine is the most widely used solvent for this purpose. Degradation of amine leads to corrosive mixtures that can destroy the system within a few days if left unchecked. Constant monitoring of the amine absorbent is needed. The need for regular maintenance and good operator care hinders the use of amine absorber-strippers in remote locations such as offshore platform and this provides an incentive to develop cost effective separation technologies with smaller footprint and easy scale-up.

2.2 Membrane technologies used for gas processing

As membrane technology broke into gas processing market in 1980s, it has been receiving more and more attention in past decades as membrane processes have been proven to be technically and economically superior to conventional absorption systems. This superiority is due to many advantages that membrane technology benefits from, including low capital investment, simplicity and ease of installation and operation, low maintenance requirements, low weight and space requirements, and high process flexibility, which makes it especially attractive for offshore gas processing (Falk-Pedersen et al., 1997).

2.2.1 Membrane separation

In the process of separation, membrane is set up between two bulk phase and the movement of any specie across the membrane is a result of one or more driving forces which can be gradients in concentration, pressure, temperature (Strathmann, 2000) or electrical potential (shown in Figure 2.2).

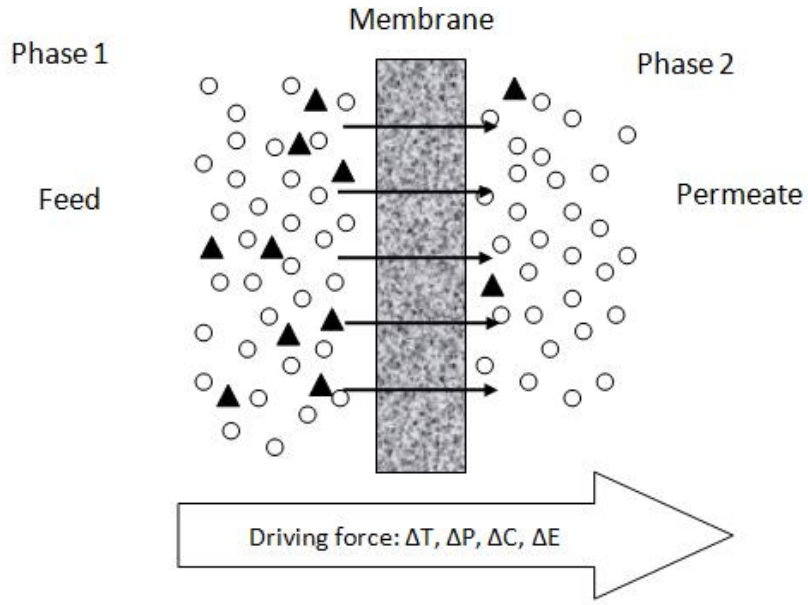

Figure 2.2: Schematic drawing of membrane separation process with different driving force is present (Strathmann, 2011)

Generally, two options are available for membrane assisted gas processing: membrane separation and liquid absorption using membrane contactors (Dindore et al., 2005). Membrane separation is a pressure-driven process in which a gas mixture is fed into the membrane module under high pressure, typically between 10 to 200 bars. The separation's driving force is the partial pressure difference of the gases in the feed and permeate. Meanwhile, the selectivity for gas components mainly relies on the property of membrane itself (Jahn et al., 2012). The first commercial use of membrane separation systems for removal of acid gases from natural gas started in 1984 with the installation of the SACROC unit by Cynara, a subsidiary of Dow (Parro, 1984) and the system was found to reduce capital cost and energy consumption comparing to conventional processing technology. Cook and his colleagues reported that (Cook et al., 1994) reported the installation of a membrane separation system to treat 30 MMscfd of natural gas

containing 11% carbon dioxide. They compared a membrane system with an amine/glycol system and concluded that the total operating costs for both systems were the same but the membrane system inherently offers more advantages such as flexibility for expansion and turndown, space savings and less cost in maintenance. In a study of a novel electrochemical membrane separator used for removal of H_2S from natural gas, and recovery of elemental sulfide and hydrogen, the membrane separator reduces the capital cost by 50%, comparing to other conventional technologies (Alexander et al., 1994). Despite all these advantages, the commercial utilization progress grows relatively slow due to low selectivity and permeability of membrane to gas components. A general tradeoff has been recognized between permeability and selectivity: Polymers that are more permeable are generally less selective and vice versa (Tabe-Mohammadi et al., 1999). Take CO_2 removal from natural gas for example, for membranes providing high permeability for CO_2, they usually encounter problem in loss of hydrocarbon, mainly methane into permeate side. Furthermore, as more CO_2 permeates through the membrane, its partial pressure decreases, resulting in decreasing of driving force as discussed above. At the same time, the partial pressure of methane increases as more CO_2 permeates through the membrane. Therefore, its permeation rate increases, resulting in higher overall methane loss. To make up for the loss of methane during this process, the idea of multistage separation was proposed which improve the recovery rate by collecting CO_2 rich permeate from the first separator and feed it into the second module. Separation performance of single and multistage membrane systems were compared and it was concluded that multistage system can improve methane recovery by 8% and 98% of methane can be recovered through multistage membrane separators (Babcock et al., 1988).

However, the increasing number of membrane units also poses challenges to applications on offshore platforms, where a space is a valuable commodity.

2.2.2 Gas absorption using membrane contactors

An alternative technology that overcomes the disadvantage of membrane separation is using membrane contactors. Unlike dense membranes used in gas separation processes, the membranes used in these types of contactors are basically non-selective in nature and the selectivity aspect is primarily determined by the solvent used. Furthermore, the total pressure across the membrane remains the same whereas the driving force for membrane gas-liquid contactor comes from the concentration difference of the absorbed species, which brings a small pressure drop and keeps the gas-liquid interface remains immobilized at the mouth of pore (Dindore et al., 2005). In addition, the interfacial area for mass transfer in a membrane gas-liquid contactor equals the geometrical membrane surface area. Thus the interfacial area is constant and not influenced by orientation or change in flow rates. The feature of orientation free area provides more flexibility for the offshore applications. Falk-Pedersen et al. (Falk-Pedersen et al.,1997) compared membrane gas/liquid contactor desorber to several types of desorption systems for CO_2 removal from gas turbine exhaust on offshore platform and the membrane contactor desorber was found to have the best potential. PETRONAS which has extensive experiences in developing high CO_2 offshore gas fields projects had made extensive evaluation on several process for gas separation namely chemical absorption (amine), physical absorption, cryogenic distillation (Ryan Holmes process), membrane system and

other current technologies (Isa et al., 2009). Different operations are ranked based on the following criteria: operating flexibility, Reliability, expandability, environment friendly, weight, foot print, CO_2 removal efficiency, CO_2 purity. It is shown clearly in Figure 2.3 that the membrane is the most optimized technology for CO_2 removal offshore.

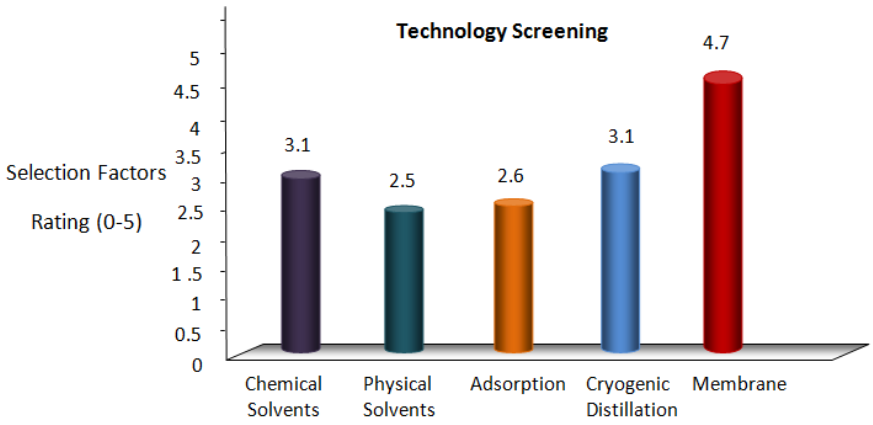

Figure 2.3: Technology screening for CO_2 removal (Isa et al., 2009)

So far, only a few of membrane contactors for gas processing have been tested in offshore fields. Kværner Oil & Gas and W.L. Gore & Associates GmbH (Gore) developed a membrane gas/liquid contactor in 1992 to separate components in gas streams as well as exhaust gases (Hoff et al., 2002). The first field test was conducted at a gas terminal north of Aberdeen, Scotland, where the test unit was fed with a slip-stream of sour gas and lean amine from one of the plant's existing gas treatment trains. Developers found that the testing results confirm previous theoretical and laboratory results, and a scale-up shows a potential of 75-85% reduction in vessel size and weight for gas sweetening. Field testing also was carried out at the Shell Fandango gas field in Zapata, Texas during the spring of 1999. The testing at Fandango aimed to test the performance of membrane contactor for

gas sweetening using a physical solvent (NFM-NAM) and gas dehydration using glycol (TEG). The results showed the potential of 60-80% reduction in footprint for gas dehydration. For exhaust gas treatment, the membrane technology was tested as both absorber and desorber in a number of laboratory units and in one field pilot plant. But it was also pointed out that the potential for the membrane gas/liquid contactor used as desorber has to be confirmed by pilot testing using real flue gas.

2.2.3 Mass transfer in membrane contactors

Membrane gas absorption is based on a gas–liquid contact across a hydrophobic porous membrane which permits mass transfer between the two phases without dispersing one phase into the other. Generally, the gas fills the hydrophobic membrane pores and meets the liquid at the opposite side of the membrane. The liquid phase pressure should be slightly higher than that of the gas phase to prevent dispersion of gas bubbles into the liquid. As long as the excess absorbent solution pressure is less than the breakthrough pressure of the membrane the solution does not penetrate into the pores and the gas–liquid interface is immobilized at the pore mouth of the membrane on the liquid side. Operation of gas–liquid membrane contactors differs from that of other membrane processes such as filtration, since there is no convective flow through the pores and only diffusive transport of certain components happen. This is the main reason that membrane contactors are less sensitive to fouling than conventional membranes. As the membrane is non-selective, the chemistry of the separation is the same as that for conventional equipment. The choice of a suitable combination of absorption liquid, membrane characteristics and operation mode determines the selectivity of the process.

During the absorption, the target gas components diffuse through the pores in membrane wall, driven by the concentration difference across the membrane (Shown Figure 2.4).

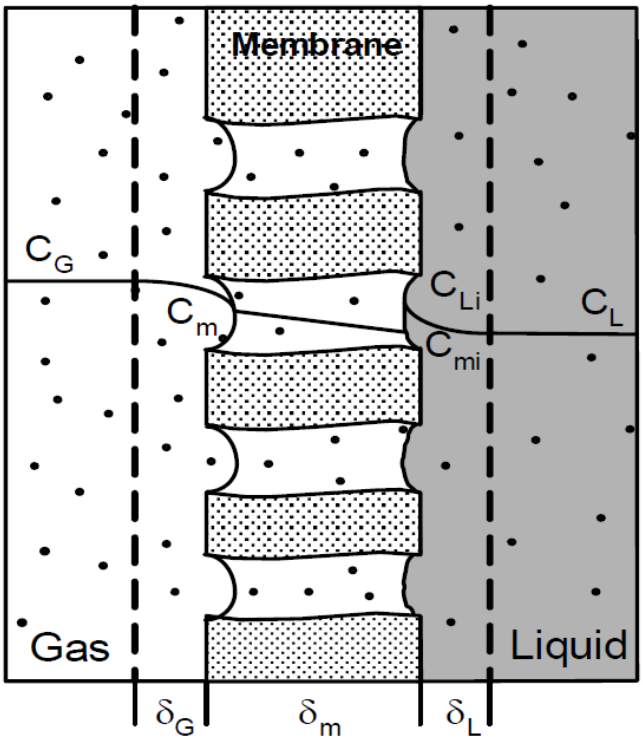

Figure 2.4: Mass transfer regions and dominant resistances in a membrane contactor (Dindore 2005).

Unlike dense membranes used in gas separation processes, the membranes used in these types of contactors are basically non-selective in nature and the selectivity aspect is primarily determined by the solvent used. This feature provides more flexibility to its application in offshore gas processing. Furthermore, the driving force for mass transfer in membrane gas-liquid contactor is mainly contributed by the concentration difference rather than a pressure gradient, which brings a small pressure drop and keeps the gas-liquid interface remains immobilized at the mouth of pore (Rangwala et al., 1996).

During the absorption, the membrane contactors are operated with the pores of membrane filled with either gas phase (non-wetted mode) or liquid phase (wetted mode), shown in Figure 2.5.

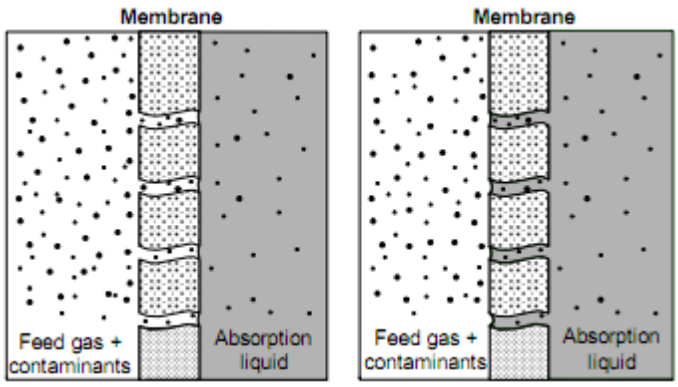

(a) Unwetted mode (b) wetted mode

Figure 2.5: Nonwetted membrane contactor and wetted membrane contactor (Dindore, et al., 2005)

The non-wetted mode is favored for gas absorption as the mass transfer resistance of the membranes becomes more significant which further results in lower mass transfer performance than the non-wetted mode. In general, the mass transfer process in the membrane contactor consists of three steps in series, the transfer from gas phase to the membrane surface, transfer within membrane pores and transfer from liquid interface to the liquid bulk. The mass transfer is determined by the consecutive steps in the three phases:

-Transport of gaseous component i from the bulk gas to the membrane wall,

-Diffusion through the totally gas-filled pores of the membrane to the membrane–liquid interface

-Dissolution into the liquid absorbent, followed by liquid phase diffusion and/or chemical reaction.

Hence, a resistance-in-series model can be used to describe the total resistance (Kruenlen et al. 1993), present in Eq. 2.1. R_{total}, defined as the reciprocal of the overall mass transfer coefficient, K_{ol}:

$$R_{total} = \frac{1}{k_{ol}} = \frac{1}{k_G} + \frac{1}{k_L} + \frac{H}{k_m} \qquad \text{Eq.2.1}$$

Where k_G is the gas phase mass transfer coefficient, k_m is the mass transfer rate through membrane and k_l is the liquid phase resistance.

For membrane contactors operated under non-wetted mode, the resistance to gas diffusion from the bulk gas to the membrane external surface and membrane can be ignored compared to other resistances (Karoor et al., 1993; Rangwala et al., 1996; Dindore et al., 2004).

To properly understand the mass transfers in the gas absorption process occurring in membrane contactors, the concentration distributions adjacent to the membrane surfaces along the module length should be fully described.

2.2.4 Modeling of mass transfer in membrane contactors

Typical approaches for predicting the shell-side mixing behavior and the mass transfer performance either require solving the continuum mass and momentum balances based on first principles, relying on completely empirical correlations or using a model which contains few empirical parameters and approximates the actual behaviour closely. The first approach would require the descretization of the complex three dimensional (3D) geometry and solving the large sets of computationally demanding equations. However, in many cases it is possible to assume simplified flow patterns. This approach is possible in more simple geometries, e.g., parallel flow in shell and tube geometry without baffles. In such cases, many researchers have assumed a simplified geometry of flow around a single fibre and Happel's free surface model (Chun et al., 1997; Karoor and Sirkar, 1993). However, these simplifications do not match with the real module performance due to uneven distribution and bending of fibres (Kreulen et al., 1993). Moreover, in the case of the cross-flow contactor such simplification of flow pattern would result in inaccurate description of the module performance due to the continuous splitting and remixing of the shell-side phase. The second approach is to derive empirical correlations to predict the mass transfer performance without knowing the details of mixing behaviour. The experimentally derived correlations are strongly influenced by the module geometry used, and are specific for the flow configuration. In addition, these correlations are subjected to suffer from channeling effects, polydispersity and uneven distribution of the fibres (Dahuron and Cussler, 1988; Wickramasinghe et al., 1992).

Another approach used to predict mass transfer in membrane contactors with complex geometry is Computational Fluid Dynamics (CFD) methodology. Computational Fluid Dynamics (CFD) methodology allows the flow of fluid to be modeled in complex geometries and offers quick analysis of the effect of design factors. Catapano et al. [9] and Gage et al. (Gage et al., 2002) have used this approach to treat the fibre bundles as porous media and to perform CFD analysis of flow in fibre bundles. When compared to experimental data, the simulation results were found agreeable.

2.3 Designing membrane contactors

Several membrane module configurations are available, both at commercial and laboratory scale respectively, for membrane applications such as filtration, gas separation etc. These module configurations can be conveniently adopted for the membrane gas-liquid contactors with relatively little modifications. Depending on the type of membranes used in the contactor, these devices can be broadly classified into two groups; the flat sheet membrane contactor and the hollow fibre membrane contactor. Flat sheet membranes are used in plate-and-frame or in spiral wound membrane contactors. Although equally efficient mass transfer operation can be carried out using flat sheet membrane contactors, hollow fibre membrane contactors are widely used due to the higher interfacial area (shown in Figure 2.6). In a research (Gu et al. 2000) carried out on CO_2 and O_2 transfer using membrane oxygenator, the pressure drop was found higher in flat membrane module comparing to hollow fiber membrane module, which makes the latter one more attractive.

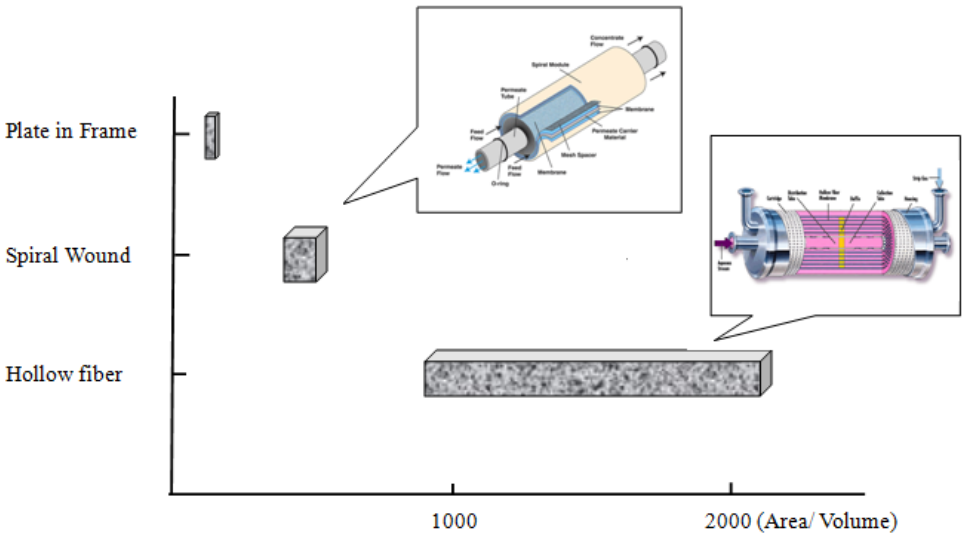

Figure 2.6: Surface areas to volume ratios of various membrane module configurations

The initial work of applying hollow fibre membrane contactor on CO_2 absorption was carried out by Qi and Cussler (Qi et al., 1993). By comparing the absorption of CO_2 into aqueous alkalis and alkanolamine solutions using polypropylene hollow fibre modules (pore-diameters 0.03 μm) and packed column, the author concluded that the key to membrane contactors is the area per volume. Hollow fibre modules have been studied more extensively than flat membrane modules because of their unique characteristics of self-support, high membrane packing density and high contact surface to volume ratio (7000–13000 m^2/m^3). Additionally, hollow fibre modules can be fabricated in different forms for various applications. In addition to the module configuration, the membrane material, selection of solvents, process design and operation conditions also play important roles in determining the module performance.

2.3.1 Selection of absorption solvent

As the key component of the membrane contactor, selection of appropriate membrane material and solvent is important to ensure effective module design. As explained in the previous section, the mass transfer rate in membrane contactor is determined by the resistance in the gas phase, liquid phase, and membrane phase. The resistance in gas phase becomes negligible when the pores of membrane are filled with gas. However, when the membrane pores are filled with the liquid (wetted), the mass transfer resistance of the membranes becomes significant (Kreulen et al., 1993), resulting into economically unviable operation. The design strategy of the membrane gas-liquid contactors for CO_2 removal should be aimed at preventing the membrane wetting for long term application by carefully selecting absorption solvent and membrane materials with good compatibility.

Absorption of CO_2 can be carried out using either physical or chemical solvents. Typical chemical solvents include aqueous solutions of alkanolamines and aqueous carbonate solutions. The mass transfer coefficients with the absorption of CO_2 in a solution of sodium hydroxide was examined and the result showed that the mass transfer process was influenced by the chemical reaction between hydroxide and carbon dioxide (Qi et al., 1993). The influence of a chemical reaction on the mass transfer by means of simulating and testing the absorption of CO_2 in KOH solution and the selective absorption of H_2S using aqueous alkanolammes was studied by several researchers (Kreulen et al.,1993). The selectivity was determined by the ratio of the partial mass

transfer resistances in the gas and liquid phase and the solubility of gas component in the absorption liquid. Aqueous monoethanolamine (MEA), 2-amino-2-methyl-1-propanol (AMP), DEA and water were compared as absorbents to separate CO_2–N_2 mixture in PTFE hollow fibre membrane contactors (Kim et al., 2000). In the presence of alkanolamines as absorbents, absorption is facilitated by chemical reaction and MEA gives the highest CO_2 removal efficiency, compared to the other absorbents.

Although amines have a long and successful track record for acid gas removal under a variety of conditions, the processes are energy intensive and are not always the best choice for offshore CO_2 removal when the CO_2 partial pressure and feed gas volumes are high (Dindore et al., 2005). Generic amine treating processes, such as DGA, DEA, or MDEA, require considerable heating and cooling duties for amine regeneration when treating gas streams with a high CO_2 content. On an offshore platform, amine regeneration by steam, hot water, or heating medium requires additional equipment, amine storage capacity, and large piping, which increases platform cost. Physical absorption using membrane can be operated under low temperature and makes regeneration of absorbents much easier. Furthermore, unlike chemical absorption, the amount of CO_2 absorbed by the solvent is determined by the vapour-liquid equilibrium of the mixture, which is governed by partial pressure and temperature. At high CO_2 partial pressure, the CO_2 loading capacity of the solvent is higher for a physical solvent than for a chemical solvent. Physical absorption processes are thus particularly appropriate for the treatment of CO_2-rich gas streams. CO_2 absorption using water as absorbent was investigated from which several empirical correlations for membrane contactors with

absorbent inside and outside the hollow fibres were presented (Yang et al., 1986). The performance of the cross flow hollow fibre membrane contactor (HFMC) for CO_2 absorption using water and propylene carbonate and both of them shows great compatibility with Propylene hollow fibres, which brings potential for long term operation. Wang et al. (Wang et al., 2006) developed detailed numerical model to analyze the absorption of CO_2 and H_2S using methanol in flat sheet membrane and the absorption efficiency can be as high as 85%.

Both chemical absorption and physical absorption have their own advantages and disadvantages, there is one common issue shared by these two operations: wetting of the membrane. As explained earlier, when the pores of membrane are filled with liquid (wetted mode), the overall mass transfer rate dramatically decreases due to the increasing in mass transfer resistance. In general, the wetting of the membrane is decided by the membrane–liquid interactions. Hence, a suitable combination of the absorption liquid and the membrane material is critical for the stability of the membrane gas-liquid contactors.

2.3.2 Selection of membrane material

For porous membranes, a minimum pressure is required for the liquid to penetrate into the pores. The higher breakthrough pressure is a key for the long term non-wetting application of gas-liquid membrane contactors. A few researchers explored the criteria of the selection of appropriate membrane-solvent combination for the development of membrane gas absorption (Dindore et al., 2005). The compatibility of organic solvents with several commercially available membrane materials were studied by examining the critical entry pressure, the contact angle of the liquid on the membrane surface and the

size and shape of membrane pores. Membranes having a high hydrophobicity and low surface energies such as PTFE, polypropylene, PVDF, polysulfone and polyethersulfone were selected.

Table 2.1: Membrane-solvent compatibility (Dindore et al., 2005)

Solvent	PTFE	PP	PVDF	PES	PS
Water	√	√	√	√	√
Propylene Carbonate	√	√	x	x	x
Selexol	√	x	x	x	x
N-methylpyrrodilone	x	x	x	x	x
Dimethyl formamide	x	x	x	x	x
Tributyl phosphate	x	x	x	x	x
Glycerol triacetate	√	x	x	x	x
n-Formyl morpholine	√	√	x	x	x

√ = compatible combination x = incompatible combination

Compared to other membranes, PTFE and polypropylene membranes were found to be compatible with some of the selected organic solvents in terms of less morphological damage, swelling, shrinkages, color change or dissolution after being exposed to selected solvents over a period of time. Compared to PP membrane, the application of PTFE is limited for its high production cost and is unavailable in small diameters while the hydrophobicity of PP membranes can be improved by various modification methods, such as pretreatment with fluorocarbonic material (Nishikawa et al., 1995), surface grafting (Xu et al., 2002), interfacial polymerization (Dickson et al., 1998) and solvent casting (Erbil et al., 2003). Therefore, PP membrane is considered as the potential candidate for designing membrane contactors for offshore gas processing in this work.

2.3.3 Operation modes of membrane contactors

Several membrane module configurations are available, both at commercial and laboratory scale respectively, for the conventional membrane applications such as filtration, gas separation etc. These module configurations can be conveniently adopted for the membrane gas-liquid contactors with relatively little modifications. Depending on the type of membranes used in the contactor, these devices can be broadly classified into two groups; the flat sheet membrane contactor and the hollow fiber membrane contactor. Flat sheet membranes are used in plate-and-frame or in spiral wound membrane contactors. Although equally efficient mass transfer operation can be carried out using flat sheet membrane contactors, hollow fiber membrane contactors are widely used due to the higher interfacial area. Based on the flow directions of the gas and liquid phase, the hollow fiber membrane contactor can be used in two different modes of operation, shown in Figure 2.7 (Dindore et al., 2005).

- Parallel flow mode: The flow of the both phases is parallel to the axis of the fiber and both fluids flow either in same direction (co-current) or in opposite direction (counter current).

- Cross flow mode: The flow of one of the fluid is perpendicular to the axis of fiber and other fluid flows parallel to the axis of fiber. Thus the two fluids flow at right angles to each other.

(a) Cross flow mode (b) Parallel flow mode

Figure 2.7: Cross flow and Parallel flow mode membrane contactors

Previous studies show that parallel flow offers the highest average concentration driving force in the case of counter-current flow and is preferred in situations where membrane or fiber side mass transfer resistance controls (Jansen et al., 1994). The choice between the co-current and counter-current operation is determined by the trans-membrane pressure variation. In the case of counter-current operation, the variation in the trans-membrane pressure is relatively high, which interferes with the interface stability and can even lead to breakthrough of one phase into another. In the case of parallel flow, the overall mass transfer rate can be significantly reduced if the shell-side mass transfer resistance is significant. In such cases cross flow configurations are attractive as flow in the direction perpendicular to the fibers leads to higher shell-side mass transfer coefficients. This is mainly because of the concentration boundary layer break-up due to continuous splitting and remixing of the fluid flowing perpendicular to the fiber. However, the higher mass transfer coefficient is obtained at the cost of a reduced overall mass transfer driving force in comparison to counter current parallel flow. The choice of the geometry of hollow fiber membrane contactors in early stages of developments was largely influenced by the simplicity of the module constructions. Conventionally, shell and tube geometry is preferred for membrane contactors due to the ease in the manufacturing of these modules

(Wickramasinghe et al., 1993). Later on, several investigators found that uneven packing and uneven flow distribution on the shell side of the shell and tube module resulted into reduced mass transfer rates (Wang et al., 2003). Hence considerable efforts have been made to explore the different module geometries in order to achieve uniform flow distribution on the shell side. In recent years, it has also been found that the use of fibers woven into fabric in the membrane module manufacture results in more uniform fiber spacing (Dindore et al., 2005) The fibers woven into a fabric have been successfully used for the manufacturing of module with different geometries such as rectangular module, helically wound fiber module, baffled shell and tube module and transverse flow module. Out of the various innovative geometries studied by several investigators, only rectangular module and shell and tube transverse flow module have been successfully commercialized. Hoechst Celanese provides shell and tube transverse flow Liqui-Cel contactors for various gas-liquid contacting applications where as rectangular cross-flow module is commercialized by TNO Environmental Energy and Process Innovation (The Netherlands) and by Kvaerner Oil & Gas in co-operation with W. L. Gore & Associates GmbH. Mass transfer in hollow fiber membrane modules with different geometries was compared with equal flow per membrane area and it was found that the flow outside and across the fibers is at least ten times more effective than flow outside and parallel to the fibers (Wickramasinghe et al., 1993). A similar conclusion was drawn based the experimental study of reactive absorption of SO_2; the mass transfer coefficient for the cross flow modules was one order of magnitude higher than parallel flow modules (Jansen et al., 1994).

References

Alexander, S.R., Winnick, J., Removal of hydrogen sulfide from natural gas through an electrochemical membrane separator, AIChE Journal, 40 (4) (1994), 613-620

Babcock, R.E.,Spillman, R.W., Goddin, C.S., Cooley, T. E., Natural Gas Cleanup: A Comparison of Membrane and Amine Treatment Processes, Energy Progress, 8(3)(1988), 135-142

Baker, R.W., Lokhandwaa, K., Natural Gas Processing with Membranes: An Overview, Ind. Eng. Chem. Res. 47 (2008), 2109-2121

Baker, R.W., Roman, I.C., Lonsdale, H.K., Liquid membranes for the production of oxygen-enriched air I. Introduction and passive liquid membranes, Journal of Membrane Science,31 (1987), 15-29

Catapano, G., Papenfuss, H.D., Wodetzki, A., Baurmeister, U., Mass and momentum transport in extra-luminal flow (ELF) membrane devices for blood oxygenation, Journal of Membrane Science, 184 (2001), 123-135

Chun, M.S., Lee, K.H., Analysis on a hydrophobic hollow fiber membrane absorber and experimental observations of CO_2 removal by enhanced absorption. Separation Science and Technology 32 (15) (1997), 2445-2466

Cook, P.J., Losin, M.S., Membranes provide cost effective natural gas Processing, Hydrocarbon Processing, (1994), 79-84

Dickson, R.M, Norris, D.J, Moerner, W.E, Simultaneous imaging of individual molecules aligned both parallel and perpendicular to the optic axis Physical Review Letter, 81(1998) 5322-5325

Dindore, V.Y., Brilman, D.W.F., Versteeg, G. F., Hollow fibre membrane contactor as a gas–liquid model contactor, Chemical Engineering Science, 60 (2005), 467-479

Dindore, V.Y., Versteeg, G.F., Gas-liquid mass transfer in a cross-flow hollow fibre module: Analytical model and experimental validation, International Journal of Heat Mass Transfer 48 (2005), 3352-3362

Esato, K., Eiseman, B., Experimental evaluation of gore-tex membrane oxygenator, Journal of Thoracic and Cardiovascular Surgery, 69(5) (1975), 690-697

Erbil, H. Y., Demirel, A.L., Avci, Y., Mert, O., Transformation of a simple plastic into a superhydrophobic surface, Americal Association for the Advancement of Science, 299(5611)(2003),1377-1380

Falk-Pedersen, O., Dannström, H., Separation of carbon dioxide from offshore gas turbine exhaust, Energy Conversion Management, 38 (1997), S81-S86

Gage, K.L., Gartner, M.J., Burgreen, G.W., Wagner, W.R., Predicting membrane oxygenator pressure drop using computational fluid dynamics, Artificial Organs 26 (2002), 600-607

Gu, Y.J., Boonstra, P.W., Graaff, R., Rijnsburger, A. A., Mungroop, H., Oeveren, W.V., Pressure drop, shear stress, and activation of leukocytes during cardiopulmonary

bypass: a comparison between hollow fibre and flat sheet membrane oxygenators, Artifiicial Organs 24(1) (2000), 43-8

Hoff, K.A., Poplsteinova, J., Jakobsen, H.A., Juliussen, O., Falk-Pedersen, O., Sevendsen, H.F., Modelling of membrane reactor, International Journal of Chemical Reactor Engineering, 1(1)(2009),A9

Isa, M.F., Azhar, M. A., Meeting technical challenges in developing high CO_2 gas field offshore, 24th World Gas Conference, Buenos Aries, Argentina,2009

Jahn, J., Bos, P.V.D, Broeke, L.J.V.D, Evaluation of membrane processes for acid gas treatment, SPE International and Operation Conference, Doha, Qatar, 2012

Jansen, A.E., Klaassen, R., Feron, P.H.M., Hanemaaijer, J.H., Meulen, B.P., Membrane gas absorption processes in environmental applications in Membrane Processes in Separation and Purification, Kluwer Academic Publishers, Dordrecht, 1994

Jassim, M.S., Rochelle, G.T., Innovative Absorber/Stripper Configurations for CO_2 Capture by Aqueous Monoethanolamine, Industrial & Engineering Chemistry Research, (2006), 45:2465

Johnson, B.M., Baker, R.W., Matson, S.L., Smith, K.L., Roman, I.C., Tuttle, M.E., Lonsdale, H.K., Liquid membranes for the production of oxygen-enriched air II. Facilitated-transport membranes, Journal of Membrane Science, 31 (1987), 31-67

Karoor, S., Sirkar, K.K., Gas absorption studies in microporous hollow fibre membrane modules, Ind. Eng. Chem. Res., 32 (4) (1993) 674–684

Kim, Y., Yang, S., Absorption of carbon dioxide through hollow fibre membranes using various aqueous absorbents, Separation and Purification Technology, 21(1-2) (2000), 101-109

Kosaraju, P., Kowali, A. S., Korikov, A., Sirkar, K., Hollow fibre membrane contactor based CO_2 absorption-stripping using novel solvents and membranes, 44(5) (2005), 1250-1258

Kreulen, H. Versteeg, G.F., Smolders, C.A., Swaaij, W.P.M.V., Microporous hollow fibre membrane modules as gas-liquid contactors II: Mass transfer with chemical reaction. Journal of Membrane Science78(3) (1993b), 217-238

Kreulen, H., Smolders, C.A., Versteeg, G.F., Swaaij, W.P.M.V., Microporous hollow-fibre membrane modules as gas–liquid contactors: 1. Physical mass transfer processes—a specific application: mass transfer in highly viscous liquids. Journal of Membrane Science, 78(1993) (3), 197–216

Nishikawa, N., Ishibashi, M., Ohta, H., Akutsu, N., Mastsumoto, H., Kamata, T. , Kitamura, H., CO_2 removal by hollow fiber gas liquid contactor. Energy Conversion and Management 36(1995)415-418

Parro, D., "Membrane CO2 proves out at SACROC tertiary recovery project," Oil Gas Journal, 82 (1984), 85-88

Poddar, T.K., Majumdar S., and K.K. Sirkar, Membrane-based Absorption of VOCs from a Gas Stream, AIChE J, 42(11) (1996), 3267-3282

Rangwala, H.A., Absorption of carbon dioxide into aqueous solution using hollow fibre membrane contactors, Journal of Membrane Science, 112(1996), 229-240

Strathmann, H. Membranes and Membrane Separation Processes; Wiley-VCH Verlag GmbH & Co. KGaA: New York, 2000

Tabe-Mohammadi, A., A review of the applications of membrane separation technology in natural gas treatment, Separation science and technology, 34 (1999), 2095-2111

Tierling, S., Jindal, S., Abascal, R., Considerations for the use of carbon dioxide removal membranes in an offshore environment offshore technology conference, Offshore Technology Conference, Rio de Janeiro, Brazil, 2011

Wang, S.Y., Hawboldt, K., Abdi, M.A., Novel dual-membrane gas-liquid contactors: modeling and concept analysis, Industrial & Engineering Chemistry Research 45 (2006), 782-789

Wang, Y. Chen, F., Wang, Y., Luo, G., Dai, Y., Effect of random packing on shell-side flow and mass transfer in hollow fibre module described by normal distribution function, Journal of Membrane Science 216 (2003), 81-93

Wickramasinghe, S. R., Semmens, M. J., Cussler, E. L., Hollow fibre modules made with hollow fibre fabric, Journal of Membrane Science, 84(1) (1993),1-14

Wickramasinghe, S.R., Semmens, M. J., Cussler, E.L., Mass transfer in various hollow fibre geometries. Journal of Membrane Science, 69(1992), 235-250

Xu, Z., Wang, J., Shen, L., Men, D., Xu, Y., Microporous polypropylene hollow fiber membrane: PartI. Surface modification by the graft polymerization of acrylic acid, Journal of membrane Science, 196 (2002), 221-229

Zhang, Q., Cussler, E.L., Microporous hollow fibres for gas absorption II. Mass transfer across the membrane, Journal of Membrane Science, 23 (1985), 333-345

Zhang, Q., Cussler, E.L., Microporous hollow fibres for gas absorption I. mass transfer in the liquid, Journal of Membrane Science, 23 (1985), 321-332

CHAPTER 3

DEVELOPMENT OF NOVEL DUAL MEMBRANE CONTACTOR FOR GAS ABSORPTION

This chapter is based on and modified based on the following paper

Cai, **J.J.,** Hawboldt, K., Abdi, M.A, Contaminant Removal from Natural Gas using Dual Hollow Fiber Membrane Contactors. *Journal of membrane science*, 377-378 (2012)9-16

Having discussed the recent trends of membrane technology and its potential for gas processing in Chapter 2, this chapter focuses on the development of novel membrane contactors for offshore gas absorption. Conventional membrane gas-liquid contactors have typically had separate absorption and regeneration system, which may not be practical for offshore gas treating due to limited space. Therefore, a novel design of membrane modules containing two sets of membranes is proposed in this chapter to achieve gas absorption and partial solvent regeneration in one unit operation. The motivation is presented in Section 3.1 whereas the details of the proposed dual membrane module are given in Section 3.2. To predict the performance of the dual membrane contactor and also the concentration change in both gas and liquid phase in the proposed modules, a numerical model based on mass balance is developed and presented in Section 3.3. In Section 3.4, the proposed numerical model is validated by comparing the modeled results and experimental measurements for CO_2 absorption. To further demonstrate the efficiency of the proposed dual membrane modules, its performance is also compared with ordinary membrane module for CO_2 absorption by varying operational conditions in the same section.

3.1 Background

In gas absorption, the absorbent must be regenerated. Compared to the extensive study in gas absorption using membrane technology, limited work has been done on the development of membrane based regeneration. For gas treatment, regeneration of absorbent is important to ensure process efficiency and keep solvent costs down. A hollow fibre membrane based absorption-stripping system was proposed to remove the

volatile organic compounds (VOCs) from nitrogen (Poddar et al., 1996). The spent absorbent liquid was regenerated in a separate hollow fibre stripper by applying vacuum through the tube side and recycled back to the absorber. Falk-Pedersen et al. (Falk-Pedersen et al., 1997) compared membrane gas/liquid contactor desorber to several types of desorption systems for CO_2 removal from gas turbine exhaust on offshore platform and the membrane contactor desorber was found to have the best potential. Kosaraju et al. (Kosaraju et al., 2005) studied the stripping of a novel non-volatile solvent for CO_2 removal. Membrane based gas absorption and stripping were used in these studies. However, the absorber and desorber were separate modules. Considering limited space on offshore platform, merging the absorber and stripper into one unit would be preferred to further minimize space and weight requirement. One option to achieve this goal is to use immobilized liquid membrane (ILM) (Teramoto et al., 1986; Hughes et al., 1986; Baker et al., 1987; Johnson et al., 1987; Kreulen et al., 1993). In this case, the liquid membrane is located in the pores of the membrane, forming a thin partition between the feed gas and stripping phase. However, the difficulty in renewal of the liquid membrane in pores (Mataon et al., 1983), critical problems in humidity control and lack of mechanical stability (Kimura et al., 1980) are issues that still need to be fully addressed. Contained liquid membrane (CLM) (Majumdar et al., 1988) has been proposed to eliminate aforementioned shortcomings. In CLM operation, a thin film of aqueous solution is held stationary in the interstitial space between two independent sets of microporous hollow fibres, where one set fibres carries a feed gas while the other set carries a sweep gas stream. This design may result in large mass transfer resistance through the layer of the membrane solution due to absorption of carrier solution in the pore of the microporous

membranes. In the aim of reducing the diffusion resistance of the liquid film, a new type of "flowing liquid membrane" was proposed for separation of ethane/ethylene, in which liquid was pumped between two microporous membranes (Teramoto et al., 1989). It was found to provide better permeability and stability than the stationary solvent. A similar idea was proposed by Bessarabov et al. (Bessarabov et al., 1993), using an integrated membrane system with a solution of silver nitrate flowing between two nonporous PVTMS membranes for separation of $CO_2/H_2/CH_4$ mixtures. This type of module has three outlets for the products and provides a higher selectivity of separation and flexibility of the gas separation.

The development of ILM and CLM shows potential in regenerating the solvent in the same unit as absorber by introducing vacuum or sweeping gas on the permeate side of the membrane. However, there is little published work on how the partial regeneration of solvent impacts gas absorption and removal efficiency. A dual membrane gas-liquid contact concept was proposed for CO_2 and H_2S removal using methanol, in which two types of flat membranes are housed into one unit (Wang et al.,m 2006). The circulating solvent of methanol is partially regenerated during the absorption. It was demonstrated that the gas removal efficiency can be substantially improved by introducing sweeping gas or vacuum on the permeate side of the membrane. However, only flat membrane under parallel flow mode (co-current or counter-current) was studied. The performance of parallel and cross flow based on the equal flow per membrane area and found that cross flow membrane were more effective as compared to parallel flow modules (Wickramasinghe et al., 1992). A similar conclusion was drawn from a study of reactive

absorption of SO_2; the mass transfer coefficient for the cross flow modules was one order of magnitude higher than parallel flow modules (Jansen et al., 1996). To analyze the performance of the cross flow hollow fibre membrane contactor for CO_2 absorption, a detailed numerical model was developed (Dindore et al., 2005). The regeneration of solvent, however, was not included in their studies. This work aims to propose a new design of hollow fibre membrane contactor to improve gas absorption by partially regenerating the absorbent during absorption through nonporous membrane.

3.2 Dual membrane contactors

In the present study, two configurations of dual membrane HFMC were proposed with their performance investigated. The proposed modules comprise two types of hollow fibres. The porous hollow fibres containing feed gas are in the same contactor as nonporous fibres, which are used for solvent regeneration. An aqueous solution flows through shell side. In Module I (outlined in Figure 3.1(a)), a low pressure is maintained on the permeate side of nonporous membrane. As indicated previously, the differential pressure across nonporous membrane can improve contaminant removal from the solvent and partially regenerate the solvent stream simultaneously with the absorption process. This results in better absorption efficiency. To further improve the removal efficiency, baffles are added in Module II (shown in Figure 3.1(b)). Based on studies conducted by Wang and Cussler (Wang et al., 1992) and those in heat exchanger, the baffles can improve mass transfer efficiency by minimizing shell-side bypass and providing a velocity component normal to the membrane surface.

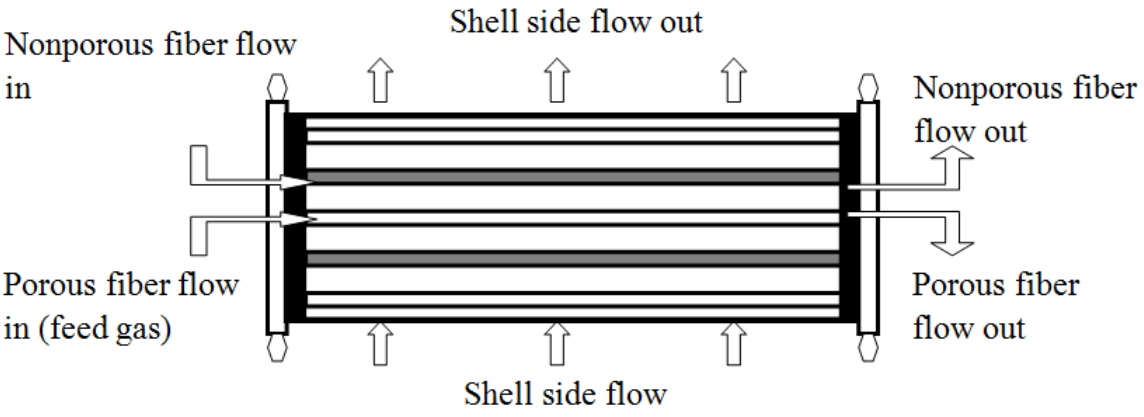

(a)

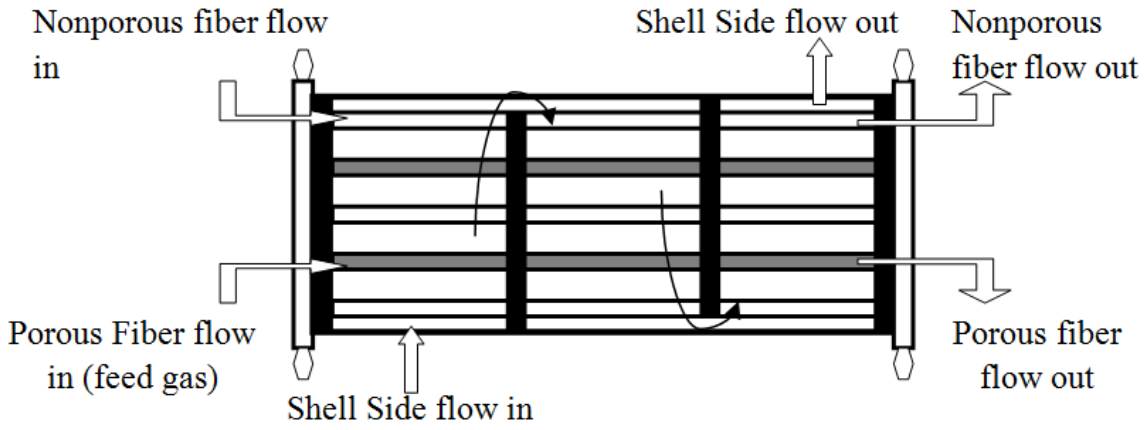

(b)

Figure 3.1 : (a) Module I - Cross flow Dual HFMC; (b): Module II - Cross flow dual HFMC with baffles

Depending on the type of solvent, the absorption of contaminant can be either chemical or physical. Solutions of chemical solvents such as amines and alkali-metal salts are widely used in natural gas treating plants. However, regeneration of these chemical solvents is energy and space intensive and is unattractive for offshore platforms. Hence, this work

mainly focuses on physical solvents. To analyze and predict the absorption performance of the proposed modules, a mathematical model has also been developed. A similar model was proposed for the first time to examine heat transfer in cross flow shell and tube heat exchanger (Hoffman, 2000). Dindore *et al*. (Dindore et al., 2005) also proposed a similar model for cross flow HFMCs. Predictions from the derived analytical expressions matched well with experimental data over a range of wide operating flow rates. In their studies, liquid was fed through membrane fibre side, which contributes most mass transfer resistance and the impact of regeneration was not included. A numerical model for liquid phase flowing in shell side was developed in this work to predict module performance. It takes impact of regeneration into consideration on absorption at the same time. The results were validated by previous experiment data from Dindore et al. (Dindore et al., 2005). Further, absorption performance of proposed module for CO_2 removal is compared with ordinary membrane module. Because two different types of membrane were employed in the module, the effect of different packing fraction for each type of membrane is also investigated.

3.3 Model Development

A number of researchers have modeled cross flow HFMC using iterative methods, finite differences, and heat transfer analogies (Zhang et al., 1985; Wang et al., 1993; Dindore et al., 2005) whereas most of these processes involve mass transfer through only one type of membrane. To describe mass transfer taking place in dual membrane contactors, a numerical model was developed to describe the mass transfer in the membrane, liquid

phase and the gas phase. The model is based on the following simplifying assumptions (Coelhoso et al., 2000):

1. Contactor is operated under steady state and isothermal conditions.
2. Physical properties including diffusion coefficient, Henry's constant, density, viscosity etc. are constant along the membrane.
3. No chemical reaction is involved, only physical mass transfer is modeled.
4. Membranes are under the non-wetted mode (gas-filled pores).
5. The pressure in gas phase is constant along the membrane.
6. The flow rate of fluid in the shell side is assumed to be steady through the contactor.

3.3.1 Overall mass transfer in liquid phase

Using the above assumptions, a material balance is applied on a differential segment of the module. The change of mass in liquid phase is due to loss of contaminant in gas in porous hollow fibre and gain of contaminant in the nonporous hollow fibre, it can be expressed as follows:

$$Q_L \Delta C_L = \Delta Q_G \Delta C_G - \Delta q_{np} \qquad \text{Eq. 3.1}$$

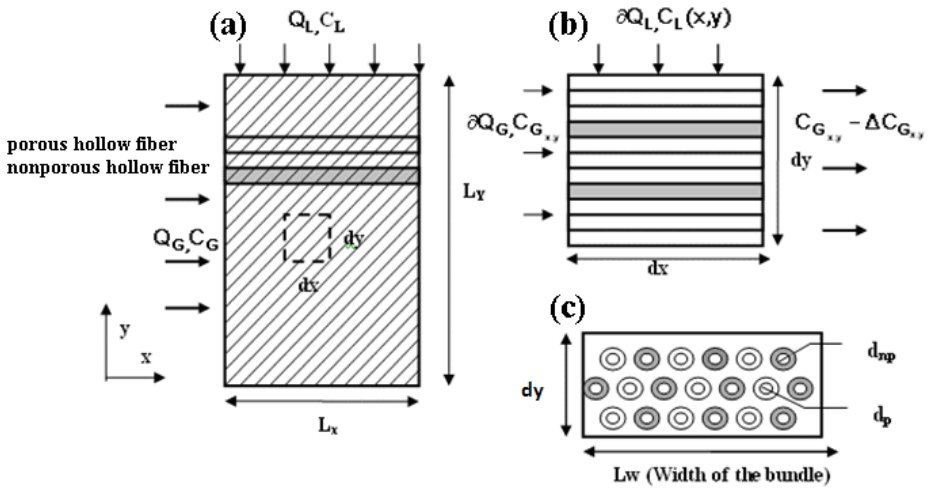

Figure 3.2 : Cross section and modeling parameters in cross flow membrane contactor (a) simplified module of cross flow dual HFMC; (b) side view of differential segment; and (c) front view of differential segment

The number of moles of contaminant absorbed by the solvent is equal to that of diffusing through the boundary. The material balance in liquid phase hence can be derived as:

$$\frac{\Delta x}{L_X} Q_L \left(\frac{\partial C_L(x,y)}{\partial y} \Delta y\right) = k_L dA_p (HC_G(x,y) - C_L(x,y)) - k_L dA_{NP} (C_L(x,y) - C_{SNP}(x,y))$$

Eq. 3.2

Where dA_P and dA_{Np} denote transfer area between gas and liquid in porous membranes and nonporous membranes, respectively. They can be obtained by multiplying membrane area of single hollow fibre (A) with the total number of fibres in differential volume (dN). Given in the following equation, C_{SNP} is concentration at the surface of nonporous membrane; dV and V are total volume of differential segment and the volume taken by single fibre.

$$dA_P = A_P dN_P = A_P \times \frac{(1-\alpha)dV}{V_P} \quad \text{Eq. 3.3}$$

$$dA_{NP} = A_{NP} N_{NP} = A_{NP} \times \frac{(1-\alpha_{NP})dV}{V_{NP}} \quad \text{Eq. 3.4}$$

where *(1- α_P)* and *(1- α_{NP})* denote the packing fractions of porous membranes and nonporous membranes in the modules. By introducing these two parameters into the model, the impact of ratio of porous membranes and nonporous membranes on the absorption efficiency can be revealed. By introducing two new variables, the steady state mass transfer balance in the porous fibre can be simplified as:

$$\frac{\partial C_L(x,y)}{\partial y} = M_p(HC_G(x,y) - C_L(x,y)) - M_{NP}(C_L(x,y) - C_{SNP}(x,y)) \quad \text{Eq. 3.5}$$

Where two new variables can be defined as: $M_P = \frac{4(1-\alpha_P)L_W L_X}{d_P}\frac{k_L}{Q_L}$; Eq. 3.6

$$M_{NP} = \frac{4(1-\alpha_{NP})L_W L_X}{d_{NP}}\frac{k_L}{Q_L} \quad \text{Eq. 3.7}$$

At the gas entrance where *x* is equal to zero, C_L is a function of *y* only, thereby, we have the following boundary condition:

$$\frac{\partial C_L}{\partial y}\Big|_{x=0} = M_P(HC_G - C_L|_{x=0}) - M_{NP}(C_L|_{x=0} - C_{SNP}) \quad \text{Eq. 3.8}$$

This expression can be solved as one of the boundary conditions on the gas side. The second boundary condition can be defined as:

$C_{L_I} = C_{L_{in,i}}$, at y=0 Eq. 3.9

3.3.2 Gas phase mass balance within porous membrane

The transfer of contaminant molecules from gas phase to the liquid consists of three steps: transfer from bulk of the gas phase to the membrane, diffusion through the gas-filled pores, and transfer from membranes into bulk of the liquid phase. The mass balance in the gas phase can be expressed as:

$$\frac{\Delta y}{L_Y} Q_L \left(\frac{\partial C_G(x,y)}{\partial x} \Delta x\right) = KdA_p (C_L(x,y) - HC_G(x,y)) \quad \text{Eq. 3.10}$$

where K is the overall mass transfer coefficient equal to k_L in this model since the membrane and the gas phase resistance can be neglected in non-wetted gas absorption, mass transfer is controlled by liquid phase under this mode. k_L can be obtained from Sherwood number (kd/D) and empirical equations (Wickramasinghe et al.,1992)

$$Sh = 0.18 \mathrm{Re}^{0.86} Sc^{0.33} \quad \text{Eq. 3.11}$$

Where the Reynolds number is calculated from the outer fibre diameter, the kinematic viscosity and superficial velocity; Schmidt number (v/D) dependence is verified by other experiments (Mavroudi et al., 2006). Equation 3.10 can be simplified as follows by introducing a new variable.

$$\frac{\partial C_G(x,y)}{\partial x} = M_G (C_L(x,y) - HC_G(x,y)) \quad \text{Eq. 3.12}$$

where the new variable can be defined as: $M_G = \frac{4(1-\alpha_P)L_W L_Y}{d_P}\frac{k_L}{Q_G}$ Eq. 3.13

The boundary conditions are

$C_{G_I} = C_{G_{in,i}}$, at x=0 Eq. 3.14

And the liquid entrance where y is equal to zero, the contaminant concentration in the gas phase is a function of module length x:

$$\frac{\partial C_{G_{in,i}}}{\partial x}\Big|_{y=0} = M_{G_{in,i}}(C_{L_i} - HC_{G_i}\Big|_{y=0}) \quad \text{Eq. 3.15}$$

This expression is the boundary condition on the liquid side.

3.3.3 Gas phase mass balance with nonporous membranes

The contaminant absorbed in the liquid phase permeates the nonporous membrane through diffusion mechanism. The flux is proportional to partial pressure difference and inversely proportional to the membrane thickness:

$$\Delta q_{NP} = \frac{k_{Per}}{t_{NP}}\left(\frac{C_{SNP}RT}{H} - P_{out}\right)\pi d_{NP}\Delta x \quad \text{Eq. 3.16}$$

Where, K_{per} denotes nonporous permeability for the gas contaminant and the membrane thickness t_{NP} is assumed to be small and therefore the outer and inner surface areas are equal. Similar analysis is also applied to the baffled module, each segment of Module II can be modeled by a set of partial differential equations; the outlet concentrations of the

previous segment in both gas and liquid phases are the initial and boundary conditions for the next segment.

The nonlinear partial differential equations established based on the mass balance in gas phase Eq. (3.12) and liquid phase (Eq. 3.5), respectively. Each equation contains two variables (C_G, C_L) in which each variable is a function of module length (x) and height (y). To describe the concentration change in both gas and liquid phase, these two partial differential equations were combined and solved using finite difference method in Maple® software.

3.4 Results and discussion

The results of models were firstly compared to the experiment data to validate the proposed model for absorption of CO_2 using water. In the following, the absorption of CO_2 from CO_2/CH_4 mixture gases of the novel dual-membrane Module I and Module II were investigated and the results were compared to the ordinary single membrane contactor under the same operating conditions. Propylene carbonate was assumed to be the absorbing solvent instead of water due to its high solubility to CO_2. The effect of different packing fractions of porous and nonporous membranes on the absorption efficiency was also investigated for future module construction reference.

3.4.1 Model validation

To validate the numerical model, the results were compared to the experimental data from Dindore et al. (Dindore et al., 2005). The module developed by Dindore differs from proposed module that the liquid solvent flows through the fibres and the mixture gas

through the shell side and only one type of membrane is used. The model parameters were adjusted accordingly for comparison. However it should be noted that the solution methodology remained the same.

Pure water was used as physical solvent to remove CO_2 from CO_2/N_2 mixture in the model validation as Dindore et al. (Dindore et al., 2005) used this combination. Earlier studies by Semmens et al. (Semmens et al., 1990) showed little mass transfer resistance across the membrane or in the gas phase. Therefore the individual mass transfer coefficient in the water is used in place of the overall mass transfer coefficient. Asymptotic correlations based on the heat transfer analogy of the Graetz-Leveque equations are widely used to predict the mass transfer coefficient on the fibre side (Kreulen et al., 1993; Leveque et al., 1928).

$$Sh = \sqrt[3]{1.67Gz} \qquad \text{Gz>20} \qquad \text{Eq. 3.17}$$

$$Sh = \sqrt[3]{(3.67^3 + 1.63^3)\ Gz} \qquad 10<\text{Gz}<20 \qquad \text{Eq. 3.18}$$

$$Sh = 3.67 \qquad \text{Gz<10} \qquad \text{Eq. 3.19}$$

The numerical model was modified to confirm module proposed by Dindore et al. (Dindore et al., 2005):

$$\frac{\partial C_G}{\partial x} = -M_G (HC_G - C_L) \qquad \text{Eq. 3.20}$$

$$C_{G_i} = C_{G_{in,i}},\ for\ x = 0 \qquad \text{Eq. 3.21}$$

$$\frac{\partial C_L}{\partial y} = M_P (HC_G - C_L) \qquad \text{Eq. 3.22}$$

$$C_{L_i} = C_{L_{in,i}},\ for\ y = 0 \qquad \text{Eq. 3.23}$$

Absorption of CO_2 with inlet concentration of 14.62 mol/m^3 and 39.33 mol/m^3 CO_2 at a constant inlet gas flow rate of $2.21 \times 10^{-4} m^3/s$ were compared to experiment results from Dindore et al. (Dindore et al., 2005) Figures 3.3 and 3.4 compare the modeled results to the experimental data. The parity plots of measured CO_2 concentration in both gas outlet and liquid outlet match well with the experiment data Dindore et al. (Dindore et al., 2005). The absorption of CO_2 in both cases is relatively how, due to the low gas residence time as a result of a high gas flow rate.

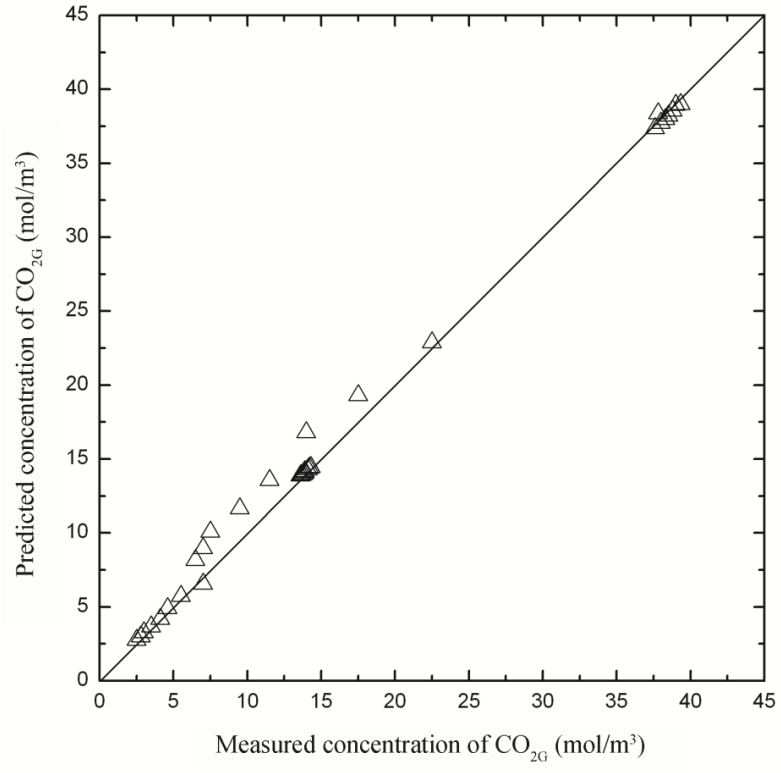

Figure 3.3 : Parity plot of model results and the experimental data (Dindore et al., 2005) for CO_2 concentration at gas outlet (Q_G=2.21×10^{-4} m^3/s)

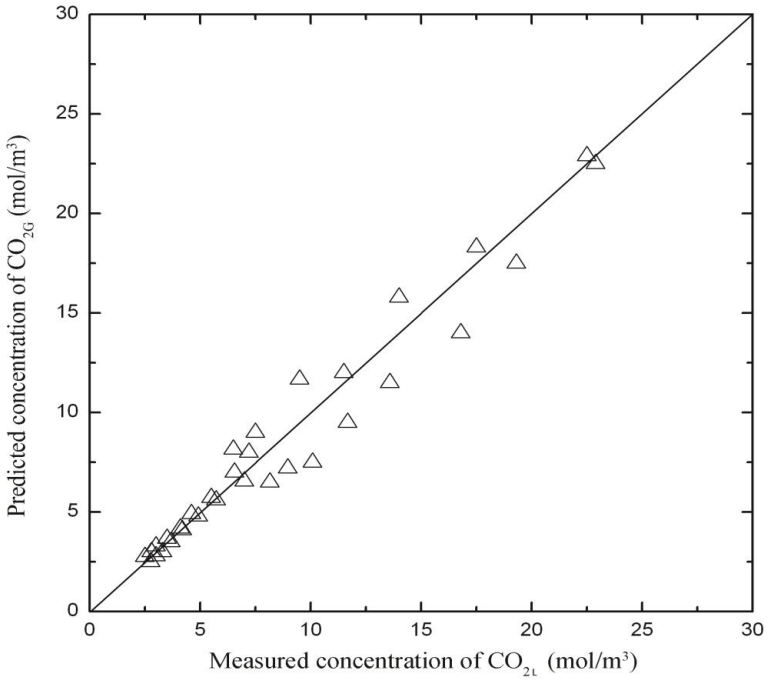

Figure 3.4: Parity plot of model results and the experimental data (Dindore et al., 2005) for CO_2 concentration at liquid outlet (Q_G=2.21×10^{-4} m^3/s)

3.4.2 The performance of dual membrane contactor

Depending on the fluid types in the shell side, absorption can be operated either with liquid passing through shell side or flowing inside the fibres. For HFMC with the liquid flows on the tube side, the pressure drop inside the tube may lead to membrane wetting quickly in the initial fibre length due to a higher trans-membrane pressure in this section than the breakthrough pressure (Mavroudi et al., 2006). Considering that the diffusion of a gaseous species in the liquid phase is much slower than in the gas phase, the membrane resistance can increase significantly if it operates in the wetted mode, as such, in our

module, the liquid flows in the shell side of HFMC. Nonporous membrane fibres are introduced with low pressure or vacuum inside the fibres, absorption of CO_2 from CO_2/CH_4 mixture is investigated. Propylene carbonate was selected as the absorbent since it offers high solubility for CO_2. Specification of modules studied in this work and parameters used in calculation are shown in Table 3.1, modified from experimental data from other researchers (Dindore et al., 2005).

Table 3.1: Specifications of module and their references

Parameter	**Value**
Module Height (m)	0.1
Dimension of module (m)	0.1×0.2
Solvent flow rate ($10^{-5}m^3/s$)	7.8
Mixture gas flow rate ($10^{-5}m^3/s$)	2.66
Diffusivity of CO_2 in propylene carbonate (10^{-9} m^2/s)	1.36
Pressure of mixture gas (10^6 PaA)	5.0
Pressure in nonporous fibres (10^5 PaA)	1.0
Number of non porous fibres	4,900
Number of porous fibres	4,900 (Dindore et al., 2005)

The absorption of CO_2 in Module I with an inlet concentration of 39.33 mol/m^3 at constant inlet gas flow rate of 2.66×10^{-5} m^3/s and liquid flow rate of 7.8×10^{-5} m^3/s is shown in Figure 3.5, where the absorbing solvent is propylene carbonate.

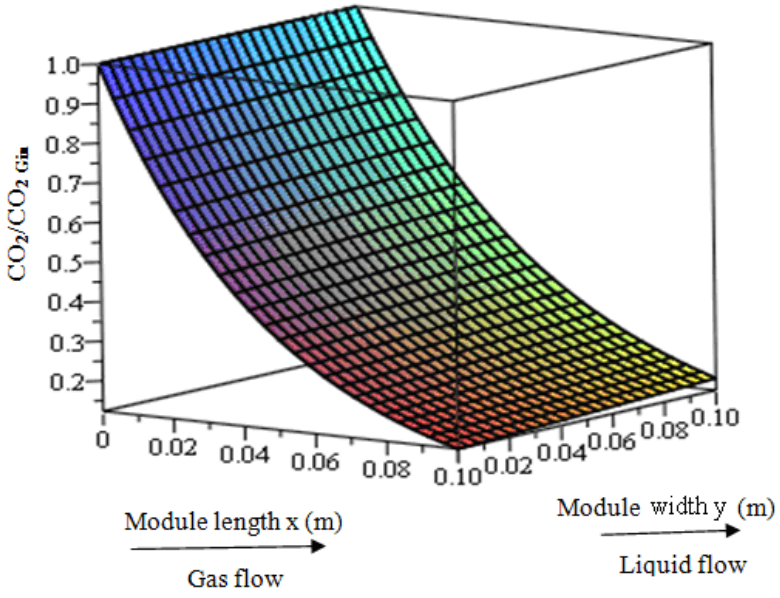

Figure 3.5: Fibre side concentration profile of CO_2 in dual membrane module for constant inlet gas flow rate of 2.66×10^{-5} m^3/s and liquid flow rate of 7.8×10^{-5} m^3/s

Figure 3.5 shows CO_2 concentration decreases along the fibre side. Compared to that at solvent exit, CO_2 concentration at the solvent entrance is lower. This is due to large driving force at the solvent entrance where feed gas first meets the clean unloaded liquid. However, at liquid outlet, solvent is partially loaded and driving force is therefore decreased, which results in higher CO_2 concentration in feed gas.

To illustrate the advantage of dual membrane module over ordinary single membrane module, absorption of CO_2 using propylene carbonate as absorbent with different liquid velocities were compared in Figure 3.6. The CO_2 concentration in feed gas is assumed to be $39.33 mol/m^3$. In both cases, the CO_2 outlet concentration drops dramatically as liquid velocity increases due to decreasing mass transfer resistance and higher driving force. Through low to high liquid velocities, the gas phase CO_2 concentration in dual membrane

module is always lower than that of single membrane module. At liquid velocity of 0.005m/s, CO_2 absorption in dual membrane module is much higher than that of single membrane. This is mainly because the partial regeneration of solvent can maintain the concentration gradient across the porous membrane. The difference gradually diminishes as liquid velocity increases. As more liquid passes through the module, more CO_2 is absorbed in less contacting time, which meanwhile minimizes the impact of solvent regeneration and therefore results in lower CO_2 concentration in nonporous fibres. Additionally, CO_2 concentration in liquid phase in dual membrane module is also found much lower compared to that in single membrane module, which again approves the regeneration function of nonporous membrane.

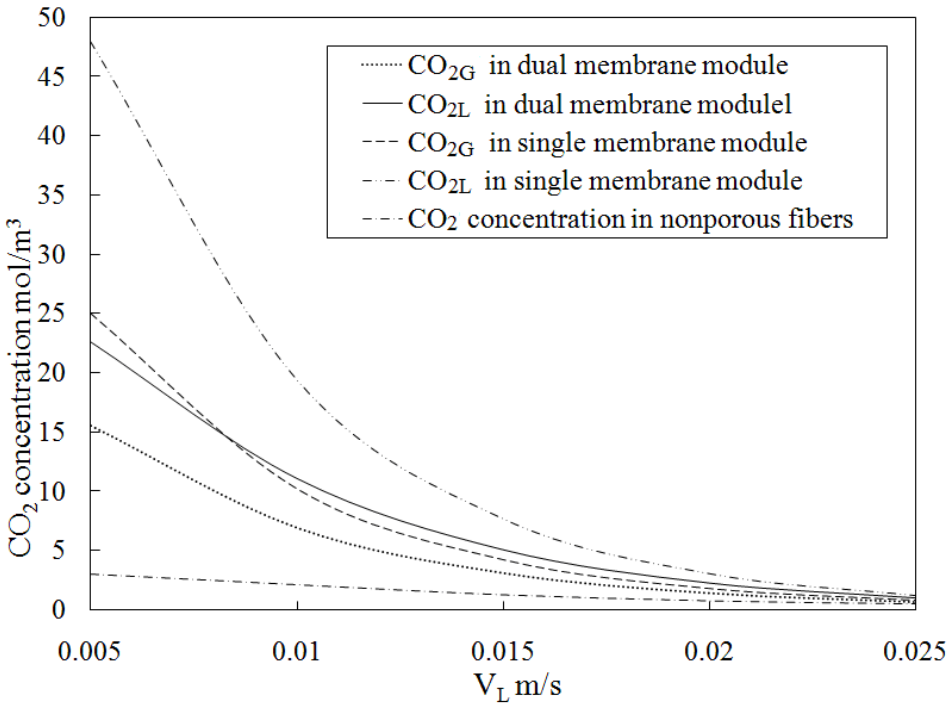

Figure 3.6: Absorption of 39.33 mol/m^3 CO_2 absorption under different liquid velocity for constant inlet gas flow rate of 2.66×10^{-5} m^3/s

To further demonstrate the impact of partial regeneration of solvent on absorption efficiency, the performance of dual membrane module (shown in Figure 1(a)) is compared with cascading of two modules shown in Figure 3.7.

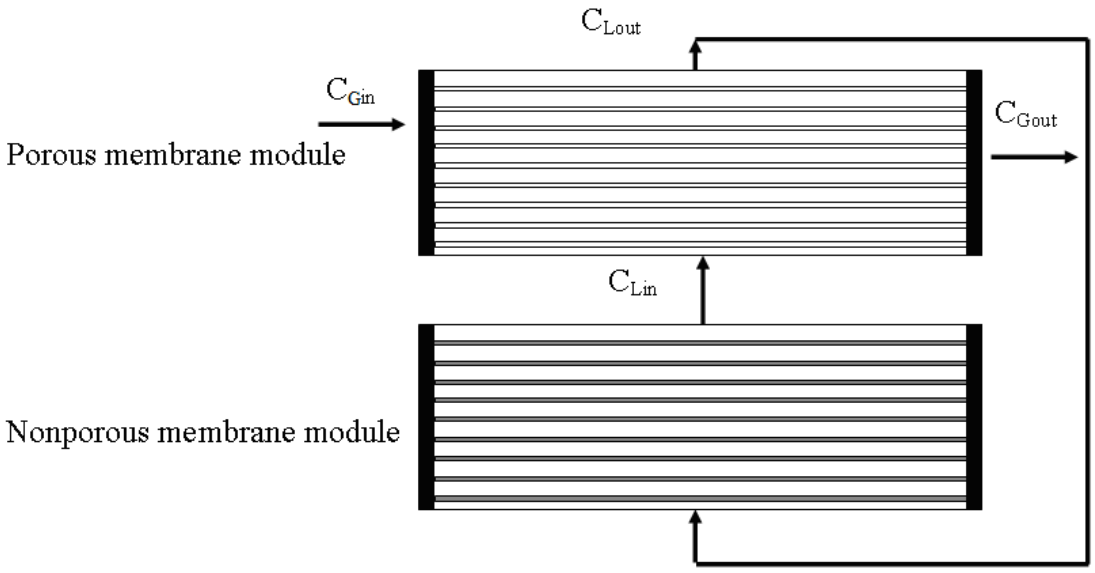

Figure 3.7: Cascading of two single membrane modules

Two single membrane modules are connected as absorber and desorber, respectively. Both absorber and desorber have the same packing fraction as dual membrane module. In each single module, fluids are in cross flow mode. The solvent coming from porous membrane module is loaded with CO_2, which can be partially stripped through nonporous membrane in nonporous membrane module. An inlet concentration of 117.99 mole/m^3 is studied when liquid flow rate is $5\times10^{-6}m^3/s$ and gas flow rate is $2.66\times10^{-5}m^3/s$. Table 3.2 compares CO_2 concentration in both gas and liquid phases in the two modules.

Table 3.2: Comparison of CO_2 concentration change in two circulating module and dual membrane module

CO_2 Concentration (mol/m^3)	C_{Gout}	C_{Lout}	C_{SNP}	CO_2 Recovery **%**
Two units module	59.49	30.63	4.16	49.45
Dual membrane module	38.53	59.49	7.84	67.34

Dual membrane module receives lower CO_2 concentration at gas outlet and higher recovery ratio compared to cascading module, due to the partial regeneration of solvent through nonporous membrane during absorption process.

Finally baffles were introduced to investigate dual membrane module performance. Similar to Module I, Module II introduces two baffles in lumen side, evenly dividing the module into three segments, as shown in Figure 3.2(b). The baffles are 0.075m in length. The liquid enters the first segment and flows across the bundle of fibres and then enters into the second segment. The baffles can also provide mechanical support for the fibres, especially when shell side flow passes the fibres in a high flow rate.

Figure 3.8 compared performance of two dual membrane modules and ordinary single membrane module under different liquid flow rates. The removal efficiency of dual membrane contactor and conventional membrane contactor were measured in terms of recovery rate in the current study. It is defined as the ratio of the quantity of target gas

component removed from gas mixture versus the original total quantity of the target gas found in feed stream. Inlet CO_2 concentrations were varied accordingly to keep gas/absorbent ratio constant. It can be noticed that, the CO_2 absorbed in two dual membrane modules is higher compared to ordinary single membrane module as previously mentioned. Low pressure in the nonporous membrane can partially regenerate the solvent during the absorption and result in a better gas removal efficiency. At liquid flow rate of 2×10^{-6} m^3/s, absorption recovery in dual membrane module without baffles is higher than that of single membrane module by 15%. CO_2 recovery in the baffled module is approximately around 70%, which mainly due to better mixing and larger residence time.

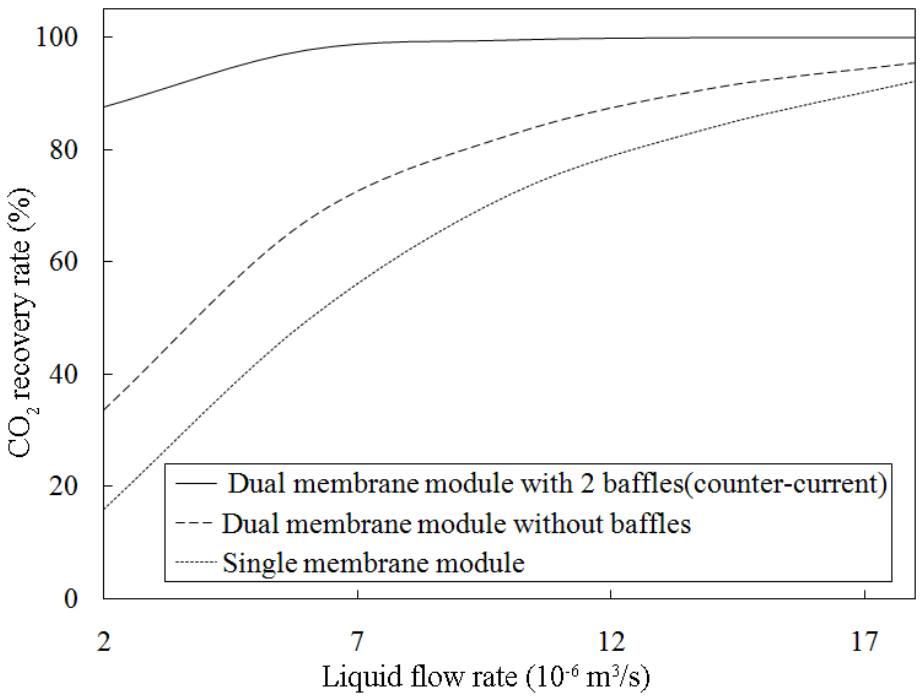

Figure 3.8: CO_2 rovery under different liquid flow rates in different modules for constant inlet gas flow rate of 2.66×10^{-5} m^3/s

Gas flow rate is an important parameter of each membrane module as it determines contacting time of gas and liquid phases. Figure 3.9 compares the dual membrane modules to ordinary membrane module under different gas flow rates when liquid flow rates keeps constant at $1\times10^{-5}m^3/s$. The figure reveals that CO_2 absorption in all three modules decreases as gas flow rates increasing due to shorter contact time. Dual membrane module along with single membrane module show an exponential decreasing trend as gas flow rate increases while baffled module shows logarithmic decreasing trend. This difference is mainly due to the existence of baffles which can prolong the liquid travel path and extends contacting time between gas and liquid phase. Through all gas flow rates, dual membrane module show higher CO_2 recovery ratio compared to single membrane module. The impact of other parameters as Henry's constant and vaccum were studied and reported in previous work of dual flat membrane modules (Wang et al., 2006)

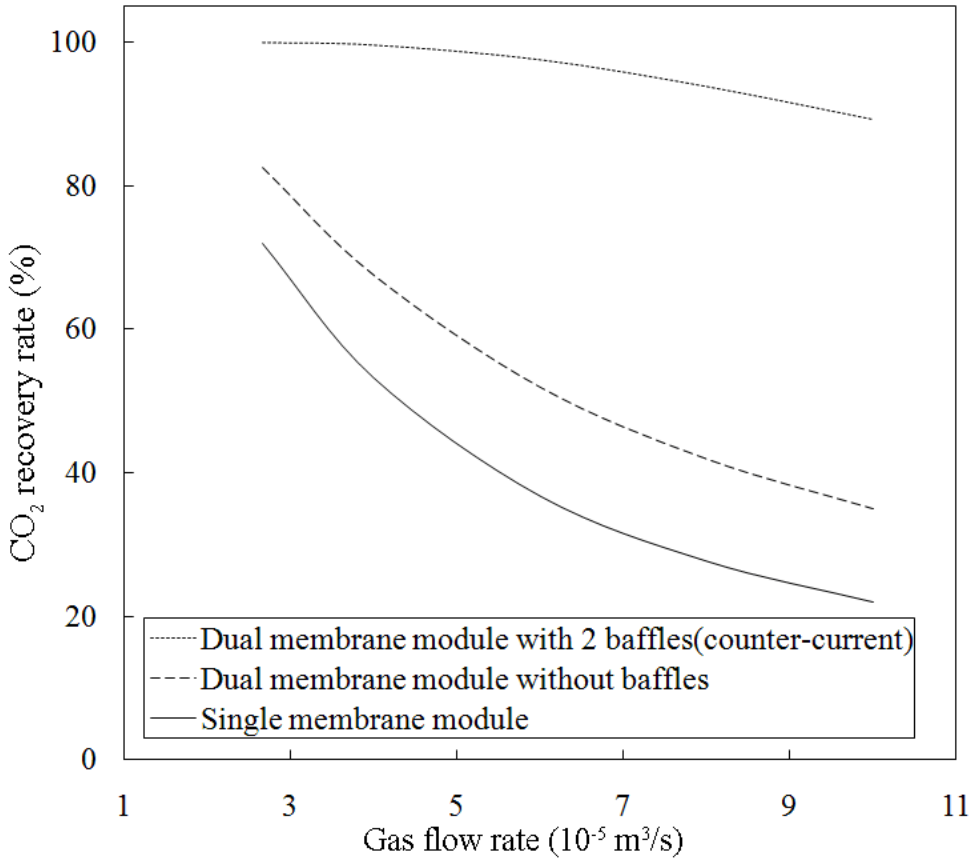

Figure 3.9: CO_2 recovery rate under different gas flow rates for constant inlet liquid flow rate of 1×10^{-5} m^3/s

3.4.3 The effect of packing fraction of membranes

The packing fraction of membranes is an important parameter in membrane modules. Figure 3.10 outlines the CO_2 absorption as a function of packing fractions of porous membranes over total membranes in the module. The total number of hollow fibres was kept constant at 9800 and the number of porous membrane fibres was varied from 0 to 9800. By increasing the porous membrane fibres, the absorption efficiency can be

improved due to increasing mass transfer area between gas phase and liquid phase. However, the increase in CO_2 absorption percentage flattens when the packing fraction of porous membrane is approximately around 65%, which also illustrates the regeneration function of nonporous membrane.

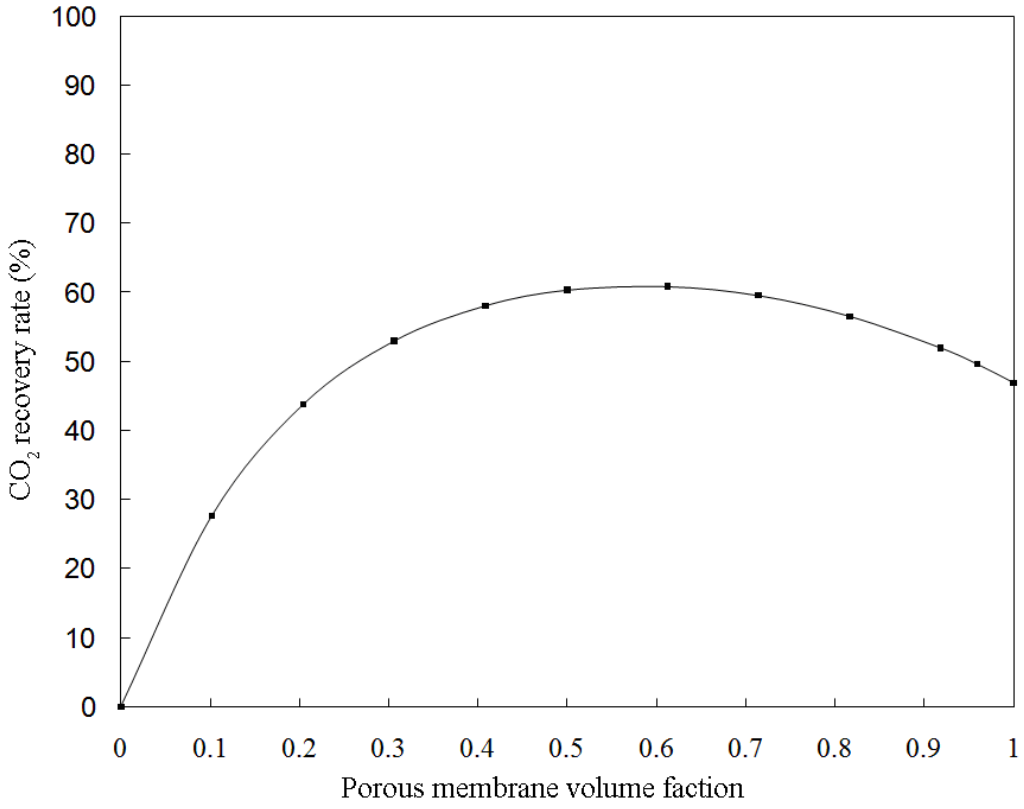

Figure 3.10: Absorption of CO_2 in modules with different porous membrane volumes ($Q_L=5\times10^{-6}m^3/s$, $Q_G=2.66\times10^{-5}m^3/s$)

3.5 Conclusion

Two configurations of hollow fibre membrane absorption-stripping systems were proposed with their performance were numerically studied. Based on the analysis presented in this chapter, it can be concluded that the nonporous membranes in the dual HFMC can partially regenerate the solvent during the absorption and result in a better overall gas removal efficiency. Consequently, it can reduce the required solvent flow rate to achieve the same CO_2 removal level. In addition, the baffles can increase the mass transfer by providing better mixing and longer residence time of the liquid phase. Of course, this must be balanced against the size and cost of the contactor. To predict removal efficiency of proposed modules, a numerical model based on mass balance was also developed in this study and it showed good agreement with previous experiment al results (Dindore et al., 2005).

All analysis and results shown in this chapter are based on mathematical models. The supporting experiments are carried out with experimental results presented in the following chapters. The liquid velocity was assumed to be constant through the module, which is not the case in practice. Therefore, fluid dynamics of liquid flow in shell side and its impacts on mass transfer coefficients is also included in the following chapters.

References

Zhang, Q., Cussler, E.L., Microporous hollow fibres for gas absorption II. mass transfer across the membrane, Journal of Membrane Science, 23 (1985), 333-345

Baker, R.W., Roman, I.C., Lonsdale, H.K., Liquid membranes for the production of oxygen-enriched air I. Introduction and passive liquid membranes, Journal of Membrane Science,31 (1987), 15-29

Bessarabov, D.G., Teplyakov, V.V. Beckman, I.N., Selective membrane valve for ternary gas mixture separation: model of mass transfer and experimental test, Industrial & Engineering Chemistry Research, 32 (1993), 2017-2022

Coelhoso, M., Cardoso, M.M., Viegas, R.M.C., Crespo, J.P.S.G., Transport mechanism and modeling in liquid membrane contactors, Separation and Purification Technology 19(2000), 183-197

Dindore, V.Y., Brilman, D.W.F., Versteeg, G. F., Hollow fibre membrane contactor as a gas–liquid model contactor, Chemical Engineering Science, 60 (2005), 467-479

Dindore, V.Y., Brilman, G. F.,Versteeg, D. W. F., Modelling of cross-flow membrane contactors: physical mass transfer processes, Journal of Membrane Science, 251 (2005), 209-222

Dindore, V.Y., Versteeg, G.F., Gas-liquid mass transfer in a cross-flow hollow fibre module: Analytical model and experimental validation, International Journal of Heat Mass Transfer 48 (2005), 3352-3362

Falk-Pedersen, O., Dannström, H., Separation of carbon dioxide from offshore gas turbine exhaust, Energy Conversion Management, 38 (1997), S81-S86

Hoffman, A., Theoretical solution for cross-flow heat exchanger, Heat Mass Transfer 36(2000), 127-133

Hughes, R.D., Mahoney J.A., Steigelmann, E.F., Olefin separation by facilitated transport membranes, Recent Developments in Separation Science, CRC Press, Cleveland, 1986

Jansen, A.E., Klaassen, R., Feron, P.H.M., Hanemaaijer, J.H., Meulen, B.P., Membrane gas absorption processes in environmental applications in Membrane Processes in Separation and Purification, Kluwer Academic Publishers, Dordrecht, 1994

Johnson, B.M., Baker, R.W., Matson, S.L., Smith, K.L., Roman, I.C., Tuttle, M.E., Lonsdale, H.K., Liquid membranes for the production of oxygen-enriched air II. Facilitated-transport membranes, Journal of Membrane Science, 31 (1987), 31-67

Kimura, S.G., Walment, G.F., Fuel gas purification with perm-selective membranes. Separation Science Technology, 15(1980), 1115-1133

Kosaraju, P., Kowali, A. S., Korikov, A., Sirkar, K., Hollow fibre membrane contactor based CO_2 absorption-stripping using novel solvents and membranes, 44(5) (2005), 1250-1258

Kreulen, H., Versteeg, G.F., Smolders, C.A., Swaaij W.P.M.V, Determination of mass transfer rates in wetted and non-wetted microporous membranes, Chem. Eng. Sci., 48(11) (1993), 2093-2102

Kreulen, H., Smolders, C.A., Versteeg, G.F., Swaaij, W.P.M.V., Microporous hollow-fibre membrane modules as gas–liquid contactors: 1. Physical mass transfer processes—a specific application: mass transfer in highly viscous liquids. Journal of Membrane Science, 78(1993) (3), 197–216

Kreulen, H., Smolders, C.A., Versteeg, G.F.,Swaaij, W.P.M.V., Selective removal of H2S from sour gas with microporous membranes, Part II. A liquid membrane of water free tertiary amines, Journal of Membrane Science, 82 (1993) 185-197

Leveque, J., Les lois de la transmission de chaleur par convection. Annls. Mines, Paris (12) (1928), 201

Majumdar, S., Guha, A. K., Sirkar, K. K., A new liquid membrane technique for gas separation, AIChE Journal, 34(1988), 1135-1145

Mataon, S.L., Lopez, J., Quinn, J.A., Separation of Gases with Synthetic Membranes, Chemical Engineering Science, 38(1983), 503-524

Mavroudi, M., Kaldis, S.P., Sakellaropoulos, G.P., Mass and momentum transfer in hollow fibre blood oxygenators, Journal of Membrane Science, 272 (2006), 103–115

Poddar, T.K., Majumdar S., Sirkar, K.K., Membrane-based Absorption of VOCs from a Gas Stream, AIChE Journal, 42(11) (1996), 3267-3282

Semmens, M.J., D.M. Foster and E.L. Cussler, Ammonia removal from water using microporous hollow fibres, Journal of Membrane Science, 51 (1990), 127-140

Teramoto, M., Matsuyama, H., Yamashiro, T., Katayama, Y., Separation of ethylene from ethane by supported liquid membranes contained silver nitrate as a carrier, Journal of Chemical Engineering of Japan., 19(5) (1986), 419-424

Teramoto, M., Matsuyama, H., Yamashiro, T., Okamoto, S., Separation of ethylene from ethane by a flowing liquid membrane using silver nitrate as a carrier, Journal of Membrane Science, 45(1989), 115-136

Wang, K. L., Cussler, E.L., Baffled membrane modules made with hollow fibre fabric, J. Membr. Sci. 85(1993), 265-278

Wang, S.Y., Hawboldt, K., Abdi, M.A., Novel dual-membrane gas-liquid contactors: modeling and concept analysis, Industrial & Engineering Chemistry Research 45 (2006), 782-789

Wickramasinghe, S.R., Garcia, J.D., Han, B., Mass and momentum transfer in hollow fibre blood oxygenators, Journal of Membrane Science, 208 (2002), 247–256

Wickramasinghe, S.R., Semmens, M. J., Cussler, E.L., Mass transfer in various hollow fibre geometries. Journal of Membrane Science, 69(1992), 235-250

Zhang, Q., Cussler, E.L., Microporous hollow fibres for gas absorption II. mass transfer across the membrane, Journal of Membrane Science, 23 (1985), 333-345

Zhang, Q., Cussler, E.L., Microporous hollow fibres for gas absorption I. mass transfer in the liquid, Journal of Membrane Science, 23 (1985), 321-332

Chapter 4

EXPERIMENTAL STUDY OF GAS ABSORPTION USING DUAL MEMBRANE CONTACTOR

This chapter is based on and modified based on the following paper

Cai, **J.J.,** Hawboldt, K., Majid, A., Improving gas absorption efficiency using a novel dual membrane contactor. *Journal of membrane science*, 510(2016), 249-258

By introducing “dual membrane concept” into the design of membrane contactor for offshore gas treatment, higher gas absorption can be achieved in a more compact membrane module with smaller footprint. The performance of the proposed dual membrane module for gas absorption has been numerically studied in Chapter 3. Our focus in this chapter is on the assessment and optimization of the absorption performance of dual membrane contactors through experimental approach. Section 4.1 reviews the experimental study of dual membrane module used for various applications. Section 4.2 presents details of a lab scale dual membrane contactor containing two types of membranes (polypropylene membrane and silicone rubber membrane) which is designed and constructed for gas absorption process. In Section 4.3, the module performance was evaluated based on permeation flux experiments for CO_2 absorption. The experimental results were compared with the predictions from a numerical model developed in our previous studies. Furthermore, the mass transfer resistance in the fabricated module was investigated using resistance-in-series model. An empirical correlation was developed to describe mass transfer coefficient under different operational conditions.

4.1 Background

As mentioned previously in Chapter 3.1, one option to minimize equipment footprint is to use two types of membranes in the same module where one membrane type functions in absorption and the other in solvent regeneration or a dual-membrane module (DMM). The dual membrane concept was first proposed and tested for H_2/CO_2 separation which allowed bulk CO_2 to be removed simultaneously with bulk H_2 recovery (Ohno et al.,

1977). Two types of membranes with different permeability for specific gases were included in the same module. A novel dual membrane reactor was designed with one tubular porous ceramic membrane as a reactant distributor and a second tubular porous ceramic membrane as a membrane separator (Chen et al., 2011). The experimental results showed that the dual membrane system can achieve ultrafine catalysts separation and product selectivity enhancement simultaneously. A few researchers have also explored the potential of dual membrane system for different applications used for reactors (Chen et al., 2014; Chen et al., 2016; Godinia et al., 2013). However, there are limited studies on improving gas absorption performance using a dual membrane system. Obuskovic et al. (Obuskovic et al., 1998) investigated the potential of dual membrane systems for VOC (volatile organic compounds) removal. Two sets of hollow fibres membranes were used in the same module, the gas to be treated was fed to the fibre side of microporous polypropylene membrane while a second set of silicone coated fibres were used as a desorber. The shell side was filled with a non-circulating liquid absorbent. Since the liquid phase in shell side was in a non-flowing mode, the system was operated in a semi-continuous mode, which required long operating time to achieve high treatment efficiencies. A parallel flow membrane system was proposed as a more compact design (Wang et al., 2006). In this system gas absorption and solvent regeneration were simulated with two types of flat sheet membrane: porous polypropylene membrane and nonporous silicone rubber membrane. The simulation showed good potential in terms of overall size reduction and gas removal efficiency. This study was further extended by proposing a cross flow dual membrane module which was composed of hollow fibre

membrane as hollow fibre membrane offers a larger interfacial area per volume than flat sheet membrane (Cai et al., 2012). The performance of this dual membrane module was evaluated through modelling approach. The result showed that gas removal efficiency of the dual membrane system was 38% higher than conventional system that uses two units in series to perform gas absorption and stripping separately. This is mainly because the simultaneous regeneration of solvent along with absorption process can help the driving force responsible for mass transfer maintain at a high level (Cai et al., 2012). Nonetheless, all these results were based on numerical modeling and needs to be further confirmed through experiments.

Therefore, the objective of this chapter is to develop a dual membrane system and conduct experiments to investigate its performance. A dual membrane system is fabricated that combines the adsorption and solvent regeneration into one unit, further decreasing the equipment footprint. The following issues will be addressed in this chapter:

1. Fabrication of a dual hollow fibre membrane contactor module;
2. Evaluation of the module performance for simultaneous absorption and stripping;
3. Development of an empirical mass transfer correlation for the system;
4. Validation of the mathematical model;
5. Optimization of the absorption process by studying the effect of operation conditions, assisted with simulation results.

In these experiments, CO_2 was removed using physical absorption as the solvents used for physical absorption generally are more compatible with porous membranes (Dindore et al., 2004).

4.2 Experiments

4.2.1 Fabrication and assembly of lab scale dual membrane contactor

The membrane core contains two type of fibre membranes, polypropylene (PP) fibre (for gas flows into system) and silicone rubber tubing (for partial regeneration of solvent). PP membranes have sufficiently low surface energy, are inexpensive, and commercially available in small diameters (Dindore et al., 2004). Silicone rubber is attractive in degassing of a liquid as there is no issue related to membrane wetting, therefore, the pressure on permeate side can be arbitrarily chosen. Ito et al. validated the feasibility to strip dissolved oxygen from water using silicone hollow fibre membranes (Ito et al., 1998). However, this material has not been applied to other gases such as CO_2 or H_2S. Compared to oxygen, the permeability of CO_2 through silicone rubber fibres is much higher. The porous PP fibre (Q3/2 membrane) purchased from Membrana GmbH has an outside diameter of 1,000 μm and inside diameter of 600 μm and a maximum pore size of 0.64 μm. Silicone rubber tubing from Dow company has outside diameter of 900 μm and inside diameter of 500 μm. The fibres were first trimmed into the same length and then potted into supporting plates at both ends (Shown in Figure 4.1). The supporting plate was made of polyvinyl chloride (PVC) and drilled through with 1.02 mm holes, arranged in a staggered pattern (Show in Figure.4.1 (a)). The use of supporting plate assures the

uniformity distribution of membrane in membrane core. Porous and nonporous fibres were then woven through the supporting plates and layered alternately. Liquid epoxy resin was applied afterwards to fix fibres to supporting plates. In this process, care must be taken to avoid damaging the membrane surface as porous membrane fibres tend to break easily. The finished membrane core was then built into a PVC housing in which the transparent PVC made it possible to observe the liquid flow in shell side. The shell housing was purposely made in a rectangular geometry instead of cylindrical geometry. As for the cylindrical module, the cross-sectional area for flow varies along the path, causing the average velocity to alternately increase and decrease. In contrast, the flow area is constant in modules with rectangular designs, which can simplify the modelling. The impact of module geometries is discussed with more details in the following chapters. As it is shown in Figure.4.1 (b), separate inlets and outlets were designed for gas absorption and stripping in the module, respectively.

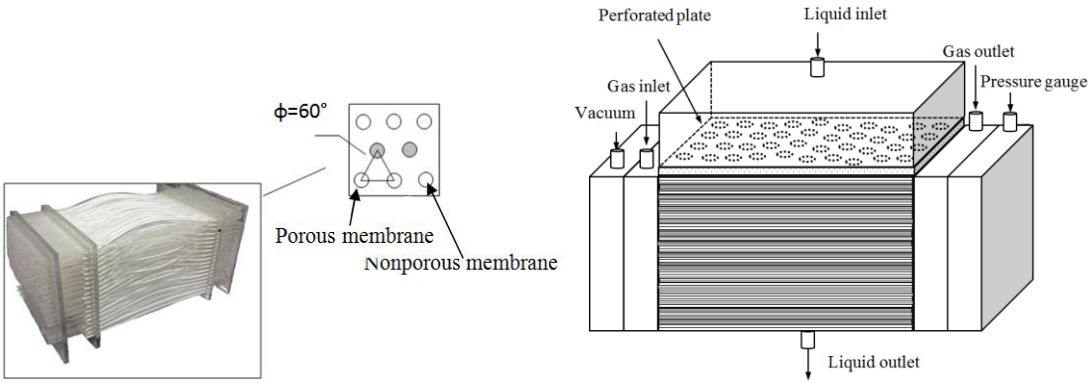

(a) (b)

Figure 4.1(a): Schematic drawing of membrane core and arrangement of dual hollow fibre membranes in lab scale module; (b) Schematic drawing of dual membrane contactor

The specification of the module is shown in Table 4.1.

Table 4.1: Specification of lab scale dual membrane module

Module length (mm)	123
Length of membrane core (mm)	103
Width of module (mm)	80
Height of module (mm)	80
Area (porous membrane)	0.18
Area (nonporous membrane)	0.18
Number of porous fiber	556
Number of nonporous fiber	285
Packing voidage of fiber bundle	0.85

4.2.2 Experimental set-up

The experimental set-up to evaluate the performance of dual membrane contactor is shown in Figure. 4.2. CO_2 was used as the targeted component to be removed from a gas stream of CO_2/N_2 mixture. Solvents tested included distilled water and propylene carbonate (purchased from Sigma- Aldrich).

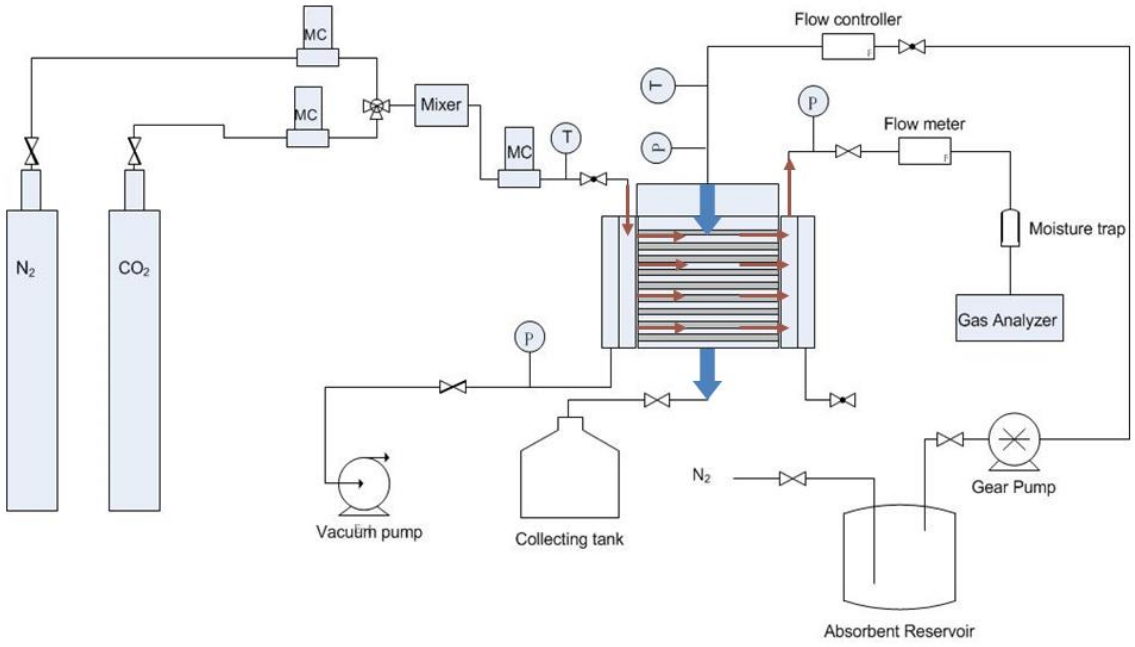

Figure 4.2: Experimental set-up for CO_2 absorption in dual membrane contactor

In all experiments, the liquid phase was continuously fed into the shell side through a gear pressure pump and liquid flow rate was controlled by a digital mass flow controller. At this stage, the solvent was operated under once-through operation during the absorption whereas the circulating mode will be discussed in the future work. All digital mass controller and flow meters used in this experiment were calibrated using rotameters before use. To ensure the absorption performance, the absorbent was degassed before use with N_2. The inlet temperature and pressure of the liquid phase were monitored throughout the experiments. To avoid gas bubbling, the pressure on the liquid side was always slightly higher than that of gas phase. The N_2 and CO_2 are premixed and the mixed gas temperature, pressure and flowrate were monitored using a high-precision mass flow controller (purchased from Alpha Controls with Model No. MFC-50LPM-D). Depending on the experimental specifications, either sweeping gas or vacuum can be

used for gas stripping in the nonporous fibre. Figure 4.2 is an example of operation with vacuum being applied. N_2 was used at a constant flow rate of 5LPM. In the case where the vacuum was applied, a vacuum pump was connected to the nonporous fibre side. The pressure was measured using a PM930SD pressure indicator (Cole-Parmer) and controlled using a high precision needle valve. Membrane wetting may occur during operation when pressure in the gas flow is insufficient therefore the mixed gas was introduced into the fibre side before liquid was introduced into the shell side. The pressure difference between the two phases was monitored in all experiments. The CO_2 was measured through portable Oxybaby®6.0 CO_2 gas analyzer at gas inlet and outlet. The average CO_2 concentration in liquid was estimated via overall mass balance. The details of experimental conditions are given in Table 4.2.

Table 4.2: Experimental conditions for test conducted in the research presented in this chapter

CO_2%	CO_2 (mol/m^3)	Operation mode (In nonporous fibres)	Sweeping Gas (flow rate 4L/min)	Vacuum (kpa below gauge)
5	2.04	No degassing	-	-
5	2.04	Sweeping gas	N_2	-
5	2.04	vacuum	-	2-30
2.5	1.02	Sweeping gas	N_2	-
30	12.26	Sweeping gas	N_2	-

4.3 Mathematical model for dual membrane module

The unique characteristic of dual membrane contactor requires modification of current HFMC models. A numerical model was developed for this type of HFMC to model the module performance with details described in Chapter 3. The overall mass balance for the liquid phase and gas phase are outlined in Eq. 4.1 and 4.2.

$$\frac{\partial C_L}{\partial y} = \frac{4(1-\alpha_P)L_Z L_X}{d_P}\frac{k_L}{Q_L}(HC_G - C_L) - \frac{4(1-\alpha_{NP})L_Z L_X}{d_{NP}}\frac{k_L}{Q_L}(C_L - C_{SNP}) \quad \text{Eq.4.1}$$

$$\frac{\partial C_G}{\partial x} = \frac{4(1-\alpha_P)L_Z L_Y}{d_P}\frac{k_L}{Q_G}(C_L - HC_G) \quad \text{Eq. 4.2}$$

where C_G and C_L are concentrations of solute in the gas phase and liquid phase, respectively. L_X, L_Y, L_Z refers to the length, height and width of module separately. k_L represents overall mass transfer coefficient by considering mass transfer resistance in gas phase, membrane phase and liquid phase. Q_L and Q_G refer to liquid flow rate and gas flow rate, respectively; H refers to the Henry's constant; x and y refer to module dimension. C_{SNP} is the concentration of the solute at the surface of nonporous membrane; $(1-\alpha_P)$ and $(1-\alpha_{NP})$ denote the packing fractions of porous membranes and nonporous membranes in the modules; d_P and d_{NP} present diameter of porous fibre and diameter of nonporous fibre, respectively.

As liquid phase is passed through shell side from top to bottom the CO_2 concentration in liquid phase is a function of module height (y).

$$\frac{\partial C_L}{\partial y}\Big|_{x=0} = \frac{4(1-\alpha_P)L_Z L_X}{d_P}\frac{k_L}{Q_L}(HC_G - C_L\big|_{x=0}) - \frac{4(1-\alpha_{NP})L_Z L_X}{d_{NP}}\frac{k_L}{Q_L}(C_L\big|_{x=0} - C_{SNP}) \quad \text{Eq.4. 3}$$

The second boundary condition can be defined as follows as no CO_2 is present in the liquid phase at liquid inlet.

$C_L = C_{Li\ y=0}$ at liquid inlet

Similarly in the gas phase, CO_2 concentration only changes with the module length (x). At the liquid entrance where y is equal to zero,

$$\frac{\partial C_G}{\partial x}\Big|_{y=0} = \frac{4(1-\alpha_P)L_Z L_Y}{d_P}\frac{k_L}{Q_G}(C_L - HC_G\Big|_{y=0}) \qquad \text{Eq. 4.4}$$

At gas inlet

$C_G = C_{Gi}$, at x=0 Eq. 4.5

By solving the above two partial differential equations simultaneously the CO_2 concentration in both liquid phase and gas phase can be predicted at any position in the module.

4.4 Results

4.4.1 Correlation for mass transfer coefficient in shell side

Compared to modules containing only porous or nonporous membrane, mass transfer in dual membrane module is more complex. For the purpose of module design and operation optimization, it is critical to generate a correlation to predict mass transfer coefficient for different operational conditions. For modules operated with liquid in shell side flowing across beds of gas filled hollow fibres, mass transfer coefficient mainly depends on liquid

flow and module geometry (Yang et al., 1986). Several empirical correlations have been developed for crossflow modules, which contain porous or porous membrane only (Yang et al., 1986; Wang et al., 1993; Wickramasinghe et al., 1993).

Therefore, a correlation was developed based on experimental results using the fabricated module. The overall mass transfer coefficient accounts for mass transfer resistance in gas phase, membrane phase and liquid phase, which can be calculated through experimental results using the following function by varying liquid flow rates:

$$K = \frac{Q_G}{A} \ln\left(\frac{C_L - HC_{Gi}}{C_L - HC_{Ge}}\right) \qquad \text{Eq. 4.6}$$

This equation was derived from Eq. 4.2 by assuming that the concentration in gas phase only varies with fiber length.

The mass transfer coefficient from experiments is incorporated into Sherwood number and plotted against liquid velocity, as shown in Figure 4.3. Sherwood number is calculated using Eq. 4.7 while shell side velocity can be expressed as Reynolds number, written in Eq. 4.7:

$$Sh = \frac{Kd_h}{D} \qquad \text{Eq.4. 7}$$

Where D is diffusivity coefficient of solute in the solvent; d_h is the hydraulic diameter. In loosely packed module with fibre beds, d_h represents the outer diameter of the fibre (for module with void fraction greater than 0.5) (Hewitt et al., 1998).

$$\mathrm{Re} = \frac{d_h \cdot u}{v} \qquad \text{Eq.4. 8}$$

Where *Re* is Reynolds number, *v* stands for kinematic viscosity of solvent and *u* represents effective velocity passing through fibre bundles, which can be calculated through dividing superficial velocity by void fraction (Hewitt et al., 1998).

The experiment was conducted using the fabricated module for CO_2 absorption where water is used as solvent. The feed gas contained 5% CO_2 and was passed through the tube side at a constant flow rate of 1.63 L/min. A sweep gas of N_2 flowed through the nonporous fibres at a flowrate of 4 L/min. The CO_2 concentration in the gas outlet was read off through gas analyzer while CO_2 concentration in liquid phase was determined by titration using 0.4M sodium hydroxide. Phenolphthalein was used as the indicator for the titration. The mass transfer coefficient, Sherwood number (*Sh*) and Reynolds number were then calculated accordingly using the known data of feed flow and module dimensions. Results for the calculated Reynolds number and Sherwood number are summarized in Table 4.3.

Table 4.3: Experimentally data and calculated Reynolds number and Sherwood number

Water flow rate Q_L($\times 10^{-6} m^3/s$)	Reynolds number	Sherwood number
1.08	0.15	3.52
2.00	0.32	5.15
2.9	0.42	5.9
3.91	0.63	7.27

6.66	1.08	9.5
9.3	1.52	11.34
10	1.63	11.75
15	2.44	14.46
19.1	3.12	16.3

A commonly used form of empirical correlation for the *Sh* is shown in Eq.4.9 (Gabelman et al., 1999):

$$Sh = \alpha Re \beta Sc^{0.33} \qquad \text{Eq. 4.9}$$

Where α and β are constants determined by fitting experimental results. The Schmidt (*Sc*) number is calculated by dividing the viscosity of the solvent by the diffusion coefficient (of solute in solvent). Based on our experimental data the correlation reduces to:

$$Sh = 0.78\,\mathrm{Re}^{0.5226} Sc^{0.33} \qquad \text{Eq. 4.10}$$

As it is shown in Figure 4.3, this correlation relates with the experimental results very well. Figure 4.3 compares the proposed correlation to another two correlations developed for porous membrane contactor and nonporous membrane contactor, respectively. These two correlations were both applicable for the range of Reynolds number examined in the present study. As presented, Sherwood number based on the current study falls in the range between two other correlations found in literature (Cote et al., 1989; Yang et al., 1993) confirming that these equations are not accurate and the new correlation is required for this dual membrane system.

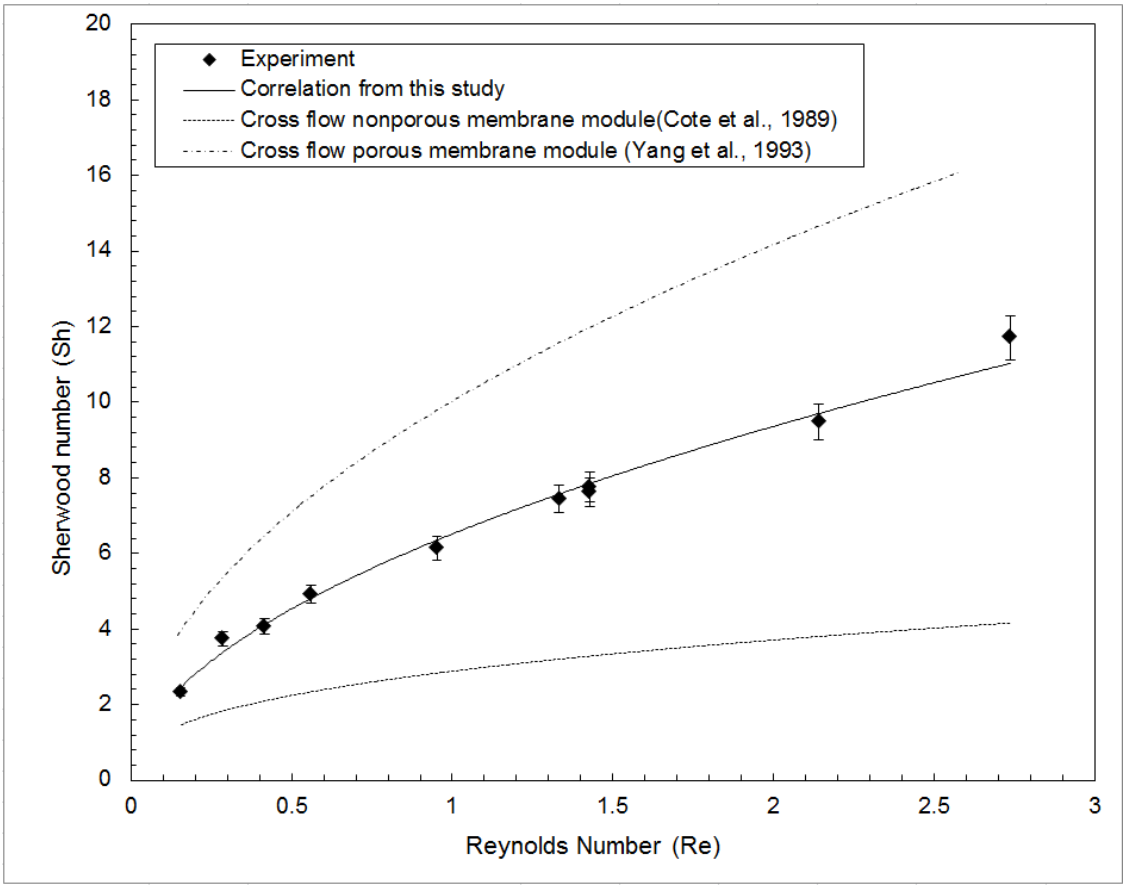

Figure 4.3: Comparison of mass transfer correlations developed for different membrane contactors

The literature correlations (Cote et al., 1989; Yang et al., 1986) for both porous and nonporous membrane modules were developed based on the assumption that the mass transfer resistance lies mainly in liquid phase. The main difference is in nonporous membrane module, that membrane resistance also needs to be accounted for. Therefore, same assumption was made in the current study. To test the assumption, a resistance-in-series model was used to describe the mass transfer (Cussler et al., 1994).

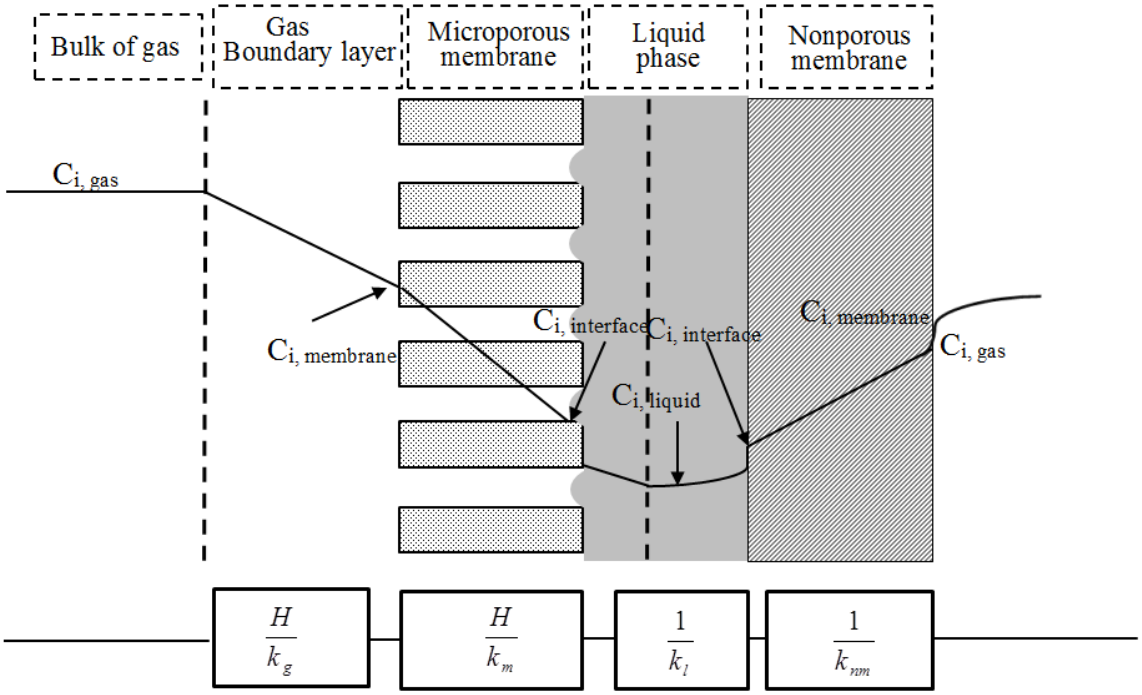

Figure 4.4 Mass transfer regions and resistance-in-series in non-wetted dual membrane contactor

Figure 4.4 depicts the mass transport of the interested gas for non-wetted mode of operation of dual membrane contactors, i.e., diffusion from the bulk gas through the membrane pores, dissolution in the liquid absorbent and stripping of dissolved contaminant from solvent. The mass transfer resistance (R_{Total}) of the above mentioned mass transfer process is mainly contributed by four parts: gas phase, liquid phase, porous membrane and nonporous membrane, as described in Eq. 4.11:

$$R_{Total} = R_g + R_{PM} + R_l + R_{NM} \qquad \text{Eq. 4.11}$$

where R_g, R_{PM}, R_l, R_{NM} represent mass transfer resistances from gas phase, porous membrane, liquid phase and nonporous membrane, respectively.

It can also be converted to a function of mass transfer coefficient, as shown in Eq. 4.12.

$$\frac{1}{K} = \frac{1}{k_g \cdot H} + \frac{1}{k_m \cdot H} + \frac{1}{k_{nm}} + \frac{1}{k_l} \qquad \text{Eq.4.12}$$

Where K and H refers to the overall mass transfer coefficient and Henry's constant separately; k_g, k_m, k_l, k_{nm} are mass transfer coefficient through gas phase, porous membrane, liquid phase and nonporous membrane respectively. The mass transfer resistance through nonporous membrane can be calculated in the following equation (Bessarabov et al., 1996; Atchariyawut et al., 2008):

$$\frac{1}{k_m} = \frac{l_{NP}}{P \cdot H} \qquad \text{Eq. 4.13}$$

Where P is the polymer permeability and l is the thickness of the nonporous membrane layer.

The Wilson plot (Atchariyawut et al., 2008), which was originally used to analyse heat transfer resistance has been used in membrane mass transfer resistance in gas–liquid membrane contacting processes. As shown in Eq. 4.10, the mass transfer coefficient can be expressed as a function of velocity:

$$\frac{1}{K} \propto \frac{1}{v^{0.5226}} \qquad \text{Eq. 4.14}$$

The plot $1/K$ versus $1/v^{0.5226}$ give a straight line as shown in Figure 4.5, where the fitting function has a R squared value greater than 0.99. The intercept corresponds to when $1/K_L$ is zero and represents the resistance from nonporous membrane. Therefore, the interception of the plot represents the resistance in nonporous membrane. Based on our

experimental results, the mass transfer resistance in the nonporous membrane contributes 7% of the overall mass transfer resistance in the range of Reynolds numbers studied (0.1-2.5), whereas in a typical nonporous membrane module, the nonporous membrane resistance is 32-73% (Bessarabov et al., 1993). The membrane resistance in this study can be further reduced by using nonporous membrane with higher permeability and thinner walls.

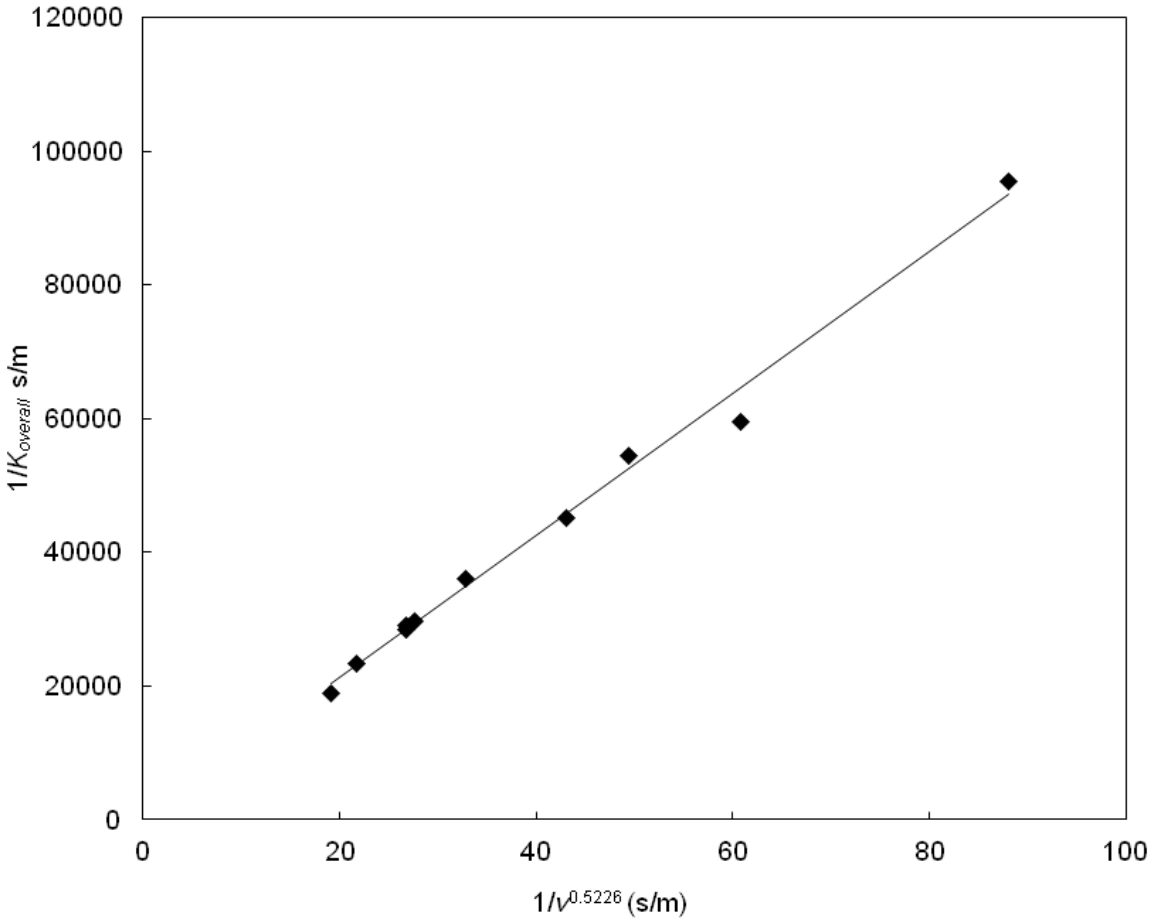

Figure 4.5: Wilson's plot for the proposed module

The relationship between Sherwood number and Reynolds number is a strong function of shell side flow and module geometry, which however should be independent of solvent selections and operation mode on the permeate side. To further confirm this assumption, experiments were carried out in this study by replacing water with propylene carbonate as solvent. Meanwhile, low vacuum was applied on the permeated side instead of sweeping gas with the vacuum pressure was maintained below 2kPa. The Sherwood number derived based on experimental results were compared against those calculated from the proposed correlation in the parity plot shown in Figure 4.6. It demonstrates that the proposed correlation can be used to predict the fibre side mass transfer coefficient in case of organic solvents. Moreover, it confirms that the Sherwood number indeed depends mainly on the module geometry of membrane contactor and independent of operation condition on permeation side.

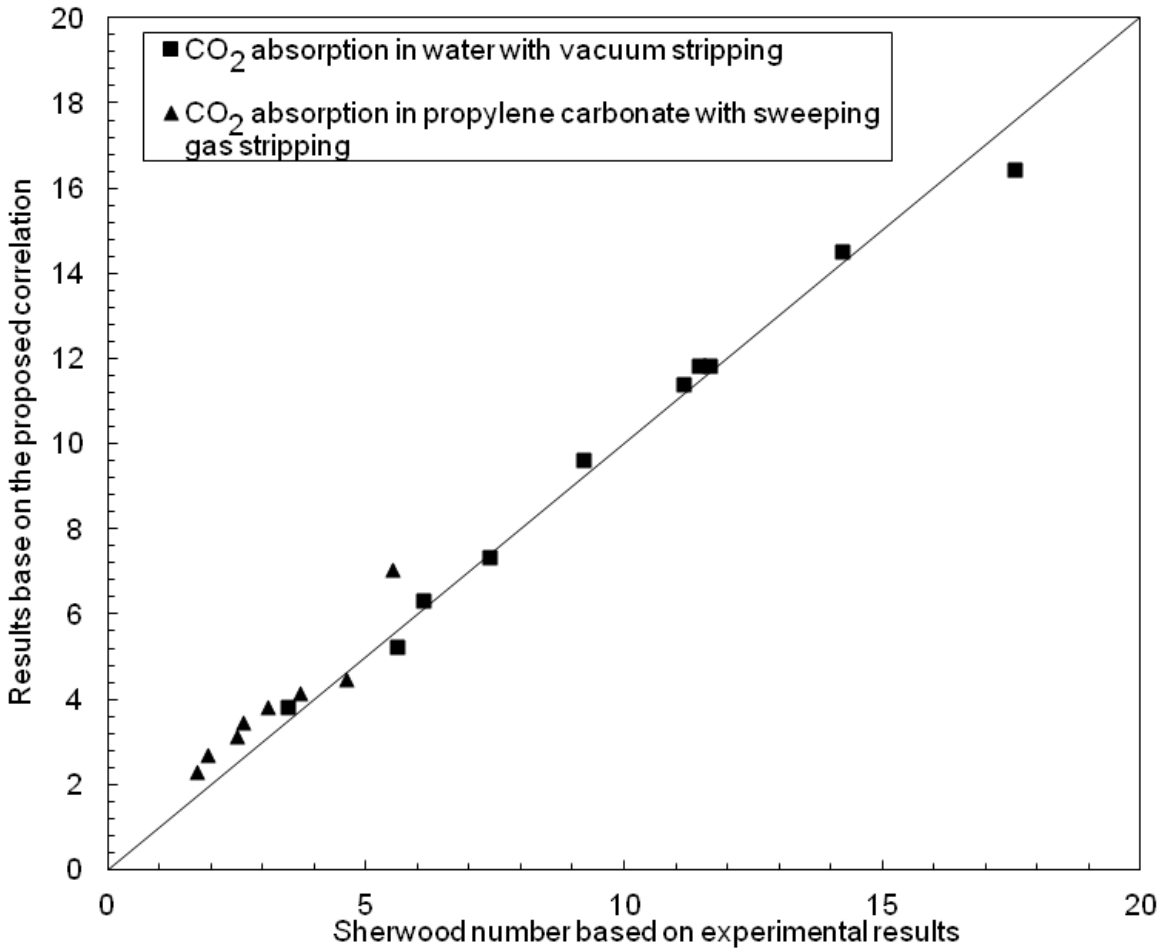

Figure 4.6 Parity plots of Sherwood number obtained for different operation conditions

Figure 4.7 compares mass transfer coefficients when two different solvent, water and propylene carbonate, were used and also demonstrates the effect of liquid flow rate on mass transfer. All the parameters and physical constants used in this study for calculation are given in Table 4.4.

Table 4.4: The parameters used in the model

Parameter	Value (Data for 298K)	Reference
Water		
Density (ρ)	995 kg/m^3	Ref. (Vargaftik, 1987)
Dynamic viscosity (v)	1×10^{-6} kg/(m s)	Ref. (Vargaftik, 1987)
Henry's constant (H)	0.82 (C_L/C_G) (at equilibrium)	Ref. (Vargaftik, 1987)
Diffusivity (D)	2×10^{-9} m^2/s	Ref. (Vargaftik, 1987)
Propylene carbonate		
Density (ρ)	1,210 kg/m^3	Ref. (Vargaftik, 1987)
Viscosity (v)	2.5×10^{-6} kg/(m s)	Ref. (Vargaftik, 1987)
Henry's constant (H)	3.5(C_L/C_G) (at equilibrium)	Ref. (Vargaftik, 1987)
Diffusivity (D)	1.35×10^{-9} m^2/s	Ref. (Vargaftik, 1987)

As it is shown in Figure 4.7, increasing in shell side velocity enhances mass transfer in both water and propylene carbonate. These results are consistent with the experimental results obtained from conventional membrane contactors operated with solvent in fibre side (Dindore et al., 2004). The mass transfer coefficient in the case of propylene carbonate is smaller than that of water. This is not unexpected as propylene carbonate is more viscous than water, resulting in a lower Reynolds and subsequently Sherwood number for the same liquid flow rate.

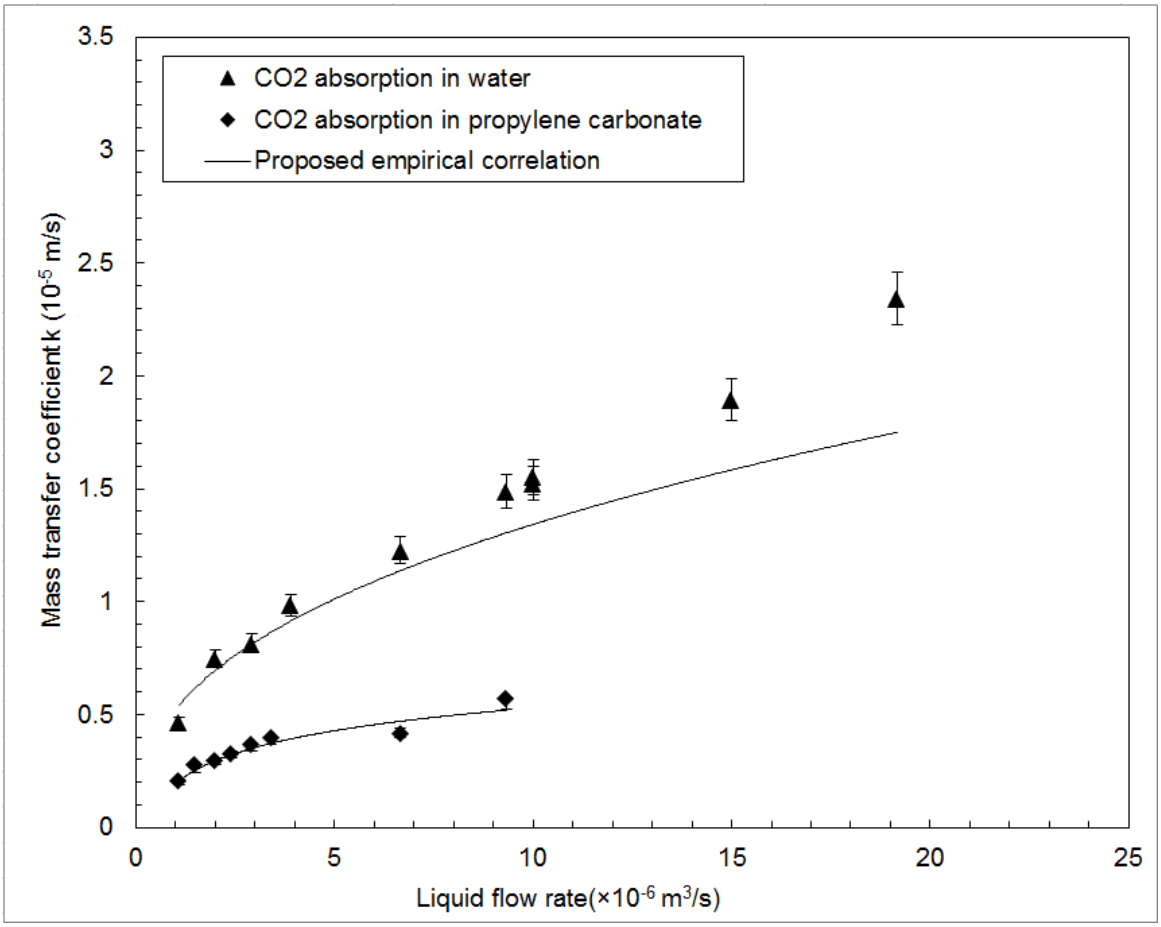

Figure 4.7 Mass transfer coefficient of dual hollow fibre membrane contactor for both solvents tested

4.4.2 The effect of liquid flow rate on mass transfer

The effect of operational conditions on module performance was investigated in the absorption of a dilute gas mixture in which CO_2 concentration in feed gas was maintained at or below 5%. Absorption of concentrated gas and the effect of solute concentration on module performance were also studied in the following section. In these experiments, a feed gas containing 5% CO_2 was passed through porous fibres at a constant flow rate of

1.63 L/min while pure N_2 was passed through the non-porous fibres at a flow rate of 4 L/min. Through all testing, temperature was kept constant at 25℃ under atmospheric pressure. The average CO_2 concentration at gas outlet and liquid outlet under different liquid flow rates were measured and presented in Figure 4.8. In general, CO_2 concentration in both gas phase and liquid phase decreases as liquid velocity increases. This further confirms that the mass transfer strongly relies on the shell side flow. Better module performance is achieved as liquid flow rate increases. The predictions from the proposed model were in a good agreement with experimental results in both phases. Concentration in liquid phase from model is slightly higher than that from experiments, which likely due to experimental error caused by titration (±3%).

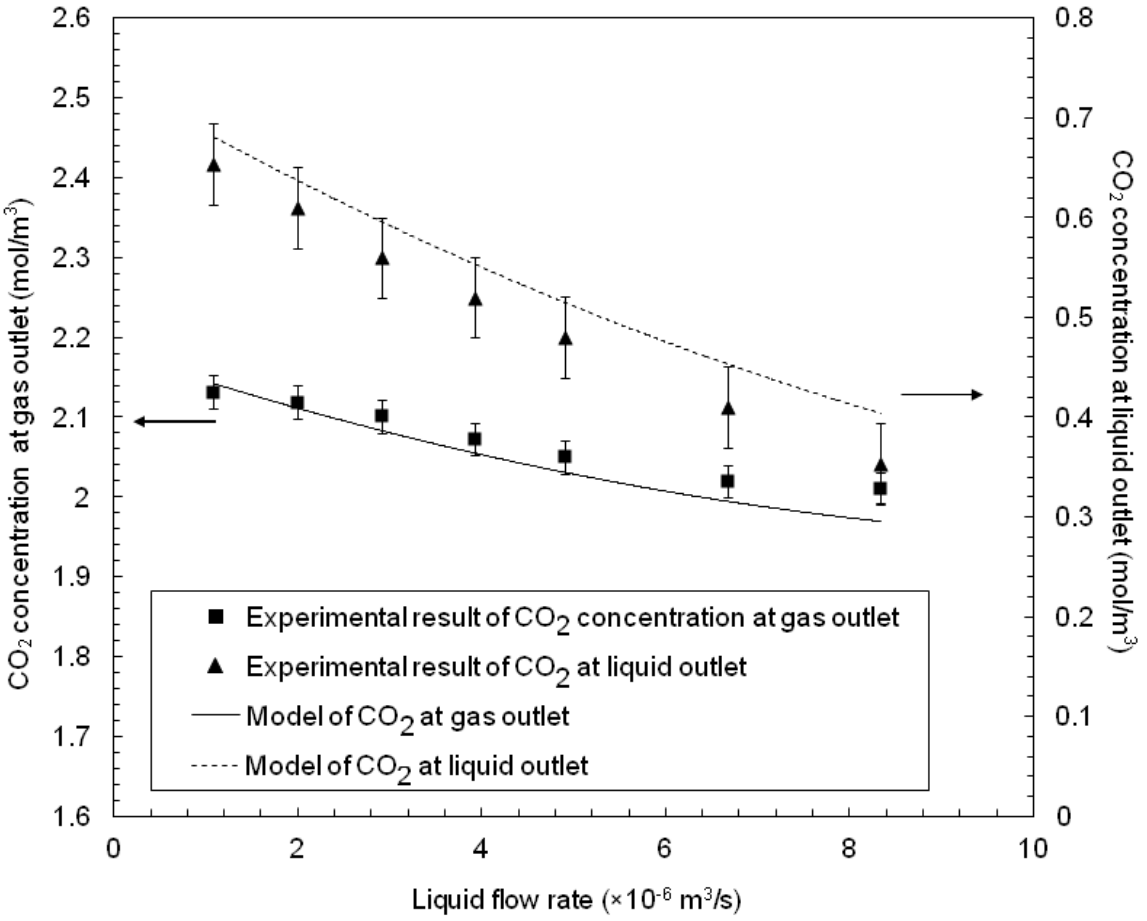

Figure 4.8 : CO2 (5%) absorption in dual membrane module with sweeping gas degassing

Parallel tests were also carried out with a vacuum pressured supplied in nonporous fibres. The vacuum pressure on permeated side was maintained slightly lower than atmospheric pressure (5 kPa). Model predictions and experimental results mirrored the results with the sweep gas and therefore are not included here. The impact of vacuum pressure on the tests results will be discussed later in this paper. Absorption flux is an indicator of process efficiency, i.e., high flux correlates to high efficiency. Absorption flux was estimated by making an overall mass balance on the contactor:

$$J_{average} = \frac{(C_{Gi}Q_{Gi} - C_{Ge}Q_{Ge})}{A} \quad \text{Eq. 4.15}$$

Where J is the molar flux (mol/m^2 s); A (m^2) effective interfacial area; C_{Gi} and C_{Ge} are the volumetric concentration of CO_2 in the feed and outlet streams, respectively. Q_{Gi} and Q_{Ge} (m^3/s) are volumetric flow rate measured at gas inlet and outlet. Figure 4.9 illustrates the effect of liquid flow rate on absorption flux under different operationalconditions. The absorption of dilute feed gas containing 5% CO_2 was firstly investigated, in which water was used as absorbent. In one set of experiments, the module was operated in a no solvent regeneration mode, that is no sweep gas or vacuum was applied to the non-porous fibres. Comparing to the absorption flux with gas stripping on permeate side, the impact of simultaneous gas stripping along with absorption placed on overall absorption flux can be determined. The absorption flux is well predicted by the numerical modelling. In general, absorption flux is enhanced as liquid flow rate increases. With a sweep gas in nonporous fibres, the absorption flux is found higher, compared to the non-regeneration mode. This is not unexpected due to the higher mass transfer coefficients resulted from high shell side flow. Meanwhile, the presence of sweep gas/vacuum further enlarges the differential partial pressure across nonporous membrane. As a result, there is enhanced permeation of the dissolved CO_2 in the liquid phase to permeate side through the nonporous membrane. It is worth mentioning that since the experiment was carried out at a relatively high gas flow rate of 1.63L/min, the overall removal efficiency is below 15%. The impact of gas flow rates on removal efficiency was further examined in the following sections.

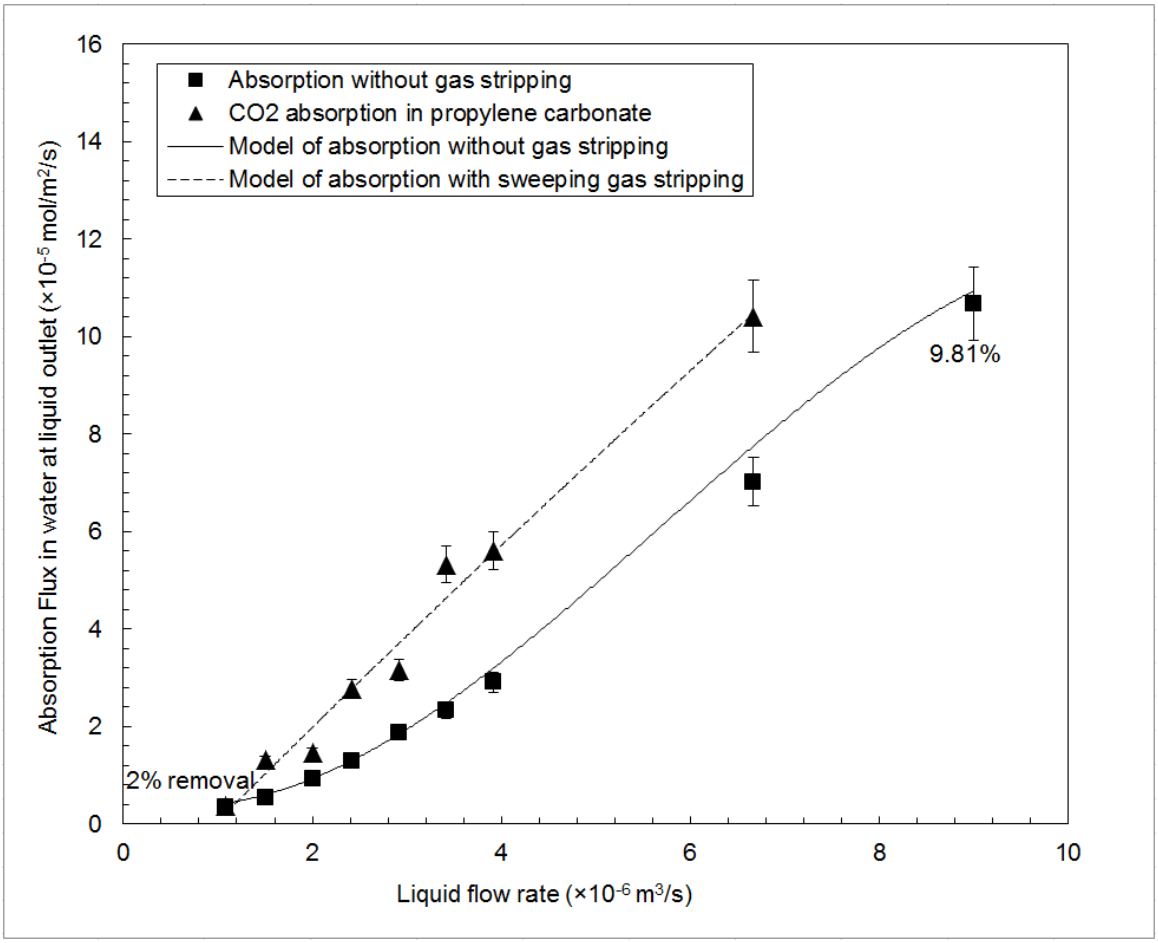

Figure 4.9 : Effect of liquid flow rate on absorption flux

Another set of experiments were carried out with the same operational conditions but replacing water with propylene carbonate to examine the effect of solvent regeneration on absorption flux. Figure 4.10 compares the experimental data and modelled results of absorption flux. Overall, higher absorption flux was achieved when propylene carbonate was used rather than water, due to higher solubility of CO_2 in propylene carbonate than water. However, the effect of sweep gas stripping on overall absorption is not as pronounced as in the experiments using water. This can be explained by the higher affinity of propylene carbonate for CO_2, which makes it difficult for CO_2 to be stripped

out of the liquid phase. The improvement in module performance through solvent regeneration is not as significant as that in water. Absorption with a vacuum instead of a sweep gas was also tested in which the vacuum pressure was maintained at 2kPa. Equivalent results were obtained without much difference in terms of absorption flux.

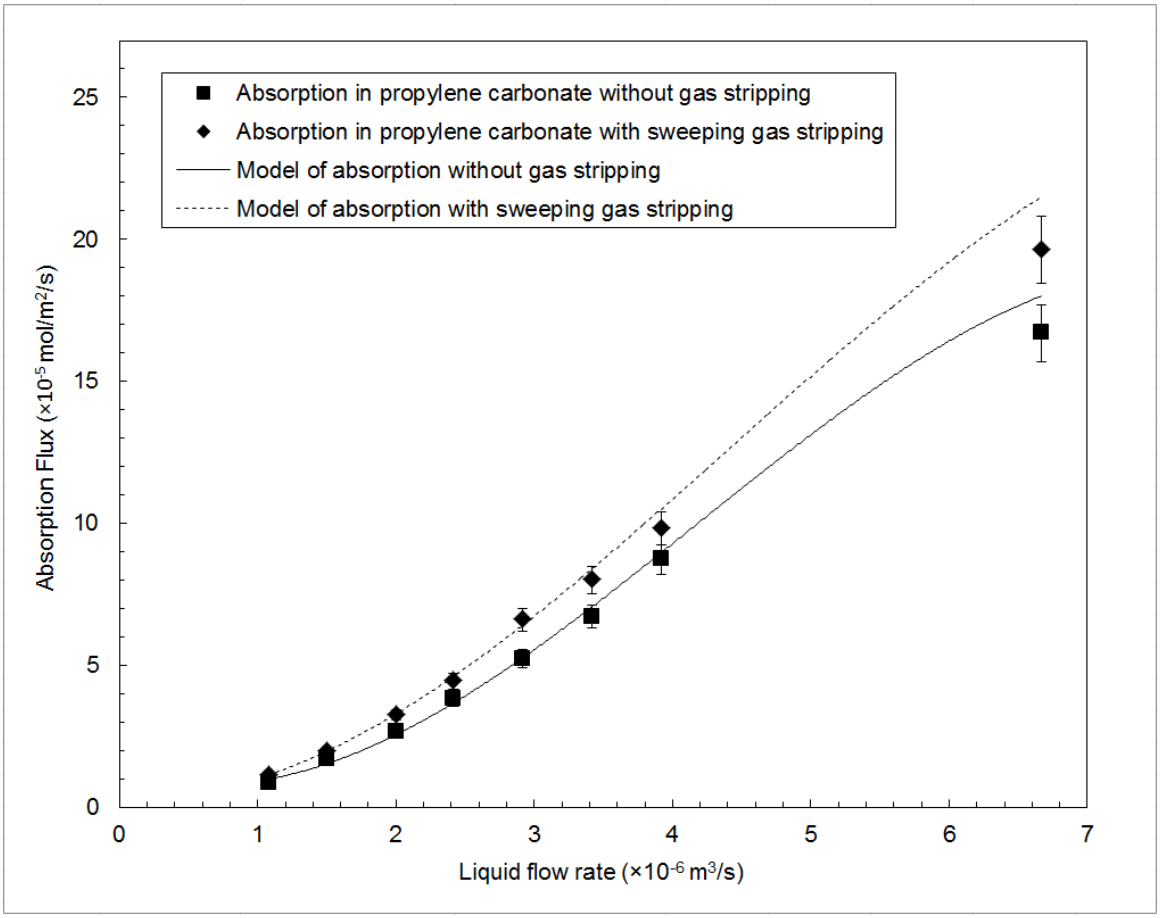

Figure 4.10: Effect of liquid flow rate on absorption flux using propylene carbonate as solvent

4.4.3 The effect of gas flow rate

The effect of gas flow rate on absorption flux is summarized in Figure 4.11. The experiments were carried out using water as absorbent at a constant flow rate of $2\times10^{-6}m^3/s$. A sweep gas of N_2 was passed through nonporous fibres at a flow rate of 4L/min. For comparison purposes, parallel experiments were also conducted without sweep gas. Gas flow rates were varied from $3.7\times10^{-6}m^3/s$ to $23.3\times10^{-6}m^3/s$. The CO_2 concentration at the gas outlet decreased with increasing gas flow rate while the absorption flux almost stays constant. This further confirms that for physical absorption in liquid-gas membrane contactor, the transfer resistance lies mainly in liquid phase. The sweep gas improved flux by approximately 50%. The lower gas flow rates show better removal from the gas due to the longer gas residence time. However, it is worth mentioning that sweep gas degassing plays a more important role at higher gas flow rates. At a relatively low gas flow rate of $3.7\times10^{-6}m^3/s$, 26.9% CO_2 was removed with the sweep gas compared to 19.3% removal rate without sweep gas, which improves the overall absorption efficiency by 39%. At a higher gas flow rate of $2.3\times10^{-5}m^3/s$, total removal efficiency decreases in both cases due to reduced gas residence time in the module. By stripping the dissolved gas with sweep gas, the removal efficiency increased from 2.46% to 4.4%, improved by 78%. It implies that simultaneous degassing during absorption has a great potential in the case that operating flow rate is high.

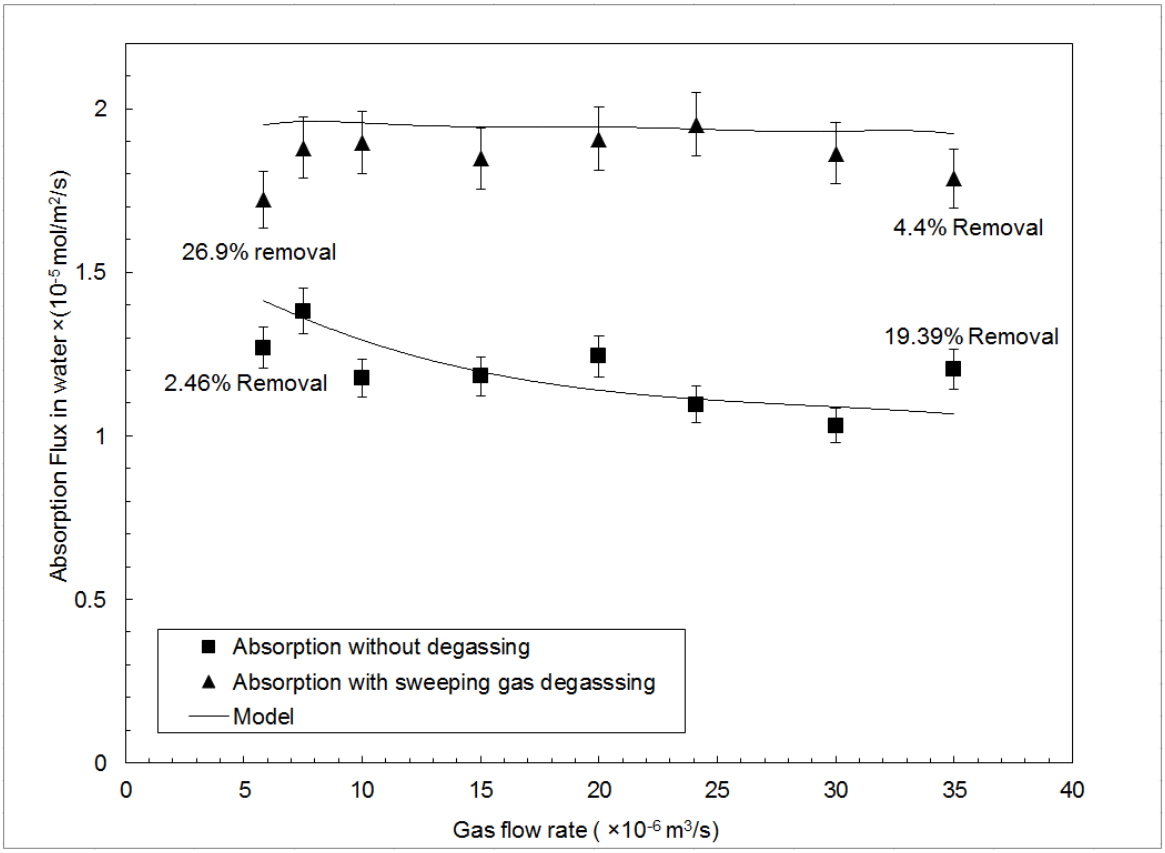

Figure 4.11: Effect of gas flow rate on absorption flux using water as solvent

4.4.4 The effect of solute concentration

When experiments were carried out at high gas flow rate using very low levels of CO_2 in the inlet gas stream, the removal rate is relatively low and therefore the volumetric gas flow rate is relatively constant. However, gas streams with high levels of CO_2 and high removal rates, the effect of a change in the volumetric flow rate of the gas stream needs to be considered. In the current study, the change in volumetric flow rate can be described using the following equation:

$$Q_G = \frac{Q_{Gi} - \frac{RT}{P} C_{Gi} Q_{Gi}}{1 - \frac{RT}{P} C_G} \qquad \text{Eq.4. 16}$$

Where Q_{Gi} is the volumetric flow rate of feed gas at inlet; C_{Gi} is the concentration at gas inlet while C_G is the CO_2 concentration any position of module; P, R, and T stand for pressure (Pascal), gas constant ($8.314 m^3 Pa/K/mol$) and temperature (K), respectively. By combining Eq. 4.16 and Eq.4.2, CO_2 concentration at gas outlet was calculated in model.

Experiments were conducted varying inlet CO_2 concentration from 2.5%, 5% and 30% under a relatively low gas flow rate of $3.7 \times 10^{-6} m^3/s$. The liquid flow rate was kept constant at 0.175 L/min. A constant flow of 4L/min N_2 was passed through nonporous fibres on the permeate side. The absorption flux from experiments is compared with the model prediction in Figure 4.12. As CO_2 concentration increases, absorption flux dramatically increases from 1.6×10^{-5} to 42×10^{-5} $mol/m^2 s$, due to the high driving force of concentration differences. The removal efficiency is also higher for the absorption of a more concentrated feed gas. As solute concentration increases, the change in gas flow rate caused by loss of solute becomes more obvious. Several models have been proposed to describe mass transfer in cross flow module, such as the heat transfer analogy (Dindore et al., 2005), however these models ignore the change in volumetric gas flow rate. As demonstrated in the figure, when this factor is not accounted, the predicted absorption flux (shown in dash line) is lower than experimental results and tends to under-predict module performance.

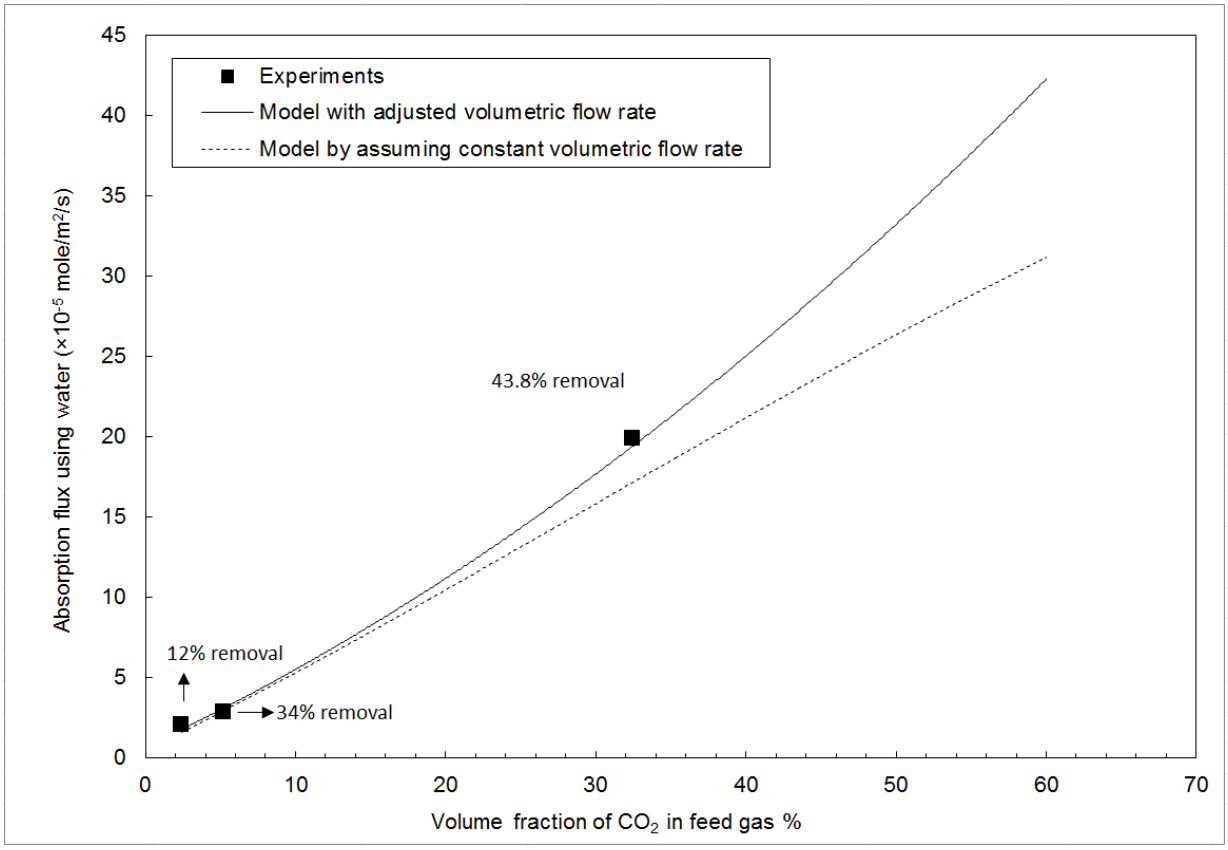

Figure 4.12: The effect of solute concentration on absorption performance

To further examine the impact of solute concentration on module performance, absorption of CO_2 using dual membrane module was compared with the module performance without solvent regeneration. CO_2 concentration in feed gas was varied from 5 to 40% while the liquid flow rate was kept constant at 0.175L/min. In one set of experiments, a flow of N_2 at 4L/min was passed through nonporous membrane and in the second set there was no vacuum or N_2 flow through the non-porous membranes (to simulate only absorption). The absorption flux obtained from these two sets of experiments was compared in Figure 4.13. Results from model were found in agreement with experimental data. Since all experiments were carried out under a high gas flow rate of 2.7×10^{-5} m^3/s,

no significant difference was observed between two operation modes when CO_2 concentration in feed gas is relatively low (>5%). As solute concentration increases, the enhancement in absorption performance due to solvent regeneration increases. This is reasonable as more CO_2 can be absorbed into liquid phase when solute concentration in feed gas is high, due to increasing driving force resulted from differential concentration across the membrane. The increasing in CO_2 concentration in liquid phase further drives more CO_2 component permeate through nonporous membrane and achieve partial regeneration of solvent. This result demonstrates the potential of dual membrane for the absorption of feed gas in which partial pressure of the target gas component is high.

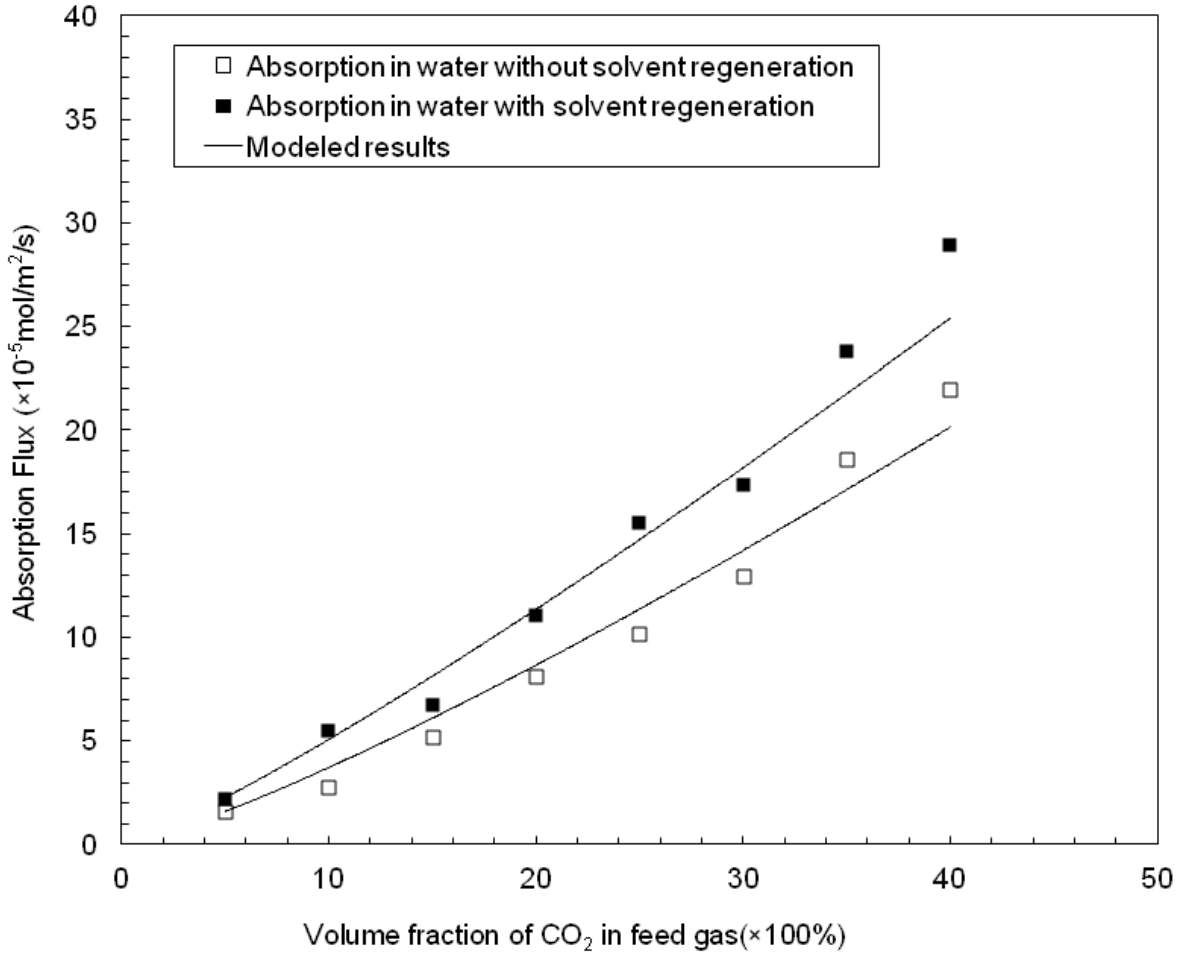

Figure 4.13: Effect of simultaneous solvent regeneration on absorption performance

4.4.5 The effect of vacuum pressure on the permeate side

Theoretically, higher fraction of CO_2 can be removed from liquid phase when the pressure on permeate side is lower as the driving force for CO_2 to permeate through nonporous membrane is the differential pressure. To maximize the absorption capacity, it is important to understand the impact of permeate side pressure on the absorption performance. Absorption of a feed gas containing 5% CO_2 was conducted using water as solvent. Gas flow rate and liquid flow rate were kept constant at $0.58 \times 10^{-5} m^3/s$. Liquid

flow rate was constant at $2\times10^{-6}m^3/s$. On the permeate side, the vacuum pressure was varied from 2 to 67 kPa.

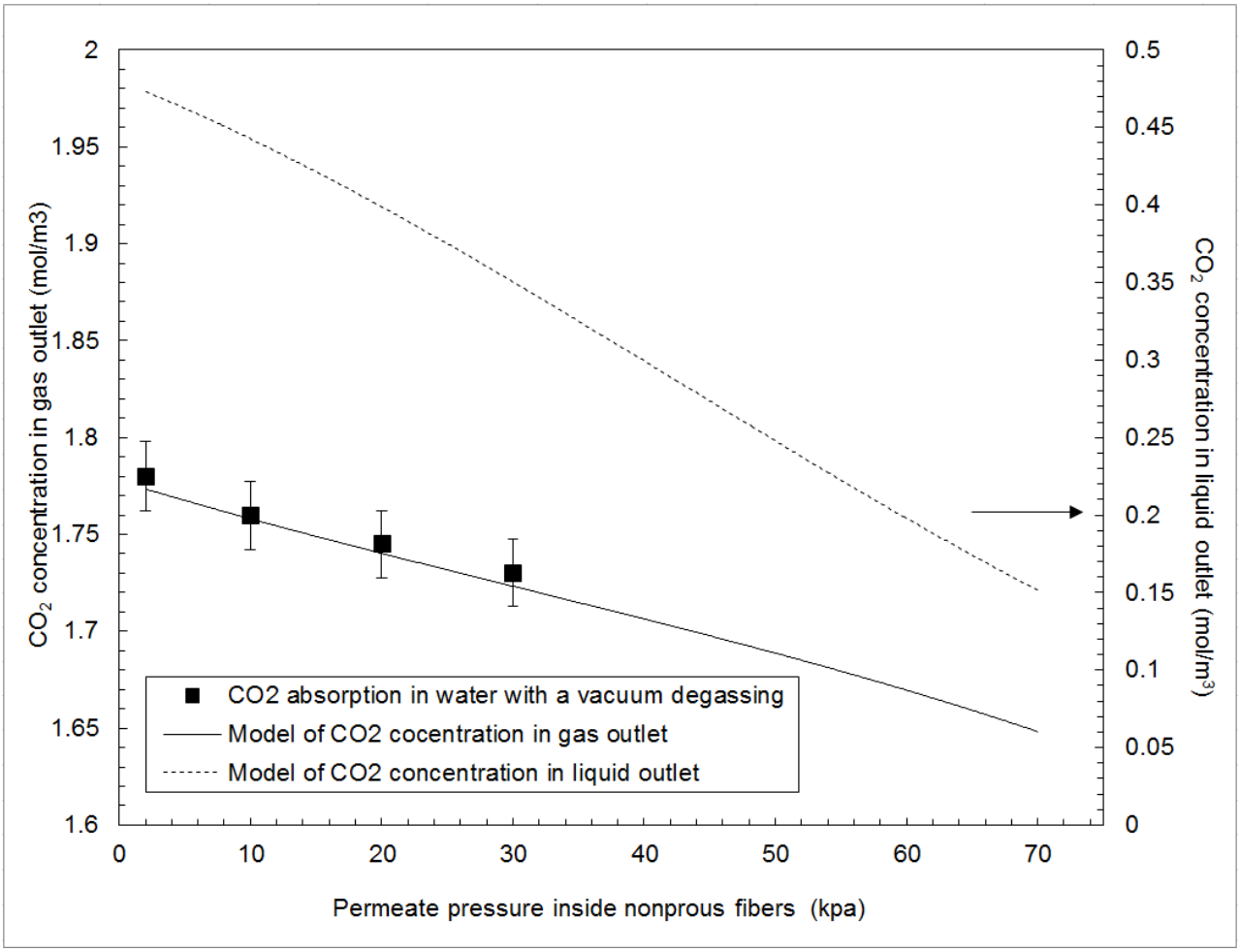

Figure 4.14: The effect of permeate side pressure to overall absorption performance

As shown in Figure 4.14, the good agreement between model and experimental results further confirms the advantage of introducing degassing along with absorption process. The CO_2 concentration in both gas phase and liquid phase decreases as higher vacuum was applied to the nonporous membranes. However, the increase in removal is small. That is, as the vacuum pressure is increased to 20kPa from 2kPa by ten times, CO_2

removal efficiency is only improved from 20% to 23.6%. The selection of appropriate pressure needs to account for the balance between energy consumption for maintaining high vacuum and removal efficiency.

4.4.6 The effect of area ratio of porous and nonporous membrane

In this type of contactor, a dual membrane, careful analysis of the ratio of one type of membrane to another is critical. For example, by increasing the porous fibres present in shell side, absorption of CO_2 into liquid phase can be enhanced but possibly at the expense of degassing due to the reduced nonporous membrane area. Given the model has been validated in the experiments; a simulation was performed where the ratio of non-porous to porous membranes was varied. Total absorption flux is compared in modules with different ratio of porous membrane area over nonporous membrane area where the total membrane area and module packing fraction were kept constant. The enhancement in absorption is also examined by comparing dual membrane module performance to the module with porous membrane only. Model results are summarized in Figure 4.15.

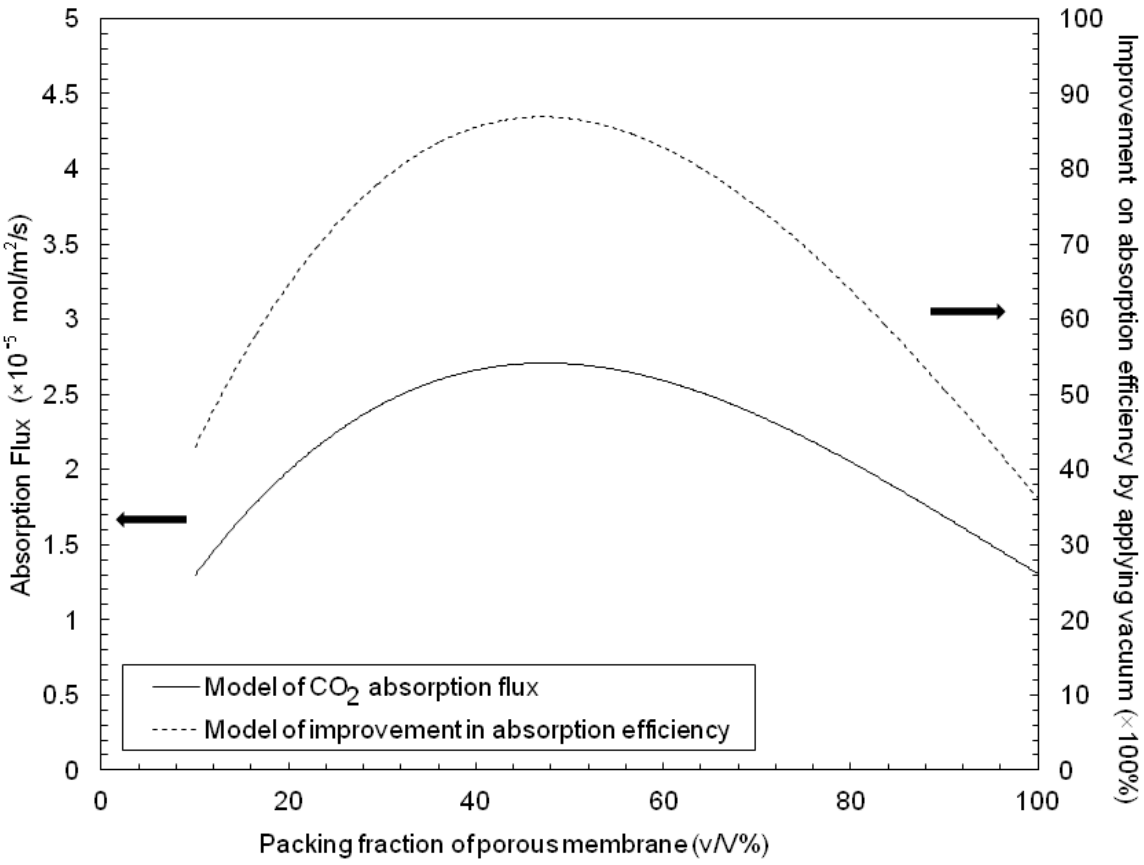

Figure 4.15: The effect of porous membrane area on absorption performance and the enhancement resulted from degassing

The ratio of porous membrane area over the total membrane area was varied from 0% to 100%. A model simulation for a feed stream containing 5% CO_2 with water as the solvent was carried out. The gas flow rate was $1.6\times10^{-5}m^3/s$ while water flow was at 0.24 L/min. The highest absorption flux occurred when porous membrane takes up 45% of the total membrane area (Shown in Figure 4.14), corresponding absorption flux 1.26×10^{-5} to $2.66\times10^{-5}mol/m^2/s$. In the case that the module is only composed of 80% porous

membrane, the removal efficiency drops to 37%. This validates our initial work present in the previous chapter in which better removal was achieved when porous and non-porous membranes were present. However the simulation also shows that there is an optimal ratio of fibres. Compared to modules operated without sweeping gas/vacuum in nonporous fibres, the enhancement in absorption efficiency is the most obvious when vacuum degassing is applied and nonporous membrane takes up to 50% of overall membrane area. This indicates that the most ideal packing ratio for porous membrane over nonporous membrane is 0.45 to 0.5This range may need to be adjusted according to the membrane material used for absorption and solvent regeneration.

4.4 Conclusion

In this work, an experimental study of a lab scale dual membrane module was carried out to investigate its performance over conventional membrane contactor and validate the numerical model developed to simulate the system. The concept of dual membrane module was first proposed by Wang et al. (Wang et al., 2006), which however has never been testified through experiment studies. In this study, a lab scale membrane contactor composed of polypropylene porous fibres and nonporous silicone rubber tubing was built and its performance was demonstrated through removal of CO_2 out from N_2/CO_2 mixed gas. Empirical correlations tailored for the proposed module was developed and the correlation was validated through experiments results. The mass transfer resistance in the designed module was also investigated using resistance in series model. The experimental results show that the resistance mainly comes from liquid film while the membrane resistance also contributes to 7% of the total resistance. Based on the results, mass

transfer coefficient was quantified through correlation for the proposed module and the experiments were then further extended to CO_2 absorption along with simultaneous degassing through nonporous membrane. Two operations were alternatively applied for degassing in nonporous membrane namely a sweep gas and a vacuum pressure. The experimental results were found in a good agreement with numerical modelling developed in previous work. In addition, it was found that by stripping dissolved CO_2 out from liquid phase through nonporous membrane, absorption on the side of porous membrane can be effectively improved. The enhancement was especially significant for the application running at high gas flow rate. High liquid flow rate and vacuum pressure are the favored conditions for the contactor to achieve maximum performance. Furthermore, the enhancement in absorption efficiency attributed by degassing was found most significant in module with 50% packing fraction of porous membrane area. This conclusion can be used for further optimization of the module. Furthermore, the proposed model is also modified in this work for absorption of concentrated gas, by accounting for the change in volumetric flow rate caused by the loss of solute. The results showed that modified model provides a more accurate prediction of module performance, particularly when CO_2% is greater than 5% in feed gas. The results were validated through experiments and it also demonstrated that higher absorption efficiency is received as solute concentration increases. It should be noted that the removal efficiencies are likely lower compared to a scaled up version of the system. This is due to the constraints introduced by the small scale module (e.g. ensuring good sealing of fibres to module, etc.), dimensions of the module (based on this work we will modify the length, height, width ratios), etc. This work served to both validate our model and to test various operational

conditions. In subsequent work presented in the following chapters, we will present the model with confidence for design optimization.

Reference

Bessarabov, D.G., Jacobs, E.P., Sanderson, R.D., Beckman, I.N., Use of nonporous polymeric flat-sheet gas-separation membranes in a membrane-liquid contactor: experimental studies, Journal of Membrane Science, 113 (1996), 275-284

Bessarabov, D.G., Teplyakov, V.V., Beckman, I.N., Selective membrane valve for ternary gas mixture separation: model of mass transfer and experimental test, Industrial & Engineering Chemistry Research, 32 (1993), 2017-2022

Cai, J.J., Hawboldt, K., Abdi, M.A., Contaminant removal from natural gas using dual hollow fibre membrane contactors, Journal of Membrane Science, 397-398 (2012), 9-16

Chen, B., Ruan, X., Jiang, X., Xiao, W., He, G., Dual-membrane module and its optimal flow pattern for H_2/CO_2 separation, Industrial & Engineering Chemistry Research, 55 (4) (2016), 1064-1075

Chen, R., Mao, H., Zhang, X., Xing, W., Fan, Y., A dual-membrane airlift reactor for cyclohexanone ammoximation over titanium silicalite, Industrial & Engineering Chemistry Research, 53 (15) (2014),6372-6379

Cote, P., Bersillon, J.L., Huyard, A., Bubble-free aeration using membranes: Mass transfer analysis, Journal of membrane science 47 (1989), 91-106

Dindore, V.Y., Brilman, D. W. F., Geuzebroek, F.H., Versteeg, G.F., Membrane-solvent

selection for CO_2 removal using membrane gas-liquid contactors, Separation Purification Technology,40 (2004), 133-145

Dindore, V.Y., Brilman, G. F.,Versteeg, D. W. F., Modelling of cross-flow membrane contactors: physical mass transfer processes, Journal of Membrane Science, 251 (2005), 209-222

Dindore, V.Y., Brilmanb, D.W.F., Feronc, P.H.M., Versteega, G.F., CO_2 absorption at elevated pressures using a hollow fibre membrane contactor, Journal of Membrane Science, 235(1-2) (2004), 99-109

Gabelman, A., Hwang, S., Hollow fibre membrane contactors, Journal of Membrane Science, 159 (1999), 61-106

Godinia, H.R., Xiao, S.M., Kima, Görkeb, O., Songa, S., Woznya, G., Dual-membrane reactor for methane oxidative coupling and dry methane reforming: Reactor integration and process intensification, Chemical Engineering and Processing: Process Intensification, (74) (2013),153-64

Hewitt, T.J., Hattler, B.G., Federspiel, W.J., A mathematical model of gas exchange in an intravenous membrane oxygenator, Annals of Biomedical Engineering, 26 (1998), 166-178

Ito, A., Yamagiwa, K., Tamura, M., Furusawa, M., Removal of dissolved oxygen using non-porous hollow-fibre membranes, Journal of Membrane Science, 145 (1) (1998),

111-117

Obuskovic, G., Poddar, T. K., Sirkar, K.K., Flow swing membrane absorption-permeation, Industrial & Engineering Chemistry Research 37 (1) (1998), 212-220

Ohno, M., Ozaki, O., Sato, H., Kimura, S., Miyauchi, T., Radioactive rare-gas separation using a separation cell with 2 kinds of membrane differing in gas permeability tendency. Journal of Nuclear Science Technology,14 (8) (1977), 589-602

S.Atchariyawut, R. Jiraratananon and R.Wong, Mass transfer study and modeling of gas–liquid membrane contacting process by multistage cascade model for CO_2 absorption, 63(1) (2008) 15-22

Sirkar, K.K., Other new membrane processes, Membrane Handbook, Chapman and Hall, New York, 1992, 885-899

Vargaftik, N. B., Handbook of Physical Properties of Liquids and Gases: Pure Substances and Mixtures, Hemisphere Publishing Corporation, 1987

Wang, K.L., Cussler, E.L., Baffled membrane modules made with hollow fibre fabric, Journal of Membrane Science 85(1993), 265-278

Wang, S.Y., Hawboldt, K., Abdi, M.A., Novel dual-membrane gas-liquid contactors: modeling and concept analysis, Industrial & Engineering Chemistry Research 45 (2006), 782-789

Wickramasinghe, S. R., Semmens, M. J., Cussler, E. L., Hollow fibre modules made with hollow fibre fabric, Journal of Membrane Science, 84(1) (1993),1-14

Yang, M., Cussler, E.L., Designing hollow fibre contactors, AIChE Journal, 32 (11) (1986), 1910-1916

Chapter 5

ANALYSIS OF THE EFFECT OF MOUDLE DESIGN ON GAS ABSORPTION IN CROSS-FLOW HOLLOW FIBER MEMBRANE CONTACTORS VIA COMPUTATIONAL FLUID DYNAMICS (CFD) ANALYSIS

This chapter is based on and modified based on the following paper

Cai, **J.J.,** Hawboldt, K., Abdi, M.A., Analysis of the effect of module design on gas absorption in cross flow hollow membrane contactors via Computational Fluid Dynamics (CFD) analysis. *Journal of membrane science*, 520 (2016) 415-424

The performance of cross flow hollow membrane contactors for gas absorption applications is greatly influenced by module characteristics. In Chapter 3 and Chapter 4, the performance of a lab scale dual membrane module with specific design has been investigated through numerical and experimental approach. The module design factors are not included in the scope. This chapter focuses on the module design and its effect on performance enhancement using computational fluid dynamics (CFD) analysis. This chapter is organized as follows: Section 5.1 provides background information on the module design of membrane contactors; In section 5.2, a CFD simulation of a lab scale cross hollow fibre membrane contactor is developed to estimate shell-side flow and overall mass transfer performance; In section 5.3, the CFD model is validated with experimental data from the lab scale module for CO_2 absorption. The validated model was then used to investigate the geometric effect of module design on the shell-side flow and consequent absorption performance. A few design factors were examined in section 5.4 such as the shell configuration, inlet geometry, header shape, fibre bed height and packing density. This work shows that a properly designed CFD simulation can be used as a useful tool to optimize module design for cross flow membrane contactors and improve absorption performance.

5.1 Background

As mentioned previously in Section 2.4.3, cross flow hollow fiber membrane modules offer higher mass transfer coefficient and lower shell-side pressure drop than parallel flow modules (Dindore et al., 2005).This could be attributed to the continuous splitting and remixing of shell-side fluid in cross flow modules, which results in more turbulence and reduced shell-side channelling. Thus far, several cross flow modules have been developed and studied for gas absorption applications whereas most of these studies focus more on the development of membrane materials and absorption process whereas less attention has been paid on the module design and fabrication (Yang et al., 1986; Dindore et al., 2005; Zhang et al., 2013).

Wichramasinghe et al. (Wichramasinghe et al., 1992) experimentally studied oxygen absorption in cross flow HFMCs with various geometries. The highest efficiency was achieved in modules operated with solvent in the shell-side versus the tube side. The overall mass transfer performance of modules with liquid phase in shell-side is strongly influenced by module design and shell geometry. This is due to the fact that in gas-liquid contacting systems, the mass transfer resistance mainly lies in liquid boundary layer. As a result, shell-side flow plays a critical role in determining overall mass transfer performance. For modules operated with liquid solvent flowing through the shell-side, the overall mass transfer coefficient is a strong function of shell-side flow behavior which in turn is determined by shell geometries. In contrast to lumen side flow which can be well described using heat transfer analogy (Skelland, 1974), shell-side flow is more complicated to correlate and scarce information is available for predicting shell-side flow

patterns and mass transfer characteristics (Dindore et al., 2005). Moreover, limited work has been done to investigate the effect of module design on shell-side flow and consequent mass transfer of cross flow modules used for gas absorption. Some researchers have derived a few empirical equations to correlate shell-side flow with mass transfer performance for cross flow modules with various geometries (Yang et al., 1993; Bhaumik et al., 1998). It was found from these studies that the shell-side mass transfer is determined by several factors and their combinations, such as the flow regime, flow distribution, hydraulic shell diameter and effective length of the module, entrance effects, fibre dispersion, and packing density (Yang et al., 2013). Thus far, very few of these factors have been studied with respect to their impacts on shell-side hydrodynamics and module performance (Yang et al., 1986; Dindore et al., 2005; Yang et al., 2013). Dindore et al. (Dindore et al., 2005) studied shell-side mixing and mass transfer in a rectangular cross flow module using residence time distribution (RTD) approach. They concluded that the shell-side velocity is the key factor determining shell-side mixing and dispersion rate. In addition to shell-side velocity, shell-side flow distribution is another important factor affecting module performance (Zheng et al., 2003). The modules with uneven shell flow distribution performed poorly compared to modules with a more uniform flow distribution in shell-side (Yang et al., 2013; Yang et al., 2014; Zheng et al., 2003). In most of these studies, the uneven flow distribution was resulted from irregular fibre arrangement. The effect of flow distribution into the shell regions of fibre bundles through external ports and manifolds has received less attention (Mat et al., 2014). The structure-induced flow maldistribution was found to have a detrimental impact on module performance when the module is operated with gas phase in shell-side (Zhang et al.,

2013). Its impact on modules with liquid in shell-side however has never been reported. Moreover, the combination effect of shell side flow distribution and shell-side flow dynamics on module performance also remains unclear.

Computational fluid dynamics (CFD) modeling has been widely adopted to simulate and analyze fluid dynamic behavior in membrane contactors (Gage et al., 2002; Catapano et al., 2001; Mazaheri et al., 2006; Fill et al., 2006). The challenge in using CFD for membrane contactors is the membrane module can be composed of thousands of fibres, resulting in long computational times and convergence problems. An alternative approach is to model the fibre bundle as porous medium with well-characterized structure, which reduces the computational time significantly. Mazaheri et al. (Mazaheri et al., 2006) and Fill et al. (Fill et al., 2006) compared CFD predictions of shell-side flow distribution where the fibre bundles were modeled as individual fibres and as approximated as a porous medium approximation. The porous medium approximation was an effective approach to replace the individual fibres. Using this approach, Zhang et al. (Zhang et al., 2007) developed a mass transfer model based on convection-diffusion equation to approximate mass transfer in membrane oxygenator through CFD analysis. The predicted results were found in good agreement with experimental results. These studies demonstrate that CFD simulations are useful and effective in evaluating the performance of membrane contactors with different module designs. However, no comprehensive study has been done using CFD analysis to investigate geometric effect on shell-side flow and mass transfer in cross flow membrane modules used for gas absorption.

In this chapter, CFD simulation is used as a design tool to study the effect of module design on shell-side flow and consequent mass transfer performance of cross flow HFMCs. The porous medium approach was used to decrease computational time. To validate the model, the simulation predictions were compared to experimental data from a lab-scale module. The objective of this work is to study: (1) geometric effect of module design on shell-side flow dynamics and structure-induced flow maldistribution; (2) performance evaluation of cross flow module with various designs; (3) appropriateness of porous medium approach to model shell-side distribution and absorption performance.

5.2 Theory

5.2.1 Momentum Equation and Porous media approach

The three-dimensional (3D) geometry and computational surface of the lab scale dual membrane contactor were generated using a computer-aided design (CAD) software package (Fluent, ANSYS, ANSYS,Inc)The computational domain for the lab scale module setup included the inlet, outlet, and a cross flow chamber containing a square fiber bed. The geometries of computational domain were discretized into grids of finite volumes with the momentum and continuity equation being solved for each grid.

In the proposed membrane process, gas flows through a porous membrane and the solute permeates through the membrane. The solute is absorbed by liquid solvent flowing in shell-side. The momentum conservation is written as:

$$\rho\nabla\bullet(\vec{v}\vec{v}) = -\nabla p + \nabla\bullet\vec{\tau} + \rho\vec{g} + S_r \qquad \text{Eq. 5.1}$$

Where, $\vec{v}$ is the velocity vector, ρ the density of the liquid, $\vec{\tau}$ the stress tensor, p the pressure, $\vec{g}$ the gravitational force, and S_r is the source term of momentum sink. This momentum sink contributes to the pressure gradient in the porous cell, creating a pressure drop that is proportional to the fluid velocity (or velocity squared) in the cell.

Rather than representing each fibre in membrane core, a porous media approach was used to simplify the CFD modeling workload and computational time. The fibre bundle (solvent, fibre walls, and gas phase) was modeled as one lumped continuum (porous medium). To model pressure drop through porous media, a momentum source term (S_{ri}) is added to the governing momentum equations where pressure drop is proportional to the fluid velocity. The flow behavior through the porous media was approximated by the Ergun equation (Fill et al., 2001). The source term at *i* direction can be written as:

$$Sr_i = -(\frac{\mu}{C_1} v_i + C_2 \frac{1}{2} \rho V_{mag} v_i) \qquad \text{Eq. 5.2}$$

Where μ is the dynamic viscosity, and V_{mag} the magnitude of local superficial velocity vector, i = (1, 2, 3) is the coordinate direction. The permeability (C_1) and inertial loss coefficient (C_2) can be derived through the Blake-Kozeny equation as fluid passing through hollow fibre bundles can be treated as laminar flow through a packed bed, and can be predicted using the following equations:

$$C_1 = \frac{{d_0}^2}{150} \frac{\varepsilon^2}{(1-\varepsilon)^2} \qquad \text{Eq. 5.3}$$

$$C_2 = -\frac{3.5^2}{d_0} \frac{(1-\varepsilon)}{\varepsilon^3} \qquad \text{Eq. 5.4}$$

Where d_0 is the diameter of the hollow fibres, and ε is the porosity of the fibre bundle.

5.2.2 Continuity Equation and Gas Transport

The following assumptions were made based on the study carried out by Catapano et al. (Catapano et al., 2001) on membrane oxygenators

1. Steady-state;
2. The porous medium was considered as a continuum;
3. Gas phase was treated as a source term in the governing equation and defined on per-unit total volume;

The mass balance equation that governs the CO_2 concentration in the liquid phase can be written as below:

$$\vec{v} \cdot \nabla C_L - D \cdot \nabla^2 C_L = S_r \qquad \text{Eq. 5.5}$$

Where $\vec{v}$ is the superficial velocity vector, D is the gas diffusivity in the continuum and defined as $D = \varepsilon D_w$, where D_w is the gas diffusivity in the solvent (water for this study), S_r is a source term used to describe solute concentration in the gas phase (CO_2 for this study):

$$S_r = k_p A(HC_G - C_L) \qquad \text{Eq. 5.6}$$

Where A is the fibre membrane surface area per unit total volume; k_p is the shell-side mass transport coefficient; H is the Henry's constant, C_G stands for CO_2 concentration in gas phase, and C_L refers to concentration of CO_2 in the liquid phase. In this study, the CO_2 partial pressure from the gas source was assumed constant along the fiber to simply the simulation of gas absorption operated under high gas flow rates. This assumption was tested and validated by comparing the predicted results to the experimental results in the following sections.

The shell-side mass transfer coefficient k_p can be calculated through Sherwood number (Sh).

$$Sh = \frac{kd_h}{D} \qquad \text{Eq. 5.7}$$

Where D is diffusivity coefficient of solute in the solvent; d_h is the hydraulic diameter. In loosely packed module with fibre beds, it is found out that d_h is the outer diameter of the fibre (for module with void fraction greater than 0.5) (Mazaheri et al., 2006). The Sherwood number can usually be expressed as an empirical correlation in the format shown in Eq. 5.7 (Gabelman et al., 1999) for cross flow HFMCs.

$$Sh = \alpha \mathrm{Re}^{\beta} \mathrm{Sc}^{0.33} \qquad \text{Eq. 5.8}$$

Where Schmidt (*Sc*) number is calculated by dividing the diffusion coefficient (of solute in solvent) with the viscosity of the solvent. Reynolds number is given by Eq. 5.9

$$R_e = \frac{d_h \cdot u}{v} \qquad \text{Eq. 5.9}$$

Where *Re* is Reynolds number, v is for kinematic viscosity of solvent and u represents interstitial velocity in the fibre bundles, which can be estimated using the average velocity across the fibre bundle.

In the present study, empirical correlations developed by Yang et al. (Yang et al., 1993) based on experimental measurement from cross flow module with different packing density were used.

For loosely packed modules (ε >50%),

$$Sh = 0.94 \mathrm{Re}^{0.4} \mathrm{Sc}^{0.33} \qquad \text{Eq. 5.10}$$

For loosely packed modules (ε <50%),

$$Sh = 1.38\mathrm{Re}^{0.34}\mathrm{Sc}^{0.33}$$ Eq. 5.11

5.3 Methodology

Absorption of CO_2 was modelled using CFD analysis and the result was compared to experimental measurements. The validated CFD model was then used to investigate different designs and operational conditions and the resulting effect on shell-side flow and module performance.

5.3.1 Experimental validations

Gas absorption experiments were carried out in a lab scale cross flow module as shown Figure 5.1. The membrane core of this module is composed of polypropylene fibres.

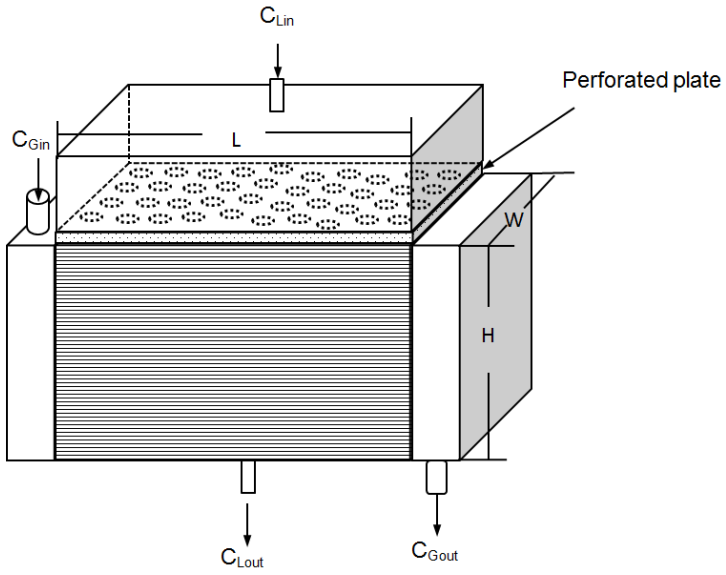

(a) Schematic drawing of lab scale cross flow module

(b) Bottom view of cross flow module

(c) Front view of cross flow module

Figure 5.1: (a) Schematic drawing of cross flow module; (b) bottom view of cross flow module; (c) front view of cross flow module

Celgard® Q10 microporous hollow fibre membranes (i.d.: 600µm, o.d.: 1000µm) (Celgard, Inc., Charlotte, NC, U.S.A.) were used in the fibre bundle. The dimensions of the flow chamber and the diameters of the inlet and outlet tubing are given in Table 5.1, The hollow fibre membrane surface area was 0.18 m^2.

Table 5.1: Specifications of cross flow module and membrane properties

Dimension of membrane core (mm^3)	103×80×88
Height of header (mm)	5
Diameter of inlet/outlet (mm)	10
Diameter of hollow fibre	2
Void Fraction	0.93
Height of inlet header (mm)	48
CO_2 inlet port (mm)	6
CO_2 outlet port (mm)	6
water inlet port (mm)	6
water outlet port (mm)	6
Membrane surface area (m^2)	0.18

The experimental set-up is outlined in Figure 5.2. The solvent was fed from a gear pressure pump via a flow controller. In all experiments, sufficient gas pressure was maintained in the contactor before starting solvent flow to prevent wetting of fibres. The solvent inlet and outlet pressures were measured using digital pressure indicators. The liquid inlet was also fitted with a digital thermometer. The average velocity of the liquid through the fibres was measured by collecting a sample over a fixed period of time.

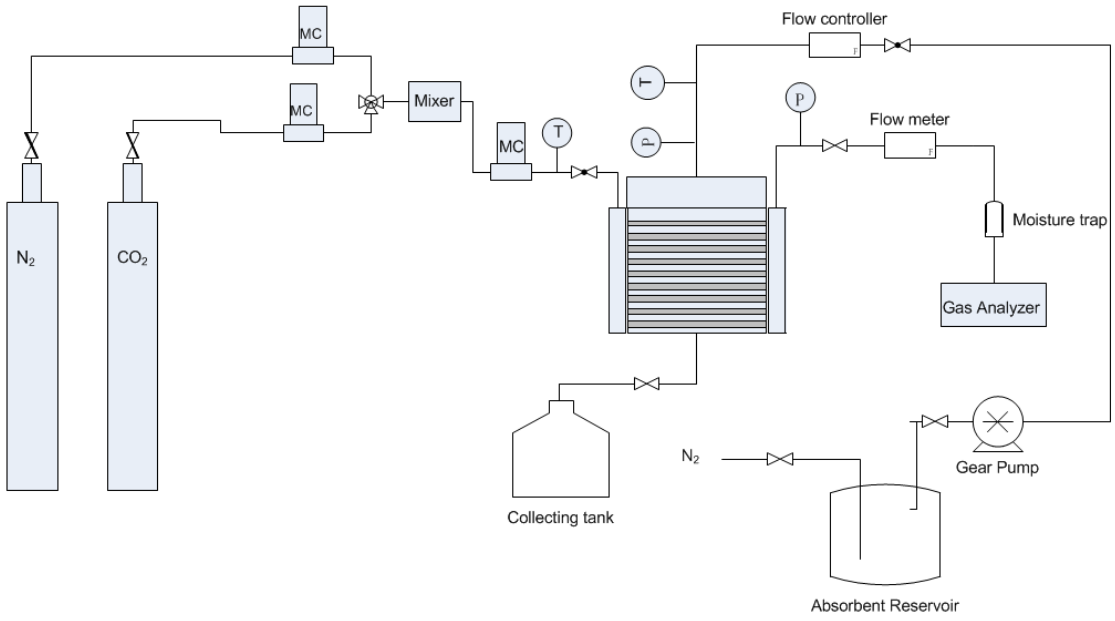

Figure 5.2: Schematic drawing of the experimental setup for CO_2 absorption using cross flow HFMC

The gas inlet and outlet pressures were measured using digital pressure indicators. The CO_2 concentration in the outlet gas stream of the contactor was measured using Oxybaby® Infrared CO_2 analyzers) (WITT Gasetechnik GmbH & Co. KG). CO_2 concentration in liquid outlet was determined through Phenolphthalein titration with experimental error of ±3%. The CO_2 absorption flux was estimated by making an overall mass balance on the system. Since the infrared analyzer provided CO_2 concentration in terms of volume percentage, it is possible to calculate both the volumetric gas flow rate and the molar concentration of CO_2 by mass balance. All the experiments were carried out at atmospheric pressure and 298 K.

5.3.2 CFD modeling approach

A three-dimensional geometry and computational surface of the lab scale module was generated using workbench, ANSYS. The 3-D geometry was then meshed using 3D Tet/Hybrid elements. An unstructured-mesh finite-volume based commercial CFD package, Fluent (ANSYS12) was used to solve the governing transport equations for CO_2 absorption in the test module.

The solvent (water) was treated as incompressible Newtonian fluid with a constant viscosity. A pressure-outlet condition was set at the outlet for all simulations. The absorption performance of the module was investigated with liquid flow rates between 0.1×10^{-5} m^3/s to 6×10^{-5} m^3/s or Reynolds numbers between 0.1 and 10 (laminar regime). Parameters and physical constants used for the CFD simulations are listed in Table 5.2.

Table 5.2: Parameter used in membrane simulation model

Parameter	Value
Water density (kg/m^3)	998
$D_{CO2/water}$ (m/s)	2×10^{-9}
Viscosity (m^2/s)	1×10^{-6}
Temperature (K)	298

5.4 Results and Discussions

5.4.1 Model validation

To validate the proposed CFD model and porous media approach, absorption of pure CO_2 was carried out in the developed lab scale module from which CO_2 concentration in liquid phase was measured at shell-side outlet and compared to the estimated results. The liquid flow rates was varied from 0.1×10^{-5} to 1.7×10^{-5} m^3/s as the gas flow rate was kept constant at $2.67\times10^{-5} m^3/s$. Figure 5.3 compares CO_2 concentration at liquid outlet estimated by CFD model and experimental measurements. The differences between the measured data and predicted values were less than 5%.

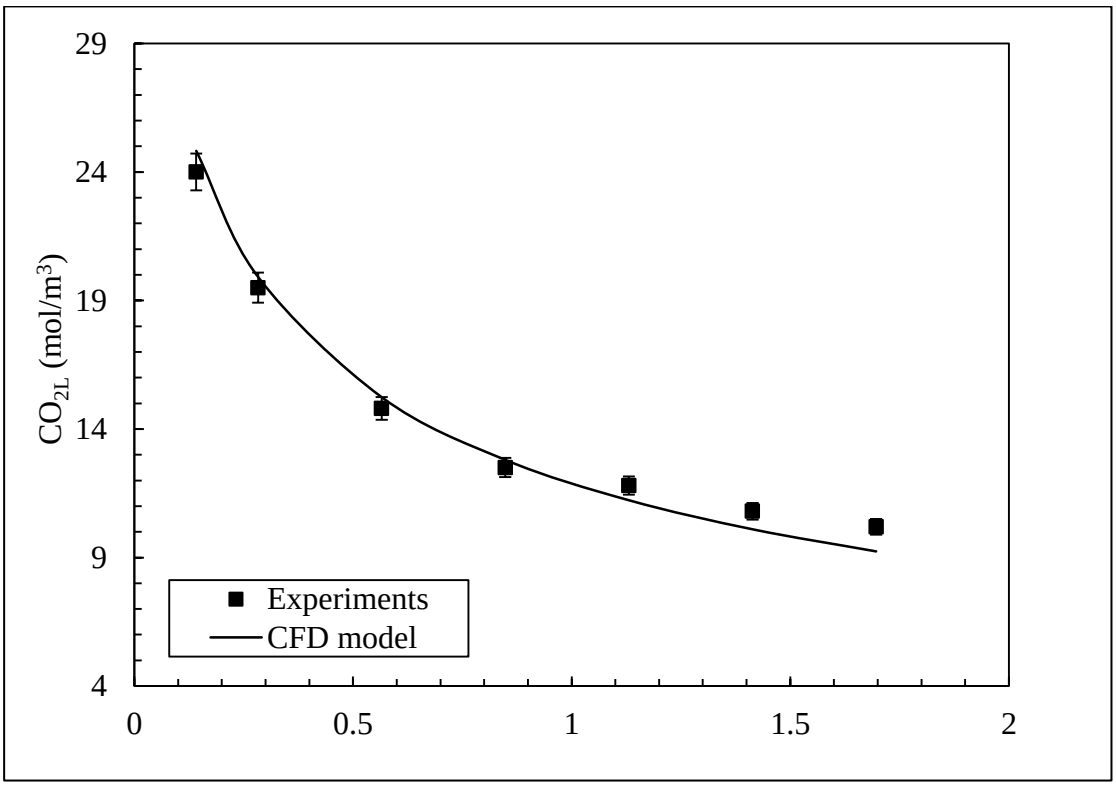

Figure 5.3: CO_2 absorption in lab scale module

A middle plane cut-view of the simulated concentration distribution for the lab scale rectangular module at a flow rate of 0.83×10^{-5} m^3/s is shown in Figure 5.4 a and b, respectively. It can be seen that the concentration in the central area is lower than in the boundary area. This is mainly caused by the jet flow behavior due to the inlet and flow chamber arrangement. This is mainly caused by the jet flow behavior due to the inlet and flow chamber arrangement. As fresh solvent enters into the shell side through the inlet manifold on the top of the module, it tends to pass through the membrane core through the center area due to the short flow path. As a result, the loaded solvent in the center area was quickly diluted and replaced with fresh solvent entering into the shell side. That is the reason that the concentration in the centre area is much lower than that in boundary area (as shown in Fig. 5.4 (a) and (b)).

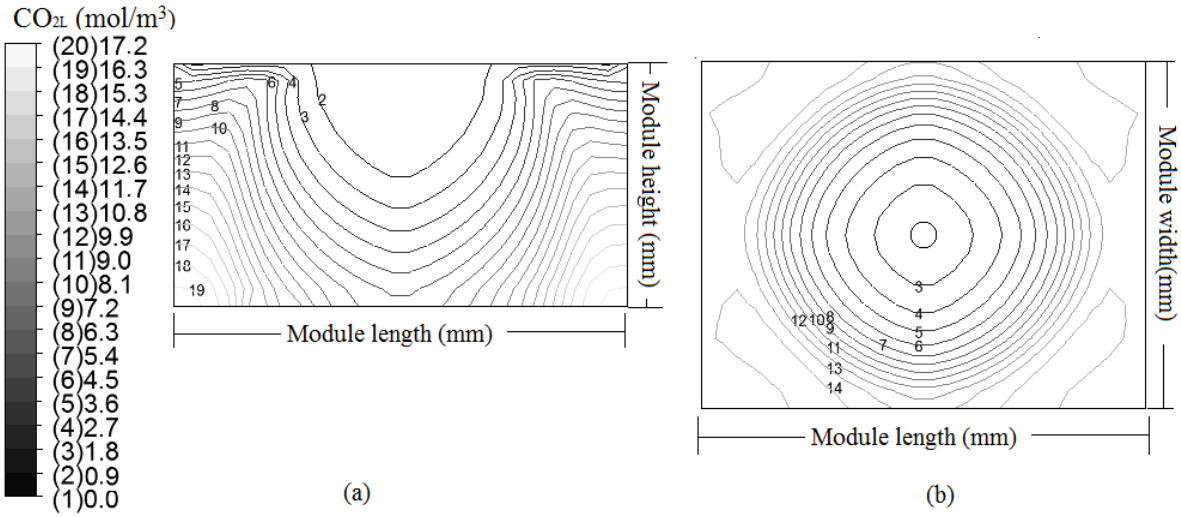

Figure 5.4: Middle-plane cut view porous zone to show the simulated concentration profile and magnitude (a) front view; (b) top view, at a flow rate of 0.83×10^{-5} m^3/s for solvent

5.4.2 Impact of module design factors

The module type, structure and geometry are critical design considerations in membrane performance. To optimize the module design for performance enhancement, the effect of a series of design factors on shell side hydrodynamic conditions and absorption performance were investigated using the proposed CFD model, including shell geometry, inlet geometry (inlet dimension and distributor manifold), fibre bed height and packing density.

Two parameters are introduced into this study to evaluate the shell side hydrodynamics in the lab scale cross flow modules: (1) the average shell-side velocity ($\bar{v}_{shell}$) and (2) flow maldistribution factor (S_g). Previous studies show that shell-side mixing behavior of the phase flowing through membrane core is a strong function of shell-side velocity (Dindore et al., 2005). By discretizing the shell side into grids of finite volumes and solving the Navier-Stokes equations for each grid, the velocity profile in shell side can be obtained. The membrane core is where the mass transfer resistance dominates, and therefore the averaged shell-side velocity can be represented by the averaged fluid velocity across membrane core (porous zone), which is calculated based on the volume weighted average on the porous zone. The uniformity of mass flow rate of liquid flow in the shell side (flow non-uniformity) was described using the flow maldistribution factor (S_g). It is a parameter used to capture the flow dynamics over a cross section of the membrane core. It has been widely used to evaluate shell-side flow distribution in the design of plate and fin heat exchangers (Jiao et al., 2003). It is introduced in the current study to evaluate the The maldistribution factor can be defined based on the ratio of standard deviation over the

mean value of the velocity distribution on the certain cross section of the membrane core, as shown in Eq.5.12:

$$S_g = \frac{\sqrt{\sum_{i=1}^{n}(v_i - v_{ave})^2}}{v_{ave}} \times 100\% \qquad \text{Eq. 5.12}$$

Where v_i is the local liquid velocity, v_{ave} refers to mean liquid velocity for a cross section.

5.4.3 The effect of shell geometry

There are two types of typical shell configurations for cross flow HFMCs: cylindrical and rectangular as shown in Figure 5.5. Though most modules being commercialized for industrial application are cylindrical, the potential to improve module performance by varying shell configuration remains unclear. In this work, the performance of cylindrical and rectangular modules was compared, keeping other design parameters and operational conditions constant. The schematic drawing of two modules was shown in Figure 5.6 while the details of module specifications are shown in Table 5.3.

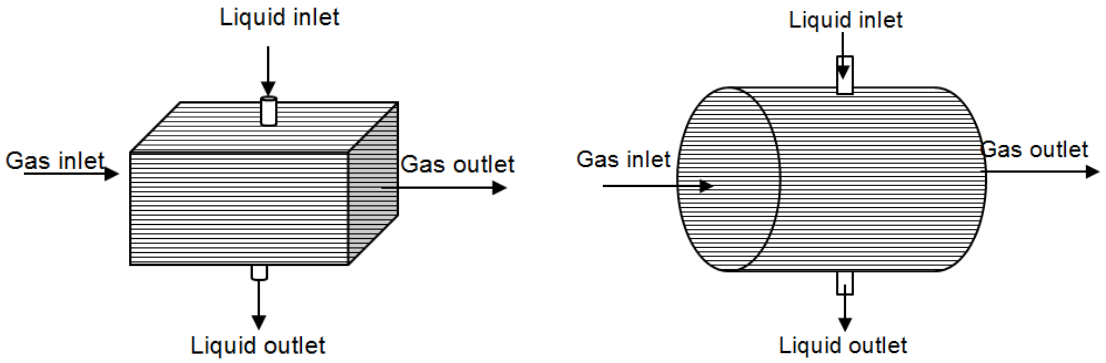

(a) Rectandular module (b) Cylindrical module

Figure 5.5: Schematic drawing of rectangular module and cylindrical module

Table 5.3: Specifications of rectangular module and cylindrical module

Module Specification	Rectangular module	Cylindrical module
Length (mm)	103	103
Width (mm)	88	-
Height (mm)	80	-
Diameter (mm)	-	94.6
Volume of membrane core(mm^3)	4.5×10^5	4.5×10^5
Total volume (mm^3)	7.25×10^5	7.25×10^5
Packing density%	15	15
Membrane area (m^2)	0.18	0.18

Absorption of pure CO_2 using water as solvent was modeled with CFD analysis. Nitrogen was bubbled through the water before use to prevent N_2 absorption, the initial CO_2 concentration in the liquid phase was assumed zero. The absorption flux was compared by varying liquid flow rate from 0.14×10^{-5} to $1.7\times10^{-5}m^3/s$. The gas flow rate was kept constant at $2.67\times10^{-5}m^3/s$. The CO_2 absorption flux can be calculated using Equation 5.13 and Equation 5.14. The average CO_2 concentration at liquid outlet was predicted by CFD modelling.

$$J_{ave} = \frac{(Q_{G,i}C_{G,i} - Q_{G,e}C_{G,e})}{A} \qquad \text{Eq.5.13}$$

$$Q_L C_{Lout} = (Q_{G,i}C_{G,i} - Q_{G,e}C_{G,e}) \qquad \text{Eq. 5.14}$$

Where, A stands for mass transfer area (m^2); $Q_{G,i}$ (m^3/s) and $Q_{G,e}$ (m^3/s) are the gas flow rate at inlet and outlet of module, respectively; Q_L (m^3/s) is the liquid flow rate and C_{Lout} (mol/m^3) refers to CO_2 concentrations at shell outlet.

Figure 5.6 shows the absorption flux as a function of the liquid flow rates. The absorption flux in both rectangular module and cylindrical module dramatically increases as inlet liquid velocity increases, highlighting the dependence of mass transfer on the liquid flow rates. Compared to cylindrical module, the rectangular module shows higher absorption flux and the difference become more pronounced as liquid flow rate increases. By using the rectangular module, the absorption performance can be improved by 65% at the liquid flow rate of $1.7\times10^{-5}m^3/s$, compared to the cylindrical modules.

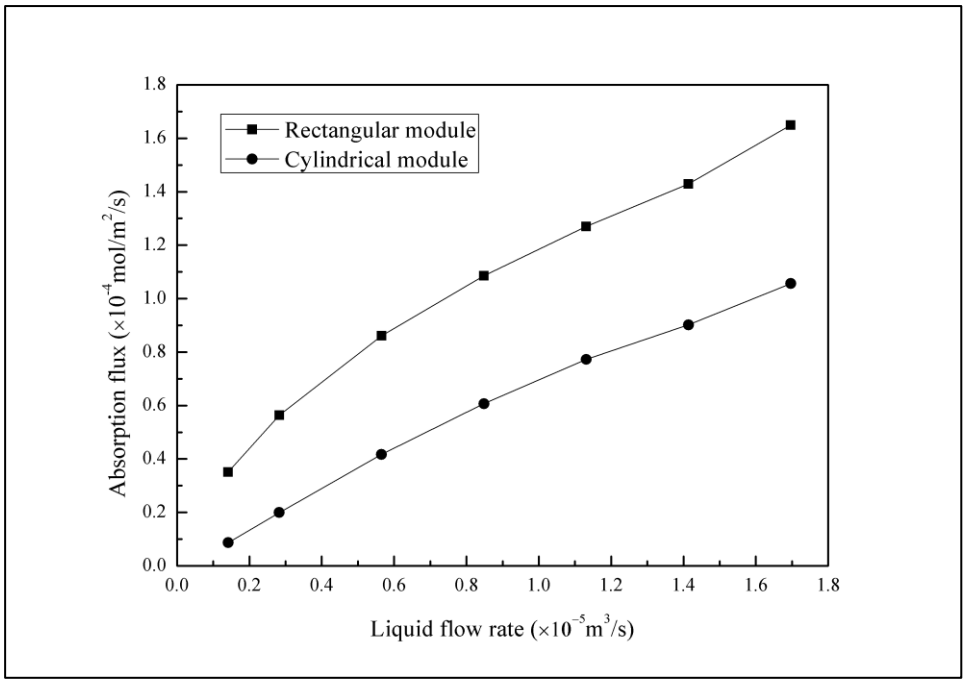

Figure 5.6: Effect of shell geometry on membrane module performance (CO_{2Gin}=44.64 mol/m^3, $Q_G=2.67\times10^{-5}m^3/s$)

As the two modules are of the same length, volume and packing density, the difference in shell-side mass transfer is likely due to various shell-side flow behaviors. Figure 5.7 compares the average shell-side velocity and flow in a cylindrical module and a rectangular module. At the same flow rate, the rectangular module results in a higher average shell-side velocity than the cylindrical module, which may explain the better absorption performance in the rectangular module. The maldistribution factor is calculated based on the velocity data from the centre of the membrane core. In general, shell side flow distribution becomes less uniform as liquid flow rate increases. Overall, the flow distribution in the rectangular module is more uniform than the cylindrical module. The pressure drop is also critical to membrane performance. Based on the simulation, the pressure drop was not significantly different between the two designs.

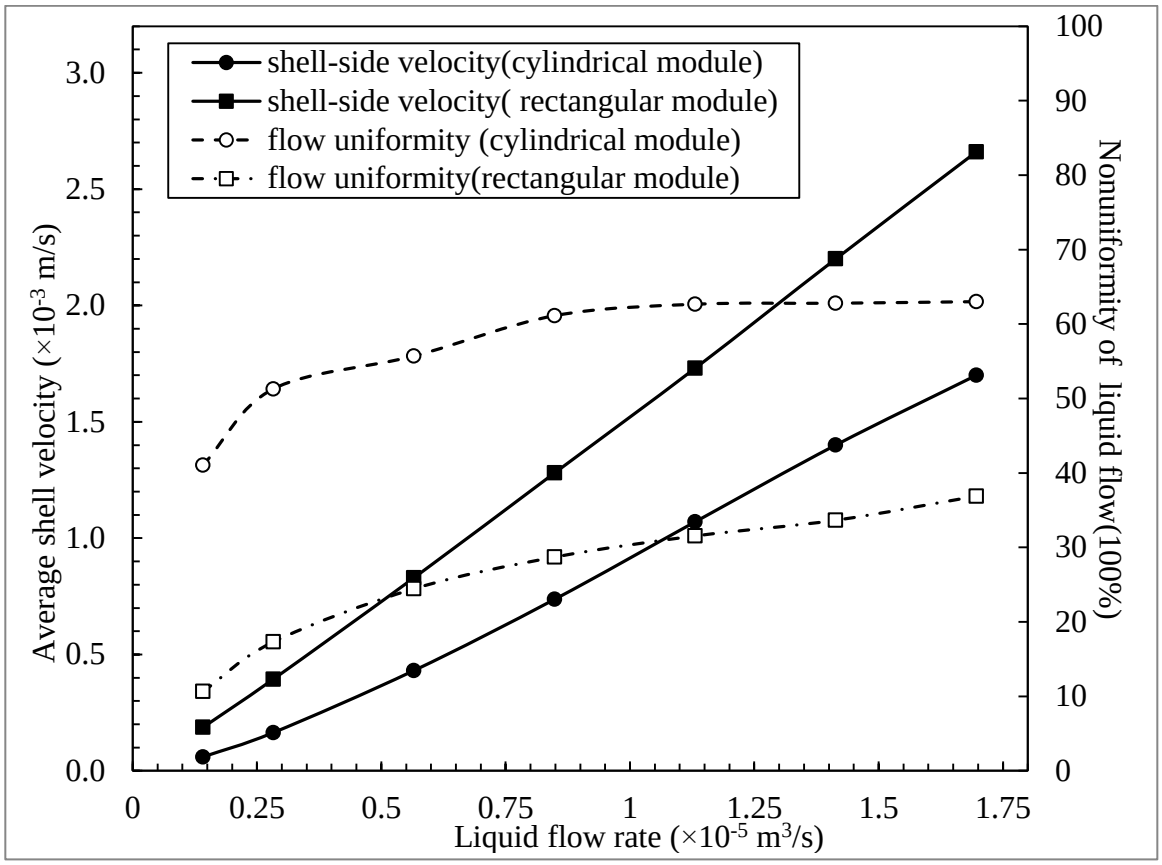

Figure 5.7: Effect of shell geometry on shell-side flow (CO_{2Gin}=44.64 mol/m^3, Q_G=2.67×$10^{-5}$$m^3$/s)

5.4.4 The effect of Inlet geometry

Inlet geometry is another influential factor on shell-side flow dynamics yet its effect on module performance can be underestimated (Frank et al., 2000). Though the inlet manifolds induced entrance effect was included in empirical correlations in few studies (Lipnizki et al., 2001), its impact on shell-side flow dynamics and gas absorption of cross flow membrane modules has not been explored for performance enhancement. In the present study, average shell velocity, shell-side flow distribution and mass transfer

performance were evaluated in modules with various inlet geometries. Two design factors were examined: 1) the inlet opening dimension and 2) the header structure.

The ratio of inlet diameter over hydraulic diameter of the module is defined as O/L. All other parameters were kept constant. The range of ratios of O/L (0.04-0.3) was selected based on the ratio of inlet cross-sectional area to the total cross sectional area of membrane core. This is similar to the method of flow area ratio investigated in compact parallel heat exchanger. CO_2 absorption in modules with different O/L ratios were modeled using the CFD analysis, with inlet diameter varying from 6 mm to 29 mm. Liquid flow rate is kept constant. Figure 5.8 plots CO_2 concentration at liquid outlet as a function of O/L ratios. The lowest CO_2 concentration at liquid outlet was found in the module with the largest inlet size. Average shell-side velocity was also compared between modules with different inlet dimension in the same plot. As expected, the module with a smaller inlet results in higher average shell velocity and better mass transfer performance in the shell-side. Modules with narrow inlets can result in high pressure drop across the membrane core. For example, a module with O/L ratio of 0.04 has an associated pressure drop of 0.3 kPa, compared to 0.3 pa in module with O/L ratio of 0.3. Therefore, there is a trade-off between the increasing pumping energy cost associated with higher pressure drop and improved absorption performance which needs to be considered for the module design stage.

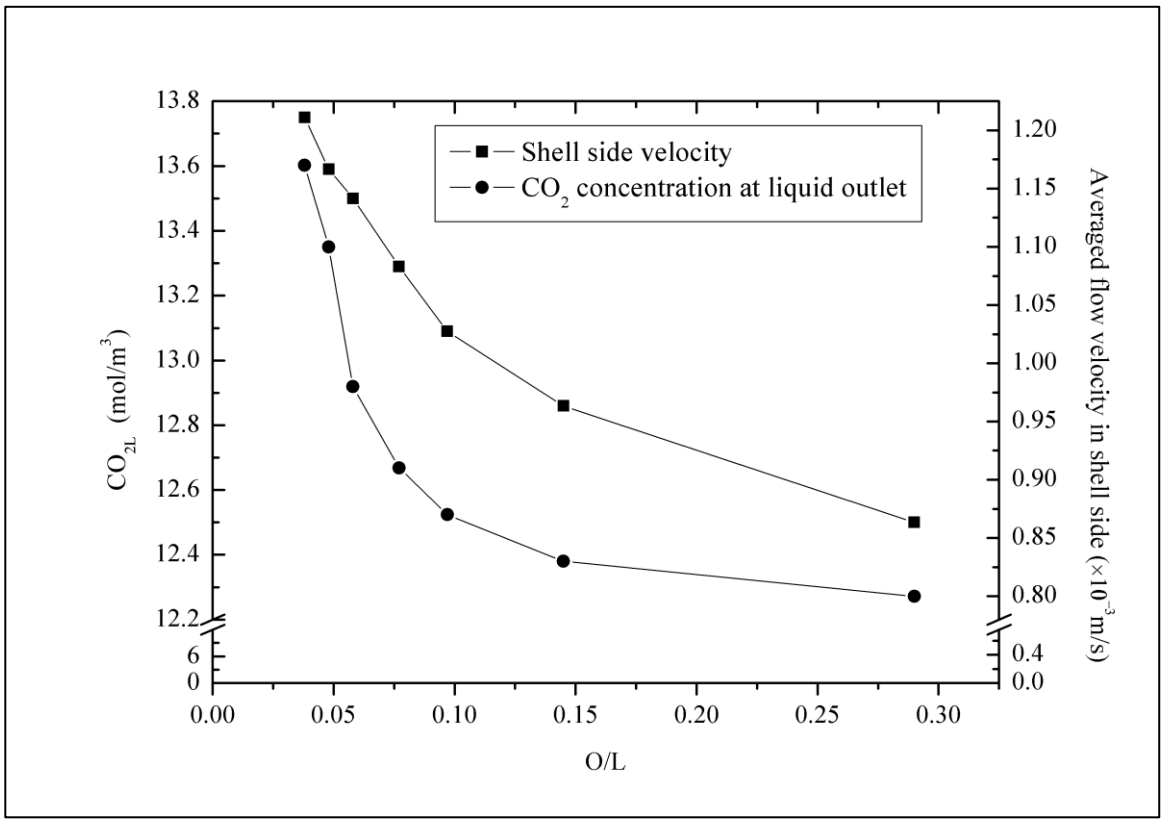

Figure 5.8: The effect of inlet dimension on shell-side flow velocity and mixing (CO_{2Gin}=44.64 mol/m^3, Q_G=2.67×10^{-5}m^3/s)

Figure 5.9 compares shell-side flow distribution and absorption flux as a function of O/L. Under the same operational conditions, absorption performance can be improved by using narrow opening inlet as absorption flux decrease as O/L ratio increases. Moreover, modules with wider inlets result in more uniform flow distribution in shell-side though there is no corresponding increase in absorption, likely a result of the aforementioned higher velocities with narrow inlets and hence higher mass transfer coefficients.

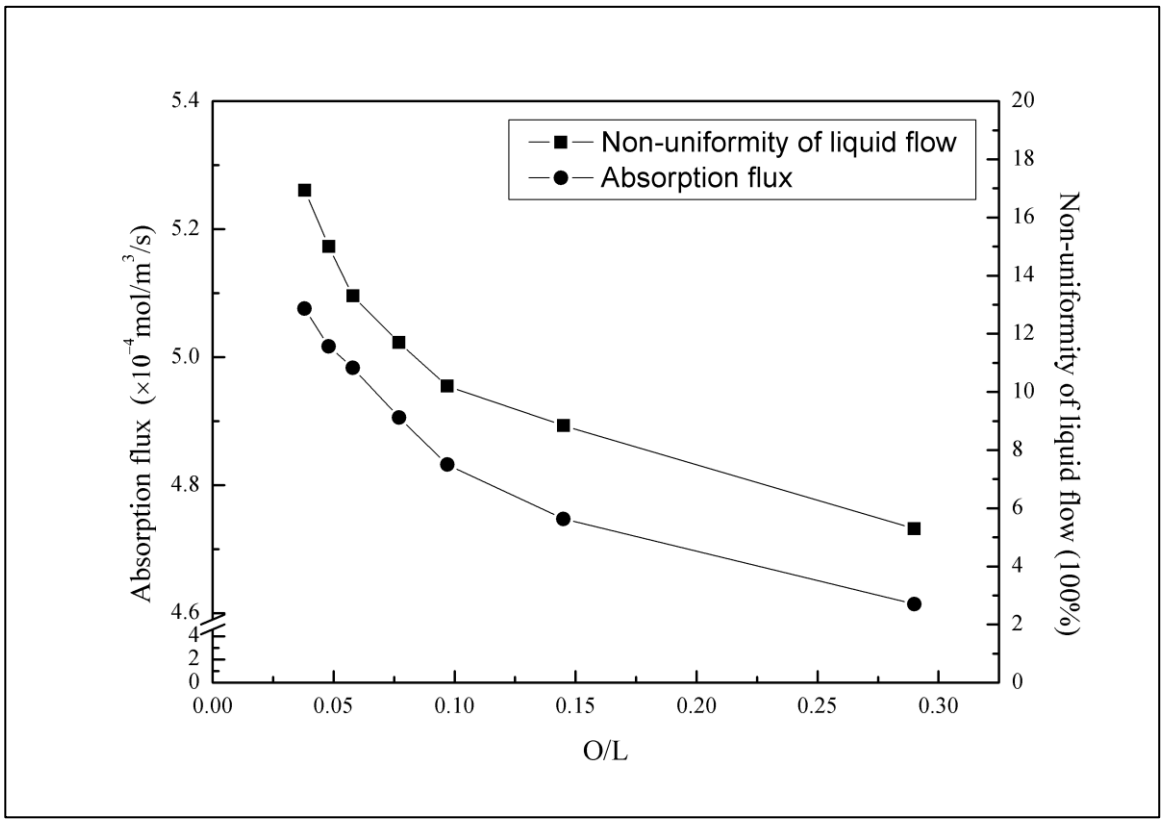

Figure 5.9: The effect of inlet dimension on shell-side flow velocity distribution and absorption flux (CO_{2Gin}=44.64 mol/m^3, Q_G=2.67×10^{-5}m^3/s)

The influence of header structure on shell-side mass transfer performance was also investigated. Park et al. (Park et al., 1986) studied the flow distribution in parallel membrane modules and found that the header design and magnitude of the velocity have a significant effect on flow distribution. A distributor or a proper design of header manifold could improve the shell-side mass transfer. Three types of modules with different header designs were proposed (Figure 5.10). Module (a) contains only an inlet, outlet, and the membrane core. Module (b) is designed with a short cone shaped header while Module (c) has a long cone shaped header. The specifications of the membrane

core are the same as the specifications in Table 5.1. CO_2 concentration at liquid outlet and average shell velocity from modules with different header geometries were compared in Figure 5.11 by varying liquid flow rates from 0.14×10^{-5} to 5.6×10^{-5} m^3/s. The impact of header design on module performance seems insignificant when liquid flow rate is lower than 0.14×10^{-5}. In general, modules with headers result in better performance. The difference becomes more obvious as liquid flow rate increases. The absorption performance can be improved by 38.4% when long header is included in module design at the liquid flow rate of 5.6×10^{-5} m^3/s, compared to the module without header design.

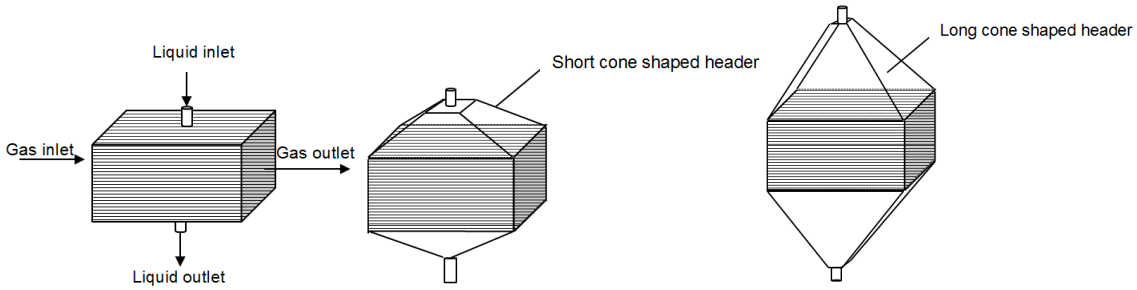

(a) (b) (c)

Figure 5.10: Schematic drawing of module with different designs of inlet geometries: (a) Rectangular module without header; (b) Module with short cone shaped header; (c) Module with long cone shaped header

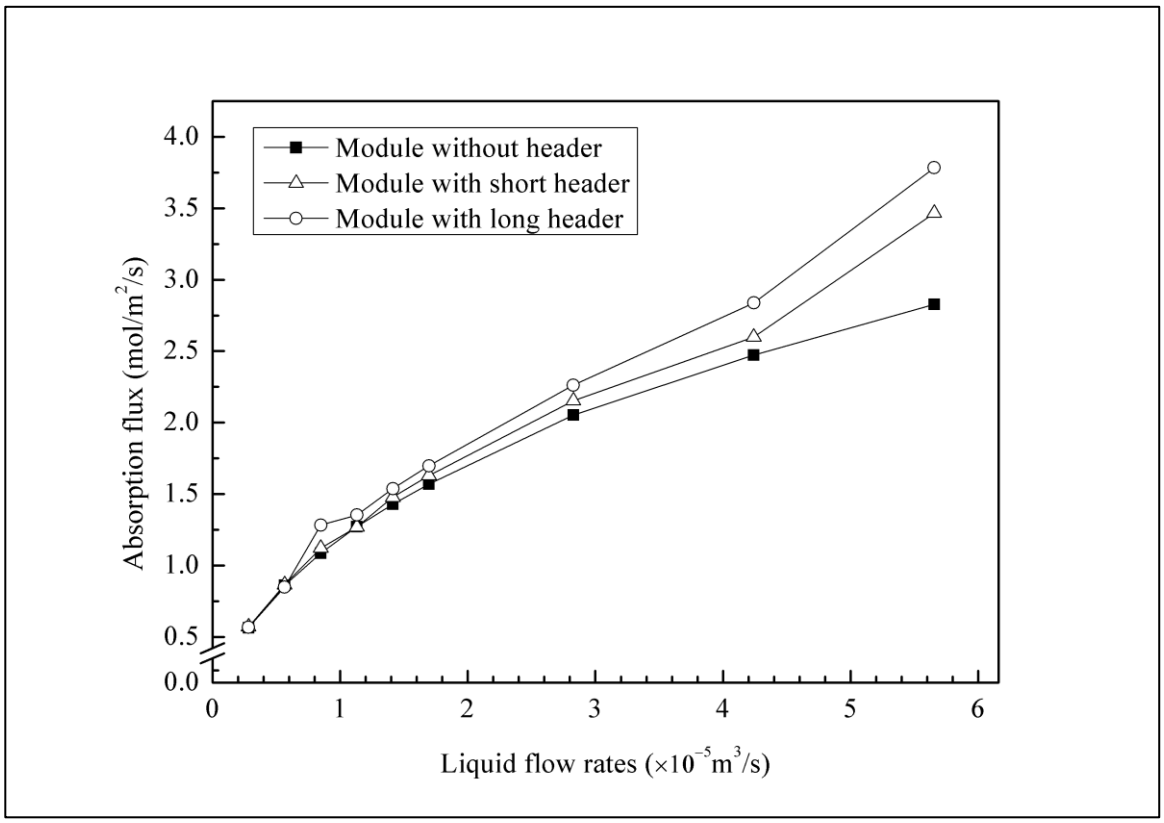

Figure 5.11: The effect of header design on absorption flux (CO_{2Gin}=44.64 mol/m^3, Q_G=2.67×$10^{-5}$$m^3$/s)

The effect of header design on shell-side hydrodynamics and flow distribution is also explored and presented in Figure 5.12. Module with longer header results in the highest average shell velocity compared to the other two modules. This difference becomes more significant as inlet velocity increases. As outlined above, higher velocities translate into higher mass transfer coefficient which explains the advantage of using long headers to prompt shell-side flow. On the other hand, shell-side flow distribution is closely linked to average shell-side velocity which is more uniform in modules without headers yet its impact on absorption performance seems insignificant.

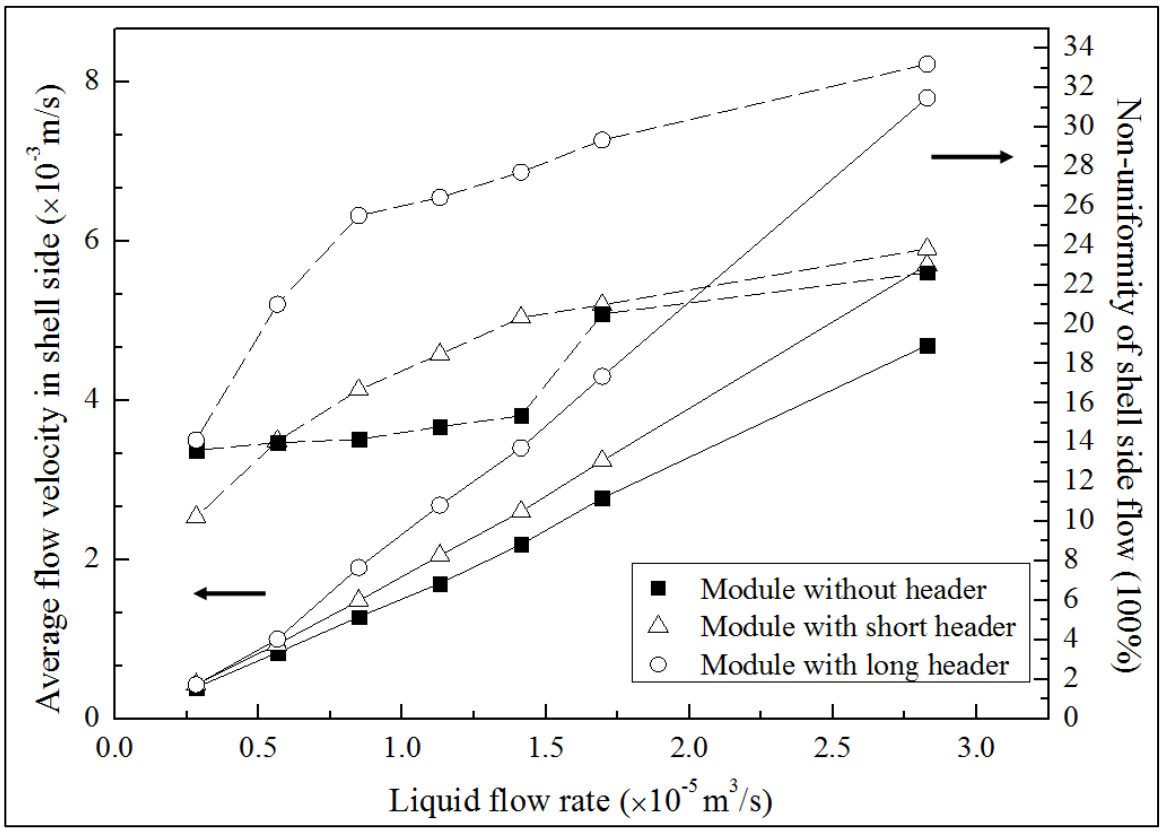

Figure 5.12: The effect of header design on shell-side flow (CO_{2Gin}=44.64 mol/m^3, Q_G=2.67×$10^{-5}$$m^3$/s)

5.4.5 The effect of membrane bed height

To scale up lab scale cross flow membrane modules for industrial implementation, the understanding of the effect of membrane bed height on module performance is critical. This is because the flow path taken by shell-side fluid strongly influences shell-side flow dynamics and module performance, which is a function of the cross section area for flow, fibre arrangement, fibre configurations and the height of membrane bed (Yang et al., 2013). Compared to extensive studies done on the other factors, the effect of membrane bed height has rarely been studied. For modules with liquid flowing in the fibre side,

varying the fibre length and number may not make a significant difference on the performance, as long as the membrane area is kept constant. This is not the case for modules with liquid flow in the shell-side. In the present study, CO_2 absorption in modules with shallow bed and deep bed was modelled using CFD analysis to investigate the effect of membrane bed height on shell-side flow dynamics and module performance. Packing density was assumed constant in all modules. Figure 5.13 compares the estimated average shell-side velocity and flow maldistribution obtained from modules with membrane bed height varying from 25 to 306mm.The highest shell-side velocity was obtained from the module with the shallowest membrane bed, which decreases as the membrane bed height increases from 25 to 125mm and flattens out as the bed height continues to increase from 125 to 306mm. In contrast to the velocity, the shell-side flow distribution in the module with the shallowest bed (i.e., containing only a few layers of fibres) showed the poorest flow distribution. As membrane bed height increases, the flow distribution on the exit membrane core is dramatically improved. This is mainly because the liquid flow is better mixed and distributed as more fibre present in modules with higher membrane bed height.

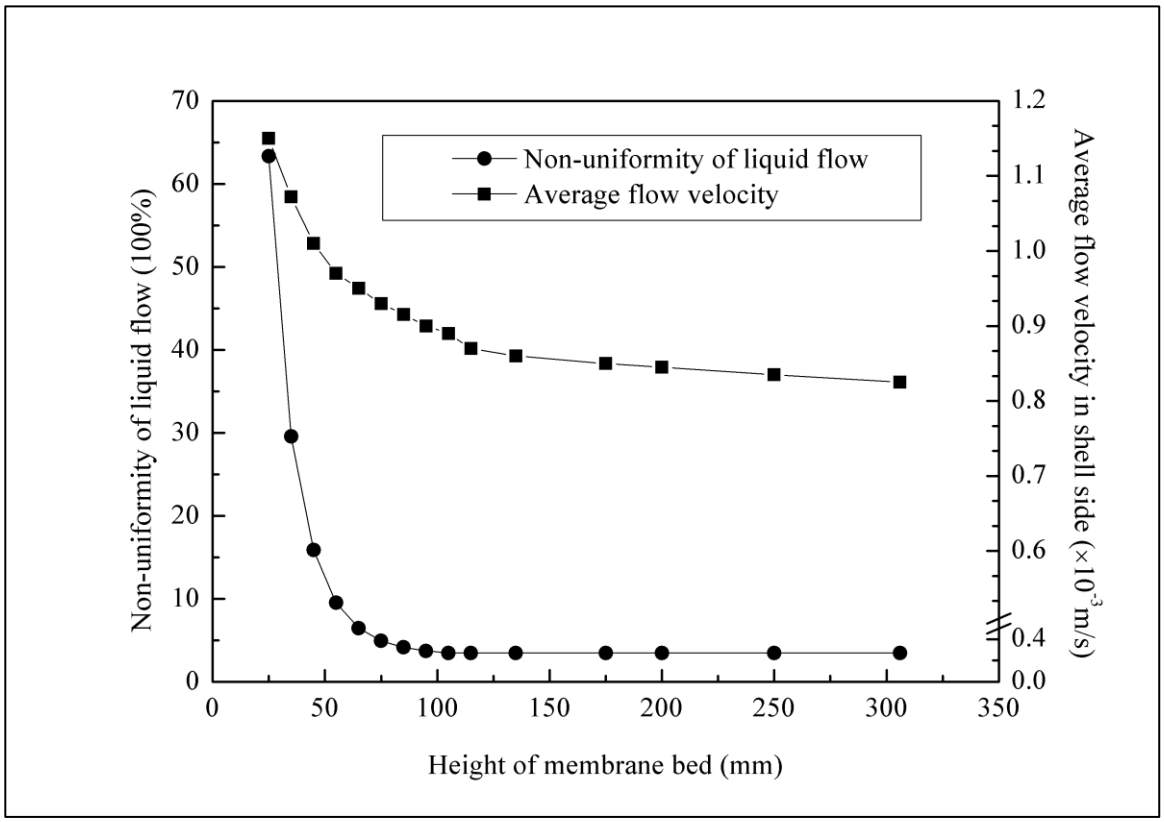

Figure 5.13: Effect of membrane bed height on shell-side flow dynamics (CO_{2Gin}=44.64 mol/m^3, Q_G=2.67×$10^{-5}$$m^3$/s, Q_L=0.85×$10^{-5}$$m^3$/s)

The effect of membrane bed height on absorption performance is described in Figure 5.14. As membrane bed height increases, higher CO_2 concentration is obtained at liquid outlet due to more membrane available for mass transfer to occur. On the contrary, module with deep membrane bed height tends to results in lower absorption flux compared to those with shallow membrane bed. This is probably because in modules with deep membrane bed, the residence time of liquid flow in shell-side is relatively long. As liquid phase is gradually becoming saturated with CO_2, the driving force responsible for mass transfer

decreases which results in lower absorption flux than modules with shallow membrane bed.

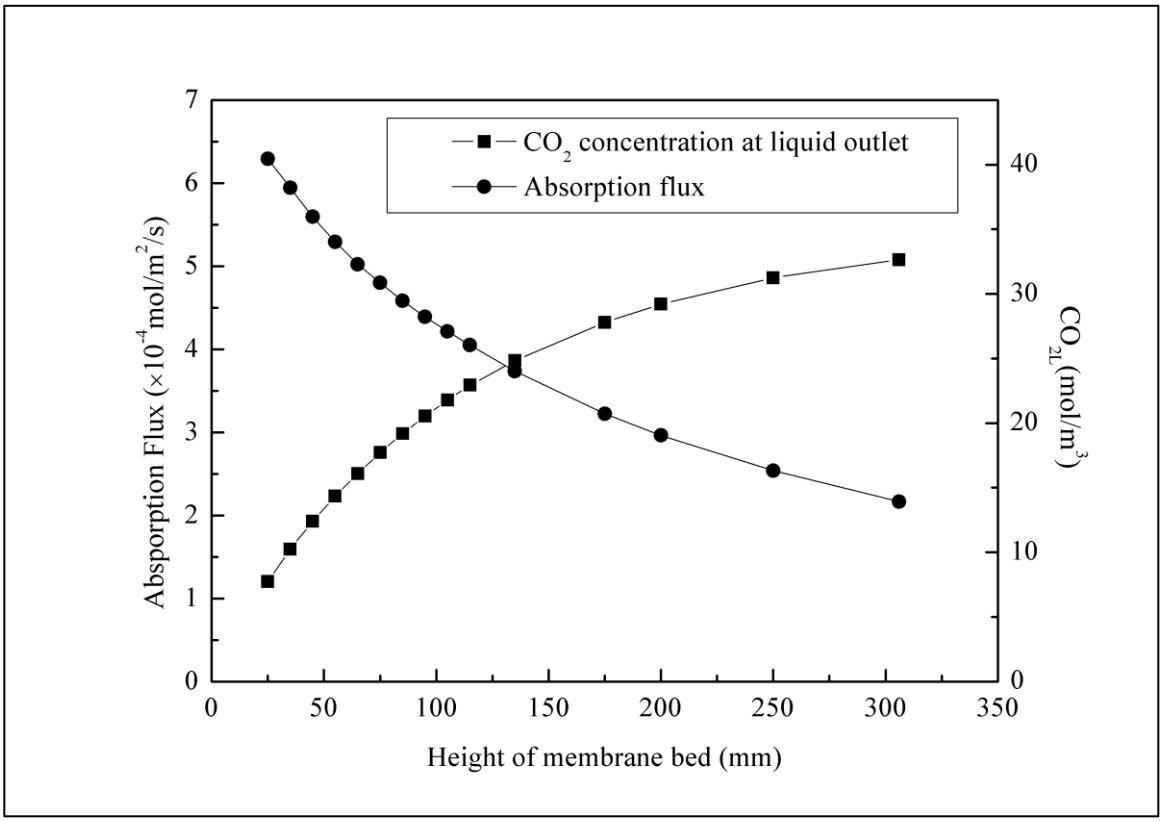

Figure 5.14: Effect of membrane bed height on absorption performance (CO_{2Gin}=44.64 mol/m^3, Q_G=2.67×10^{-5}m^3/s, Q_L=0.85×10^{-5}m^3/s)

5.4.6 The effect of packing density

The diameter of the fibres and packing density control the surface area to volume ratio, However there is an accompanying negative impact on the flow distribution when packing density increases. Tightly packed fibres can impede flow and cause regions of stagnation, while loosely packed systems not only have low surface area to volume ratios

but also may also limit liquid mixing thereby decreasing mass transfer rates. Figure 5.15 compares the average shell-side velocity and flow distribution across the membrane core exit surface for lab scale modules with different packing densities. Modules with high packing density tends to results in lower shell-side velocity and more uniform flow distribution compared to loosely packed modules. This again demonstrates the very different effects in module with liquid in the shell-side and the important role velocity distribution and magnitude paly in module performance.

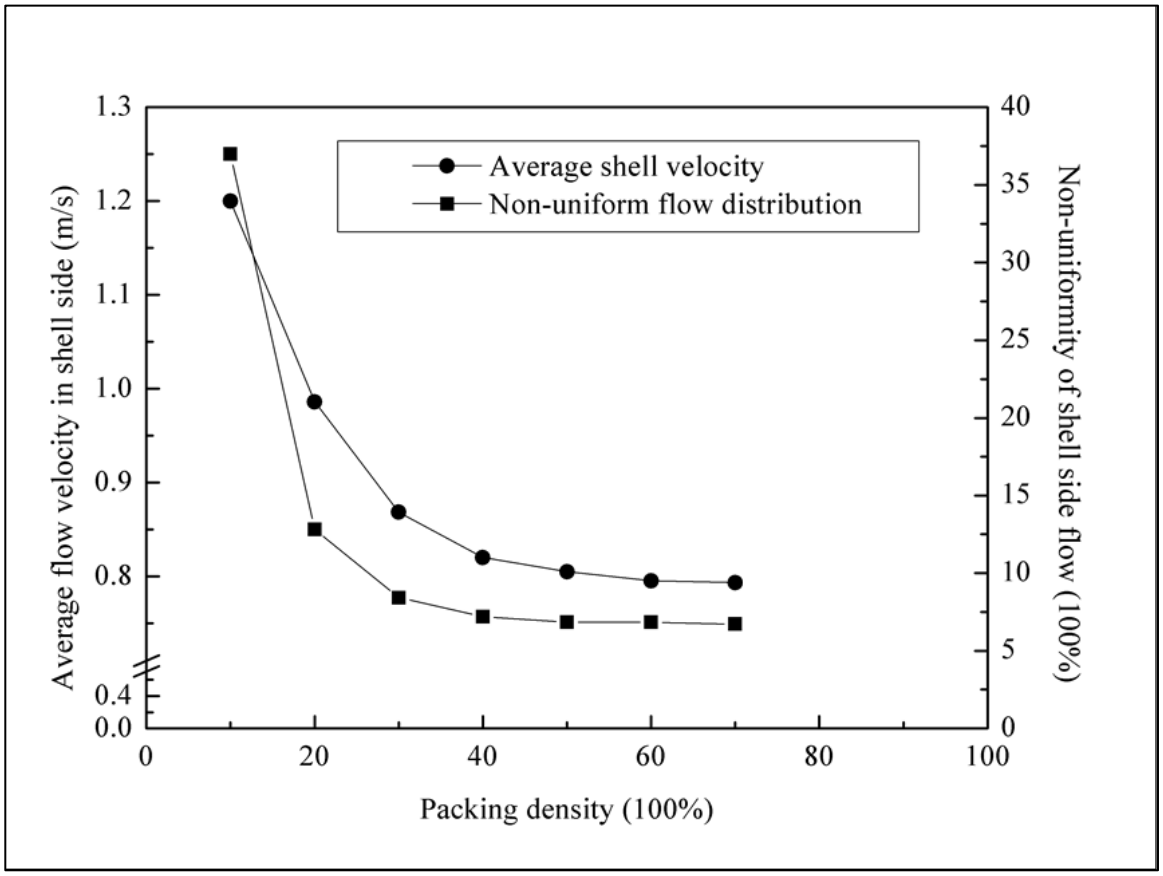

Figure 5.15: Effect of packing density on shell-side flow dynamics (CO_{2Gin}=44.64 mol/m^3, Q_G=2.67×$10^{-5}$$m^3$/s, Q_L=0.85×$10^{-5}$$m^3$/s)

Two empirical correlations were used to predict the shell-side mass transfer coefficient based on a study using cross flow membrane modules with different packing densities (Yang et al., 1986) (Shown in Equation 5.10 and 5.11). As shown in Figure 5.16, the CO_2 concentration at liquid outlet increases from 8.1 to 30 mol/m^3 as the packing density increases from 10% to 50%. The increasing rate gradually flattens out as packing density continues to increase from 50% to 90%. Less densely packed modules result in higher absorption flux compared to tightly packed modules while the absorption flux decreases as packing density increases. This is probably due to higher liquid flow resistance between fibres in tightly packed modules. As a result, compared to less densely packed modules, the residence time of liquid in the shell-side is higher in tightly packed modules, which decreases the driving force for mass transfer. This result agrees well with the Taskin et al. (Taskin et al., 2010)

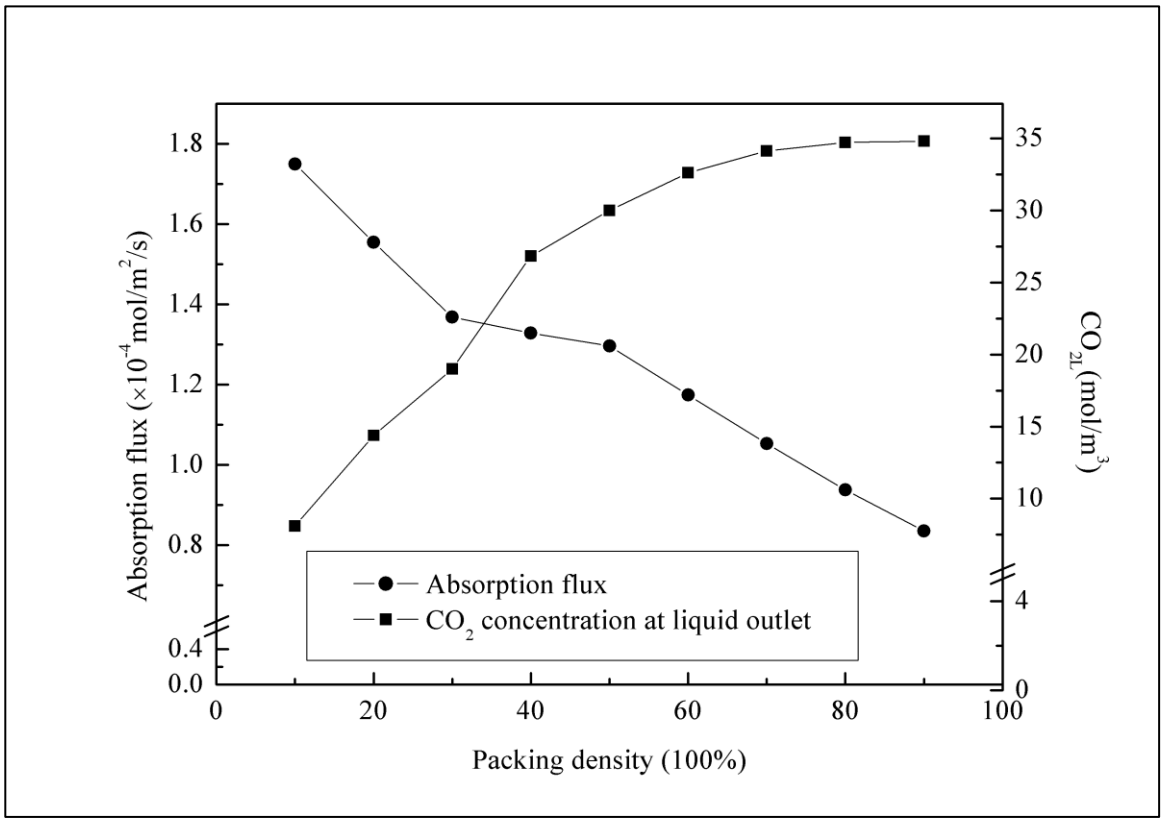

Figure 5.16: Effect of packing density on absorption performance (CO_{2Gin}=44.64 mol/m^3, Q_G=2.67×$10^{-5}$$m^3$/s, Q_L=0.85×$10^{-5}$$m^3$/s)

5.5 Conclusions

The complex nature of the liquid flow in the shell-side of a HFMC makes lab scale design and optimization challenging. A CFD model was developed to study the impact of various design parameters on the performance of a lab scale module. Porous medium approach was used to simulate the fibres and verified experimentally. The model was then applied to modules with different design configurations by varying operating conditions to study the effect of different design factors on gas absorption in cross flow membrane

contactors for performance enhancement. When operated under the same conditions, the rectangular module results in higher shell-side velocities and more uniform shell-side flow than the cylindrical module. The impact of module design factors such as shell configurations, inlet geometry, header geometry, fibre bed height and packing density on shell-side flow dynamics and absorption performance were also investigated. It was found that the overall shell-side velocity is a key controlling factor in the performance of lab scale cross flow modules and reduces the impact of shell-side flow distribution. This study also shows how CFD analysis can be effectively used in the design, scale-up, and operation of lab scale HFMC. The methodology developed here could be used to eliminate assumptions (such as constant velocity) which result in inadequate designs and potentially decrease time and costs associated with residence time distribution and other tracer tests when evaluating liquid flow characteristics in a lab setting.

Reference

Bhaumik, D., Majumdar, S., Sirkar, K.K., Absorption of CO_2 in a transverse flow hollow fibre membrane module having a few wraps of the fibre mat, Journal of Membrane Science, 138 (1998), 77-82

Catapano, G., Papenfuss, H.D., Wodetzki, A., Baurmeister, U., Mass and momentum transport in extra-luminal flow (ELF) membrane devices for blood oxygenation, Journal of Membrane Science, 184 (2001), 123-135

Dannström, H., Natural Gas Sweetening Using Membrane Gas/Liquid Contactors, presented at The 49th Annual Laurance Reid Gas Conditioning Conference, Norman, Oklahoma, 1999

Dindore, V.Y., Cents, A.H.G., Brilman, D.W.F.,Versteeg, G.F., Shell-side dispersion coefficients in a rectangular cross-flow hollow fibre membrane module, Chemical Engineering Research and Design, 83(A3) (2005), 317-325

Fill, B.J., Gartner, M.J., Johnson, G., Ma, J., Horner, M., Porous media technique for computational modeling of a novel pump-oxygenator, ASAIO Journal, 51 (2) (2006), 18A.

Frank, A., Lipscomb, G.G., Dennis, M., Visualization of concentration fields in hemodialyzers by computed tomography, Journal of Membrane Science, 175(2000), 239-251

Gabelman, A., Hwang, S., Hollow fibre membrane contactors, Journal of Membrane Science, 159 (1999), 61-106

Gage, K.L., Gartner, M.J., Burgreen, G.W., Wagner, W.R., Predicting membrane oxygenator pressure drop using computational fluid dynamics, Artificial Organs 26 (2002), 600-607

Jiao, A., Zhang, R., Jeong, S., Experimental investigation of header configuration on flow maldistribution in plate-fin heat exchanger, Applied Thermal Engineering, 23 (2003), 1235-1246

Karoor, S., Sirkar, K.K., Gas absorption studies in microporous hollow fibre membrane modules, Industrial & Engineering Chemistry Research, 32 (4) (1993), 674–684

Lipnizki, F., Field, R. W., Mass transfer performance for hollow fibre modules with shell-side axial feed flow: using an engineering approach to develop a framework, Journal of Membrane Science, 193 (2001), 195-208

Mat, N.C., Lou, Y., Lipscomb, G.G., Hollow fibre membrane modules, Current Opinion in Chemical Engineering, 4(2014), 18-24

Mazaheri, A.R., Ahmadi, G., Uniformity of the fluid flow velocities within hollow fibre membranes of blood oxygenation devices, Artificial Organs, 30 (1) (2006), 10-15

Park, J.K., Chang, H.N., Flow distribution in the fibre lumen side of a hollow fibre module. AIChE Journal, 32(1986), 1937-1947

Skelland, A.H.P., Diffusional Mass Transfer, John Wiley and Sons, New York, USA, 1974

Taskin, M. E., Fraser, K.H., Zhang, T., Griffith, B.P., Wu, Z. J., Micro-scale modeling of flow and oxygen transfer in Hollow Fibre Membrane Bundle, Journal of Membrane Science, 362(1-2) (2010), 172-183

Wickramasinghe, S.R., Semmens, M. J., Cussler, E.L., Mass transfer in various hollow fibre geometries. Journal of Membrane Science, 69(1992), 235-250

Yang, M.C., Cussler, E. L., Designing hollow-fibre contactors, AIChE Journal, 32 (11) (1986), 1910-1916

Yang, X., Wang, R., Fane, A. G., Tanga, C. Y., Wenten, I.G., Membrane module design and dynamic shear-induced techniques to enhance liquid separation by hollow fibre modules: a review, Desalination and Water Treatment, 51(2013), 16-18

Yang, X., Wong, R., Fane, A.G., Novel designs for improving the performance of hollow fibre membrane distillation modules, Journal of Membrane Science 384(1-2) (2011), 52–62

Zhang, J., Nolan, T.D.C., Zhang, T., Griffith, B.P., Wu, Z.J., Characterization of membrane blood oxygenation devices using computational fluid dynamics, Journal of Membrane Science, 288 (2007), 268-279

Zhang, L.Z., Li, Z.X., Zhong, T.S., Pei, L.X., Flow maldistribution and performance deteriorations in a cross flow hollow fibre membrane module for air humidification, Journal of Membrane Science, 427 (2013), 1-9

Zheng, J., Xu, Y., Xu, Z., Flow distribution in a randomly packed hollow fibre membrane module, Journal of Membrane Science, 211(2003), 263-269

Chapter 6

NUMERICAL STUDY OF GAS ABSORPTION-DESORPTION IN DUAL MEMBRANE CONTACTORS USING CFD MODELING

This chapter is based on and modified based on the following paper

Cai, **J.J.,** Hawboldt, K., Abdi, M.A., Numerical Study of Gas Absorption-Desorption with Dual Membrane Contactors Using CFD Modeling, *Chemical Engineering Journal*, under-review

As discussed in Chapter 5, the CFD modeling approach is an effective design tool to explore and evaluate novel design of cross flow HFMC used for gas absorption. In Chapter 5, the CFD model was used to investigate the impact of shell geometry on the shell side flow dynamics and the impact of shell geometry on the overall module performance. One critical assumption made to develop the model in Chapter 5 is that the partial pressure of target gas component from the gas source was constant across a cross sectional area (e.g. in the radial or y-direction). This assumption is useful for studying liquid flow dynamics, but would not be valid for actual operation, where locale mass transfer will impact overall rates. Therefore, in this chapter, the CFD model is expanded to model the local concentration profile in both fibre and shell side of the proposed dual membrane contactor.

In sections 6.1 and 6.2 the modified CFD model is outlined. In section 6.3, experiments are compared to modeled results to validate the model. In section 6.4, the model is used as a design tool to study the performance of HFMC with more complex geometries such as baffled modules and modules containing unevenly distributed fibre bundles.

6.1 Background

Currently, one of the most commonly used approaches to predict shell side flow and mass transfer module performance of cross flow membrane contactors is to develop empirical correlations for modules with specific designs (Yang et al., 1986; Gabelman et al., 1999; Dindore et al., 2005). This approach is effective in predicting overall module performance but cannot provide information on concentration profile and local concentration driving

force in the shell side. To gain an understanding of the driving force and concentration profiles within the module, Dindore et al. (Dindore et al., 2005) used an analytical approach based on heat transfer to describe the mass transfer in cross flow contactors. The heat transfer analogy tends to over-predict the module performance at the higher removal rates as the impact of volumetric flow is not accounted for in the model. In the same study, a numerical model was developed to describe and predict local concentration profiles taking into account shell-side mixing. This model however is limited to modules with solvent flowing in fibre side. In addition, the model cannot account for flow distribution in the shell, which has proved to be a critical factor in module performance. Hence, efforts are still needed in developing more rigorous models that can be used to predict shell side flow and performance of modules with complex geometries on shell side flow patterns.

Computational fluid dynamics (CFD) has been proven useful tool in characterizing shell side flow dynamics and mass transfer performance in membrane modules (Darcovich et al., 1997; Rezakazemi et al., 2011; Taskin et al., 2010). It can also be used to investigate the connection of module fabrication and processing engineering. Cai et al., (Cai et al., 2016) developed a CFD model as a screening design tool to evaluate the performance of cross flow membrane modules with various configurations. One critical assumption made in this study was that the partial pressure of target gas component from the gas source was constant across a cross sectional area (e.g. in the radial or y-direction). Though the proposed model was effective in predicting the overall performance of membrane module, the locale mass transfer could not be accurately reflected.

Liao et al. (Liao et al., 2003) attempted to simulate local mass transfer in membrane artificial kidney by coupling together shell-side, fibre-side, and transmembrane flows. Darcy's equations were employed to simulate shell-side flow, Navier-Stokes equations were employed to simulate fibre-side flow, and Kedem-Katchalsky (K-K) equations were used to approximate transmembrane flow. However, the computational domain of shell side did not include the inlet/out, only the membrane core. As such, the entrance effect of the inlet was not considered. For cross flow modules, entrance effects could significantly impact shell side flow and mass transfer, which should be accounted for in the process modelling. The K-K equations used to describe for trans-membrane flux were developed for the transport of a solvent and a single solute across a membrane which cannot be used to describe gas absorption into solvent through porous membranes. The hollow fibres were assumed to have uniform space between fibres whereas the impact of uneven fibre distribution on module performance was not considered.

The objective of this study is to develop a CFD model as a design tool to optimize the module design and enhance overall performance of cross flow membrane contactors used for gas absorption/desorption. The fibre bundle was treated as a porous medium in the CFD simulation for the shell side flow. An overall mass transfer coefficient correlation developed in this work which is present in Chapter 4 was incorporated into the CFD model. Gas flow in the fibre side was simulated in a separate CFD model. The two CFD models are coupled and solved using an iterative process (described below) to simulate mass transfer in the whole module. The combined CFD models were validated through experimental results obtained from a lab scale cross flow membrane module. Further, the

absorption performance of baffled modules and the module with unevenly distributed fibre bundles were also modeled using CFD analysis for the design purpose.

6.2 Materials and methods

The model was validated with experimental measurements from a lab scale dual membrane module (shown in Figure 6.1) by comparing the results of CO_2 absorption from CO_2/N_2 mixture. This module is composed of a rectangular inlet header, rectangular membrane core and outlet. A perforated plate is used between the inlet header and membrane core to improve shell side flow distribution. The specifications of the lab scale module can be found in Table 6.1. In contrast to conventional cross flow membrane modules, the membrane core in this module is composed to two types of fibres: porous polypropylene fibres and nonporous silicone rubber fibres, which are arranged in alternate rows. The porous membrane is used as an absorber for the targeted gas component to diffuse through while the nonporous membrane functions as a desorber through which the dissolved gas component is stripped out of solvent, driven by the differential pressure. The solvent flows in the shell side. The details of the mass transfer performance in this dual membrane module can be found in our previous studies (Cai et al., 2016).

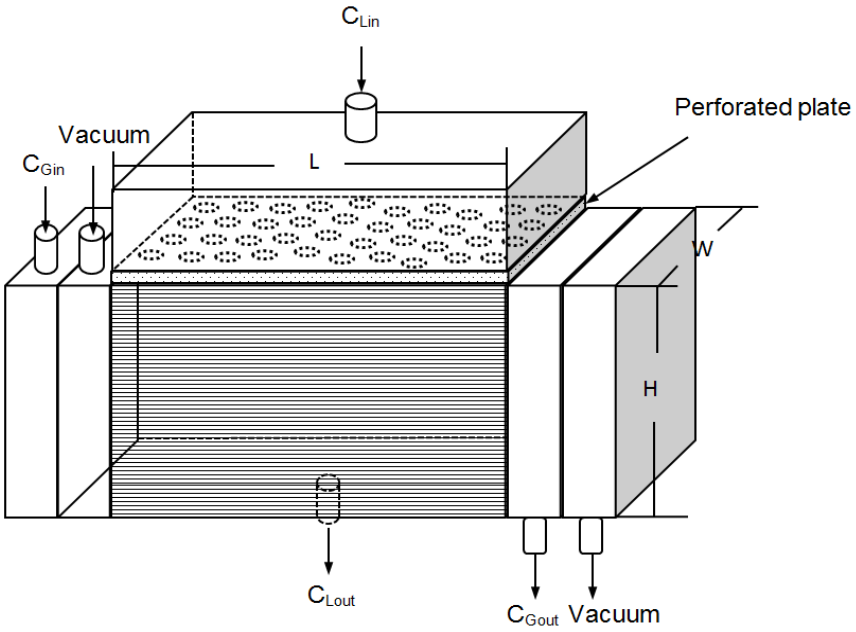

Figure 6.1: Schematic drawing of lab scale module

Table 6.1: Specifications of cross flow module and membrane properties

Dimension of membrane core (mm^3)	103×80×88
Height of header (mm)	5
Diameter of inlet/outlet (mm)	10
OD/ID of porous fibre (mm)	1/0.6
OD/ID of nonporous fibre (mm)	0.96/0.5
Void Fraction	0.93
Height of inlet header (mm)	48
CO_2 inlet port (mm)	6
CO_2 outlet port (mm)	6
water inlet port (mm)	6
water outlet port (mm)	6
Membrane surface area (m^2)	0.18

6.3 Mass transfer model

The model was developed based on the following assumptions:

1. Steady state in both shell and fibre side;
2. Ideal gas behavior is imposed;
3. The membrane pores are filled with gas mixture (non-wetted mode);
4. In shell side, the fibre bundle was modeled as a porous medium where the gas phase was treated as source term in the governing equation and defined on per-unit total volume.

These assumptions will be discussed in detail below.

6.3.1 CFD model for shell side flow and mass transfer

The shell side flow behavior is a function of the module inlet/outlet, membrane core and fibre arrangement. Ideally, the flow fields and local mass transfer inside the module should be modelled simultaneously. However, this is computationally expensive and time consuming due to the simulation of thousands of fibres individually. Therefore, in this study, the membrane core is treated as a porous media in the CFD simulation to predict the flow fields in shell side. That is, the fibre bundle (solvent, fibre walls and gas phase) was modeled as one lumped continuum (porous medium). Since the gas absorption was carried out in our lab scale dual membrane module with Reynolds numbers between 0.3 and 3 for all experiments, the shell side flow is laminar and the mass transfer in the shell side can be described with Navier-Stokes equations in the steady state as follows.

$$\rho(V \cdot \nabla)V + \nabla p = \nabla \cdot \bar{\tau} + \rho\bar{g} + S_r \qquad \text{Eq.6.1}$$

Where V, p, ρ, g and τ denote the velocity vector (m/s), the pressure (Pa), the density of the fluid (kg/m^3), the dynamic viscosity (kg/m/s), and gravitational force and stress tensor, respectively. The porous media is modeled by the addition of a momentum source term (S_r) to the standard fluid flow equations. The source term is composed of two parts: a viscous loss term (Darcy, the first part of Eq.6.2), and an inertial loss term (the second part of Eq.6.2) (Ergun 1952):

$$S_r = (-\frac{\mu}{C_1}v_i + \frac{1}{2}C_2\rho V_{mag}v_i) \qquad \text{Eq.6.2}$$

Where μ is the dynamic viscosity, V_{mag} is the magnitude of local superficial velocity vector. i (i = 1, 2, 3) is the coordinate direction. The permeability (C_1) and inertial loss coefficient (C_2) were estimated by the following equations (Ergun, 1952):

$$C_1 = \frac{d_0^2}{140}\frac{\varepsilon^3}{(1-\varepsilon)^2}, C_2 = \frac{3.5}{d_0}\frac{(1-\varepsilon)}{\varepsilon^3} \qquad \text{Eq.6.3}$$

Where d_0 is the outside diameter of the hollow fibres, and ε is the porosity of the fibre bundle.

The specifications of the crossflow dual membrane module can be found in Chapter 4.

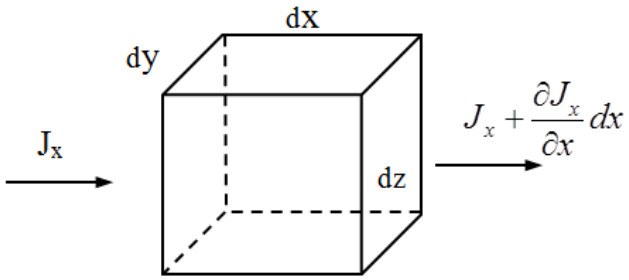

Figure 6.2: A Cartesian control volume in the porous media for derivation of the species conservation equation.

For a fluid control volume shown in Figure 6.2, mass balance equation can be established as follows:

$$\sum J_D + \sum J_C + \sum J_S - \sum J_r = \sum J_\Delta \qquad \text{Eq.6.4}$$

Where J_D is the mass transfer by diffusion; J_C is the mass transfer by convection; J_S is the target gas component source from the gas-phase; J_R is the mass transfer rate of dissolved target gas stripped out of solvent; J_Δ is the rate of mass production within the control volume. At the steady state, the above equation can be derived and simplified into Eq.6.5:

$$\vec{v} \cdot \nabla C_L = D_{eff} \nabla^2 C_L - r_1 \qquad \text{Eq. 6.5}$$

Where C_L refers to the concentration of target gas in solvent (mol/m^3); v is the superficial velocity vector (m/s), D_{eff} (m/s) is the effective gas diffusivity in the porous medium and defined as $D_{eff} = \varepsilon D$, where D is the diffusivity of target gas in solvent. S_r is the source term and represents the solute from gas phase to liquid per unit volume (Eq.6.6); r is the sink term representing the dissolved gas stripped out of solvent (Eq.6.7); The porous

media was approximated by the Ergun equation. For a simple homogeneous porous media, a momentum source term is added in the governing momentum equations:

$$S_G = kA_P(HC_G - C_L) \quad \text{Eq. 6.6}$$

$$r = kA_{NP}(C_L - C_{SNP}) \quad \text{Eq. 6.7}$$

Where A_P and A_{NP} are porous and nonporous fibre membrane surface areas per unit volume; k (m/s) is the overall mass transport coefficient in liquid phase; C_L and C_{SNP} (mol/m^3) are concentrations of target gas in liquid and at the surface of fibre, respectively. Mass transfer of target gas stripped out of solvent is mainly driven by the differential pressure across the nonporous membrane; therefore, C_{SNP} is a function of pressure in nonporous fibre which can be calculated using Eq.6.8. The derivation of this equation can be found in the details in our previous work (Cai et al., 2010).

$$C_{SNP} = \frac{C_L + \frac{k_{per}}{kt_{NP}} P_{out}}{1 + kt_{NP}\frac{RT}{H}} \quad \text{Eq.6.8}$$

Where, k_{per} denotes nonporous permeability for the gas contaminant and t_{NP} is the membrane thickness; P_{out}, R, T and H represent the pressure in nonporous fibre (Pa), ideal gas constant (m3Pa/K/mol), Temperature (K) and Henry's constant, respectively.

The overall mass transfer coefficient (k) of hollow fibre membrane contactor mainly depends on the fibre arrangement, module geometry and shell side flow dynamics and is

calculated using the Sherwood number, which is expressed as an empirical correlation in the format shown in Eq. 6.9 (Vargaftik et al., 1987) for cross flow HFMCs.

$$Sh = \alpha Re^{\beta} Sc^{0.33} \qquad \text{Eq. 6.9}$$

Where α=0.78, β=0.526 are constants determined by fitting experimental results from our lab scale dual membrane module (Cai et al., 2016). The Schmidt (*Sc*) number is calculated by dividing the diffusion coefficient (of solute in solvent) with the viscosity of the solvent. Reynolds number is given by Eq. 6.10

$$\mathrm{Re} = \frac{d_o h \cdot V_i}{v} \qquad \text{Eq. 6.10}$$

Where *Re* is Reynolds number, v stands for kinematic viscosity of solvent and V_i represents the interstitial velocity in the fibre bundles, which can be estimated using the average velocity across the porous media of fibre bundle.

Therefore, mass transfer coefficient *k* can be then calculated as below:

$$Sh = \frac{k d_h}{D} \qquad \text{Eq.6. 11}$$

Where *D* is diffusivity coefficient of solute in the solvent; d_h is the hydraulic diameter. Hewiit et al. (Hewiit et al., 1998) determined for a packed fibre bundle, with $\varepsilon<0.5$, the hydraulic diameter can be expressed as the outer diameter of an individual fibre, d_o, and the fibre bundle porosity ε: $d_o=dh(\varepsilon/(1-\varepsilon))$; For a less densely packed fibres $\varepsilon>0.5$, the hydraulic diameter is more accurately described by d_o.

6.3.2 CFD model for fibre side flow and mass transfer

The arrangement of two types of fibre membrane is shown in Figure 6.3.

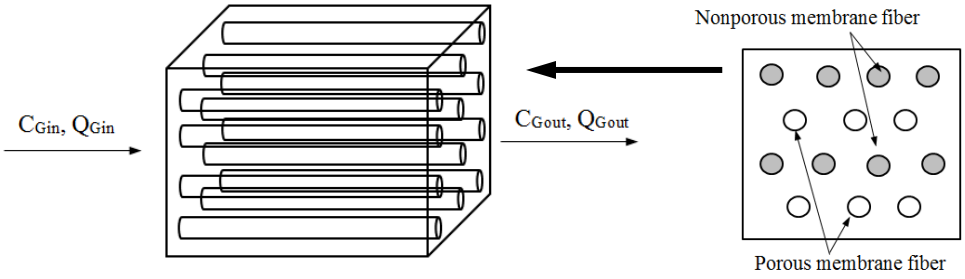

Figure 6.3 : Schematic of fibre bundles in the shell side of cross flow dual membrane module

The flow through porous and porous membrane is shown in Figure 6.4.

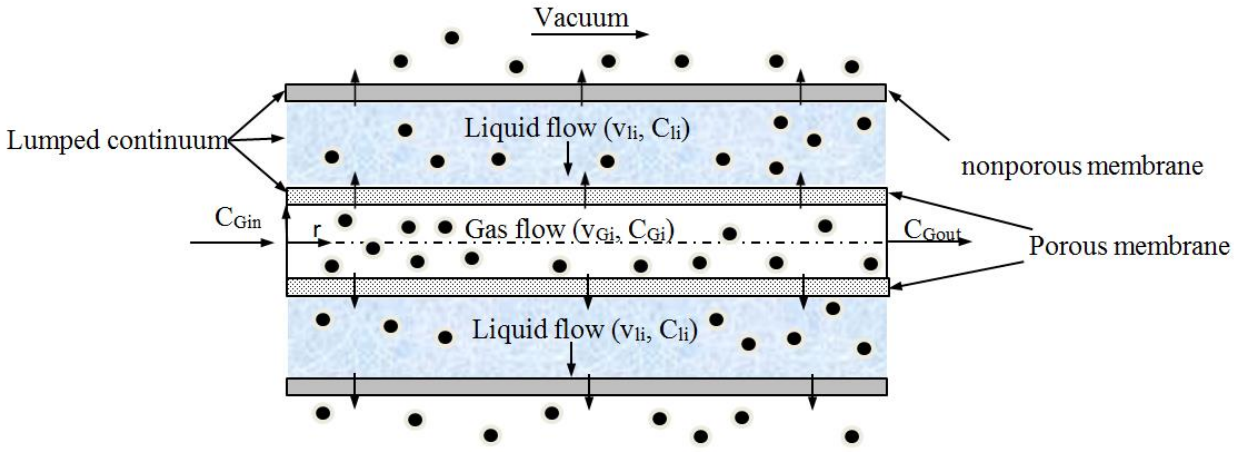

Figure 6.4 : Schematic drawing of computational domain for fibre side in the cross flow dual membrane contactor

The purpose of the model is not to simulate the non-porous membrane removal independently but rather the impact of liquid flow dynamics on the removal rate. As such,

to save computational time the liquid and non-porous fibres are grouped together as a sink term (see below). The mass transfer of solute from gas phase can be described by a modified convection-diffusion equation shown in Eq.6.12. That is, the mass transfer rate in the porous fibre side is determined by convection and diffusion in the gas phase and diffusion through the membrane wall and liquid layer.

$$\vec{v} \cdot \nabla C_G = D_{eff} \nabla^2 C_G - r_2 \qquad \text{Eq.6.12}$$

Where v is the velocity vector of gas phase which can be calculated by solving the momentum equations of gas phase in the fiber side (m/s), r_2 is the sink term and represents target gas diffusing into the solvent/non-porous fibres:

$$\mathrm{r}_2 = -kA_p(HC_G - C_L) \qquad \text{Eq.6.13}$$

The overall mass transfer coefficient is determined through an empirical correlation developed in our previous studies (Cai et al., 2016)

At the inlet of fiber side, the concentration of target gas component was kept constant for each fiber, which can be used as the boundary condition to solve Eq. 6.12.

$$C_G = C_{Gi}\text{, at x=0} \qquad \text{Eq.6.14}$$

6.3.3 Solution methodologies and computer algorithm

The computational domain of the lab scale cross flow module was generated using computer-aided design software (Workbench from ANSYS). The computational domain is then divided into a mesh. The resolution of the final mesh was determined varying grid

resolutions (coarse to fine) to ascertain that the results were grid-independent and converged quickly. Fluent (v6.2.16, ANSYS, U.S.A.), was used to solve the governing transport equations.

The overall solution algorithm is outlined Figure 6.5. The equations describing shell side flow are solved first to calculate the distribution of velocity and concentration in the shell side. Since the initial concentration distribution in the gas phase is unknown, for the first iteration the concentration in the gas phase is assumed to be constant along the length of the fibre and equal to the inlet concentration. The velocity and concentrations obtained from shell side CFD model are used as input to the fibre side CFD model. The fibre side CFD model is then run and updated gas concentration profiles in the fibres side (C_G). The results are fed back to the shell CFD model to generate updated concentrations in the liquid. This process is repeated until the gas concentration in the liquid and gas phase converge. The convergence criterion is set as $(C^{n+1}-C^n)/C^n<10^{-6}$. Parameters and physical constants used in this study are summarized in Table 6.2.

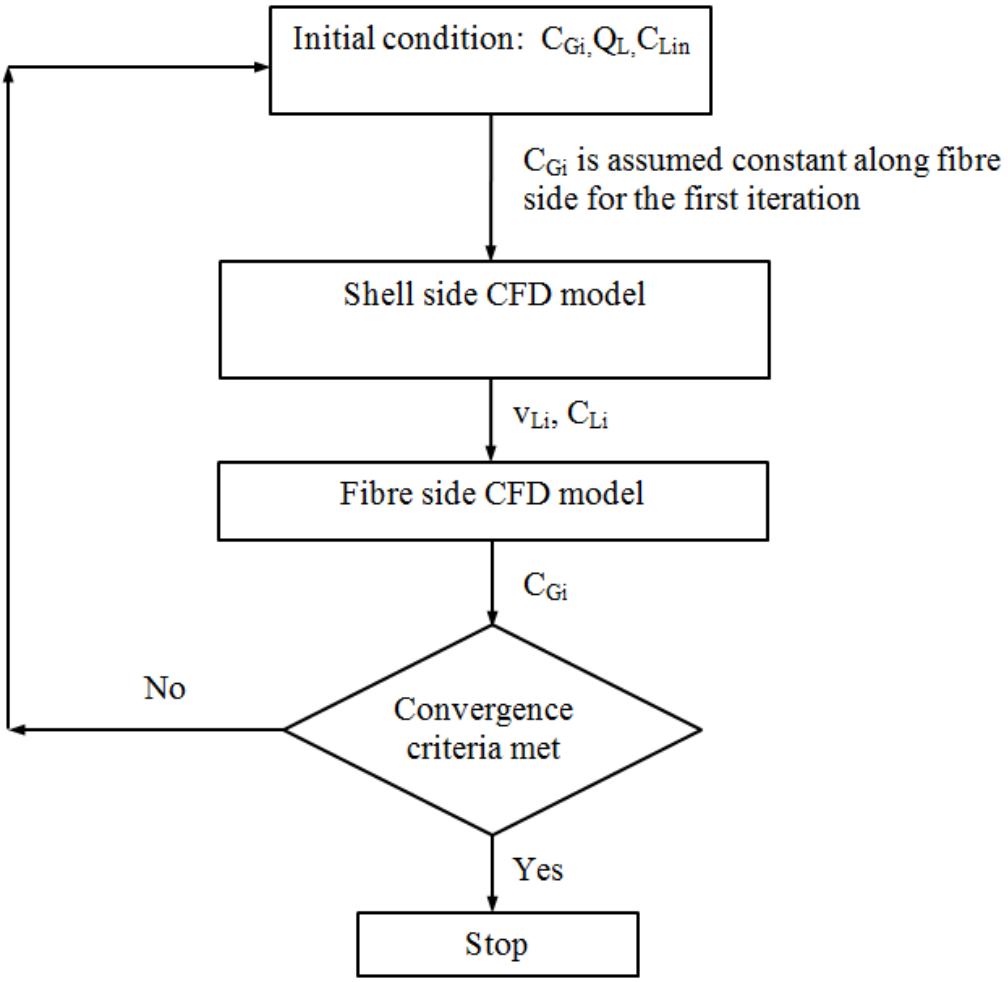

Figure 6.5 : Flow chart of computer algorithm.

Table 6.2: Physical and transport properties of the hollow fibre membrane cores

Parameter	Value (Data for 298K)	Reference
Water (solvent)		
Density (ρ)	995 kg/m^3	Ref. (Vargaftik 1987)
Dynamic viscosity (v)	1×10^{-6} kg/(m s)	Ref. (Vargaftik 1987)
Henry's constant (H) for CO_2 in water	0.82 (C_L/C_G) equilibrium)	Ref. (Vargaftik 1987)
Diffusivity (D) for CO_2 in water	2×10^{-9} m^2/s	Ref. (Vargaftik 1987)

6.4 Experimental validation

The membrane core contains two type of fibres, polypropylene (PP) fibre (for gas flow into system) and silicone rubber tubing (for partial regeneration of solvent). The porous PP fibre (Q3/2 membrane) purchased from Membrana GmbH has an outside diameter of 1,000 μm and inside diameter of 600 μm and a maximum pore size of 0.64 μm. Silicone rubber tubing from Dow company has outside diameter of 900 μm and inside diameter of 500 μm. Separate inlets and outlets were designed for gas absorption and stripping in the module, respectively. The details of module specifications are given in Table 6.3.

Table 6.3: Module specifications of cross flow dual membrane module

Module length (mm)	103
Module width (mm)	80
Module height (mm)	80
Porous membrane area (m^2)	0.18
Nonporous membrane area (m^2)	0.0832
Voidage	0.85
Height of the header (mm)	20
Size of perforated holes (mm)	4
Height of perforated plate (mm)	2

The experimental set-up to evaluate the performance of dual membrane contactor is shown in Figure 6.6. CO_2 was used as the targeted component to be removed from a gas stream of CO_2/N_2 mixture. Solvents tested included distilled water and propylene carbonate (Sigma- Aldrich).

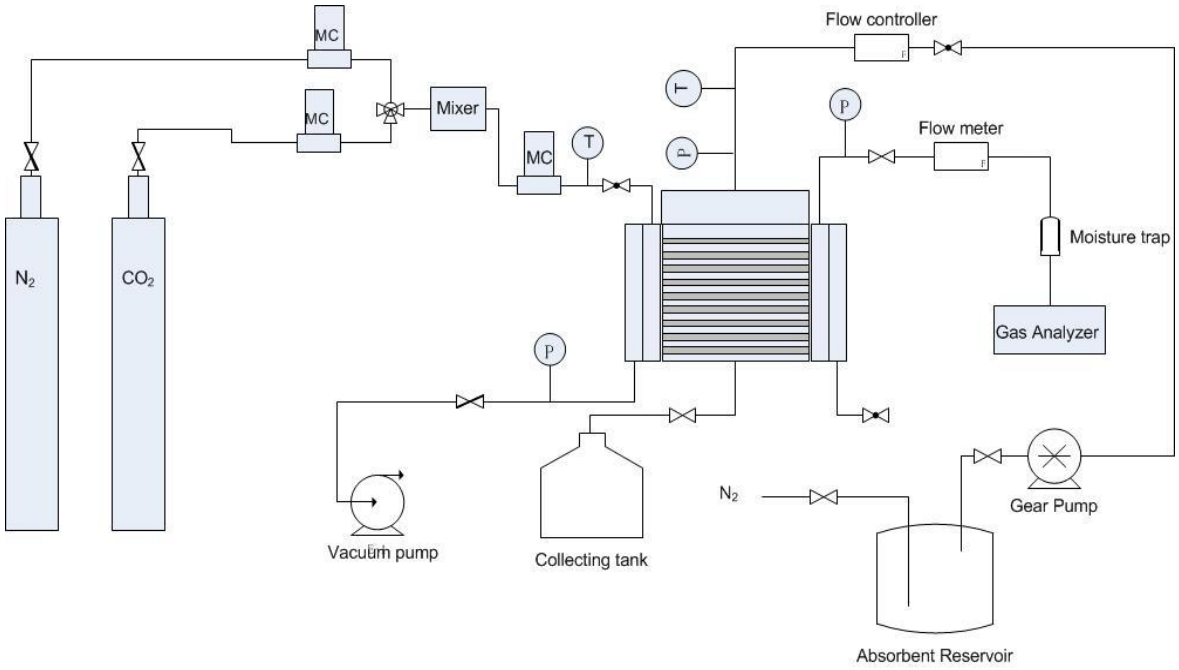

Figure 6. 6 : Experimental set-up for CO_2 absorption in dual membrane contactor

In all experiments, the liquid phase was continuously fed into the shell side through a gear pressure pump and liquid flow rate was controlled by a digital mass flow controller. The solvent was stripped off CO_2 by bubbling N_2 before use. The inlet temperature and pressure of the liquid phase were monitored throughout the experiments. To avoid gas bubbling, the pressure on the liquid side was always slightly higher than that of gas phase. The N_2 and CO_2 are premixed and the mixed gas temperature, pressure and flowrates were monitored by a high-precision mass flow controller (Alpha Controls Model No. MFC-50LPM-D). A vacuum was maintained in the nonporous fibres and the pressure was monitored using a PM930SD pressure indicator (Cole-Parmer) and controlled using a high precision needle valve. The pressure difference between the two phases was monitored in all experiments. The CO_2 was measured through portable Oxybaby®6.0

CO_2 gas analyzer at gas inlet and outlet. The average CO_2 concentration in liquid was measured via titration.

6.5 Results

6.5.1 Experimental validation of CFD model

Experiments were carried out in our lab scale module for CO_2 removal from a gas mixture of N_2/CO_2 using water as solvent. Two sets of experiments were carried out using gas mixtures containing 5% and 30% CO_2 respectively. The experimental results were compared with the simulation results from CFD analysis in terms of CO_2 concentration at gas outlet and liquid outlet. As shown in Figure 6.7, the modelled results agree well with experimental results. In general, the outlet gas concentration decreases as liquid flow rate increases due to the fact that the mass transfer resistance resides in the liquid phase is reduced by increasing the circulating rate of liquid flow.

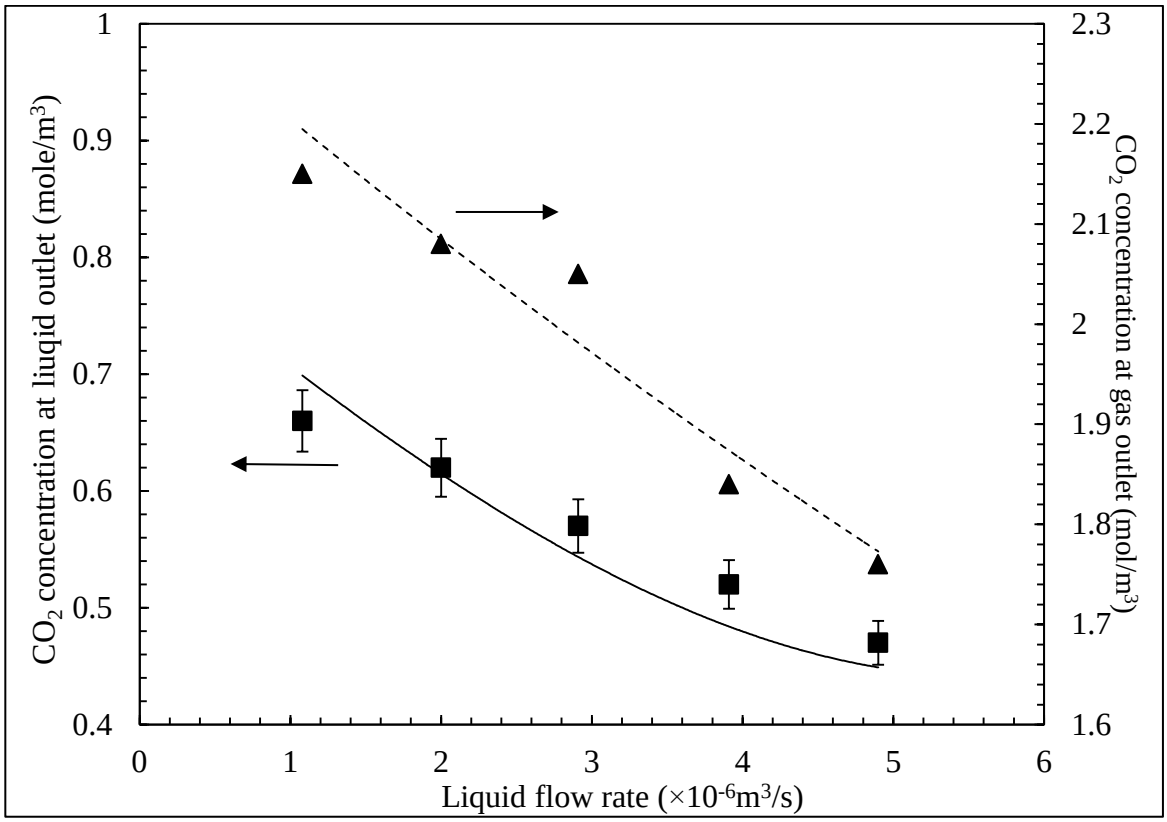

Figure 6.7: A comparison of modelled results with experimental measurement

(CO_{2in}%=5%, Qg=5.6×$10^{-6}$$m^3$/s)

In cross flow mode, the CO_2 concentration not only varies along the fibre length, but also varies with the module height. Therefore, the concentration in Figure 6.7 is an averaged concentration at the gas outlet. The CFD model was further verified by comparing the modelled results for absorption operated under different gas flow rates. CO_2 concentration in feed gas was kept constant at 5%. The CO_2 concentration from experiments at gas outlet and liquid outlet are compared with CFD model results in Figure 6.8 and 6.9, respectively. The predicted concentration in both phases is in a good agreement with experimental results. These two plots further validate the CFD model.

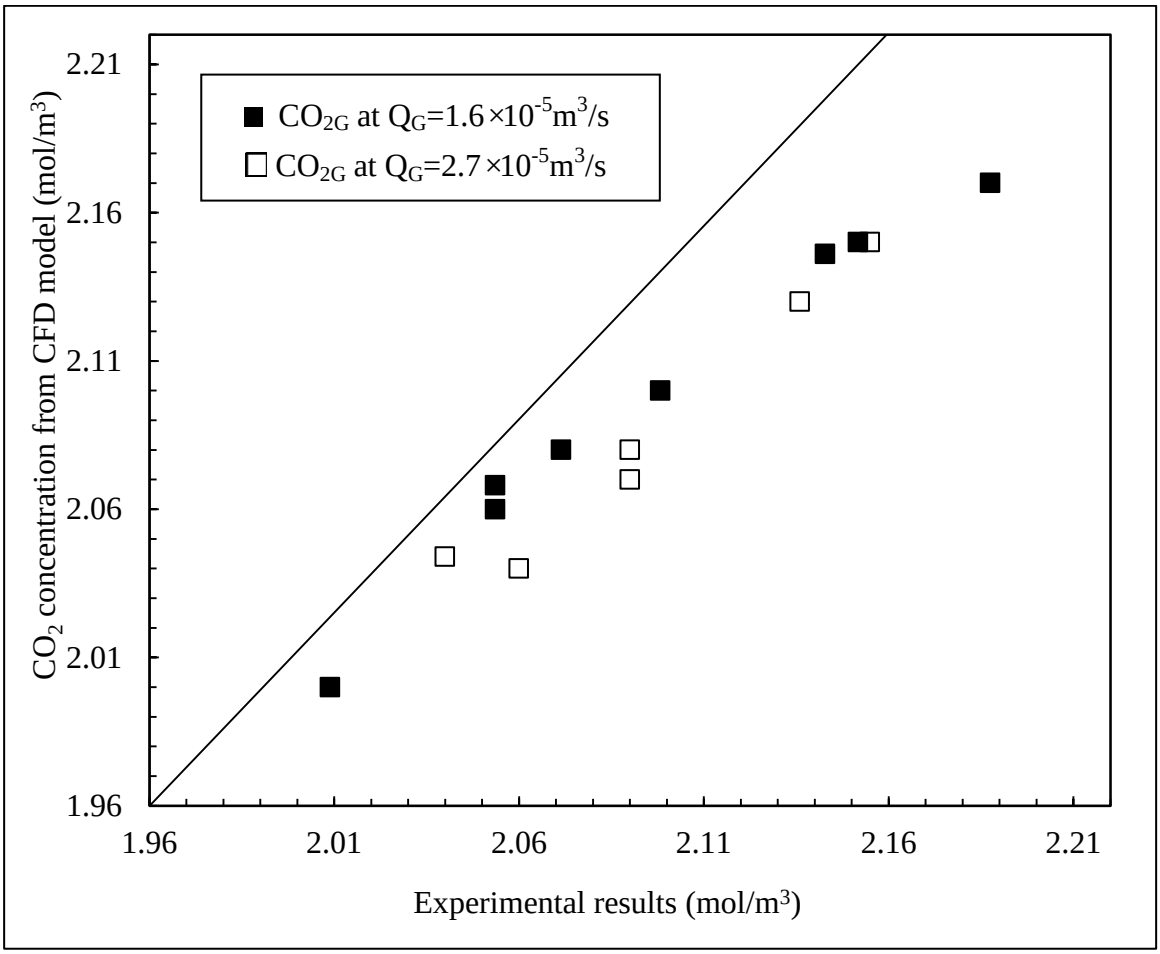

Figure 6.8: Comparison of CO_2 at gas outlet between experiment and CFD model (CO_{2in}%=5%, Q_L was varied from 10^{-6}m^3/s to 8.33×10^{-6}m^3/s)

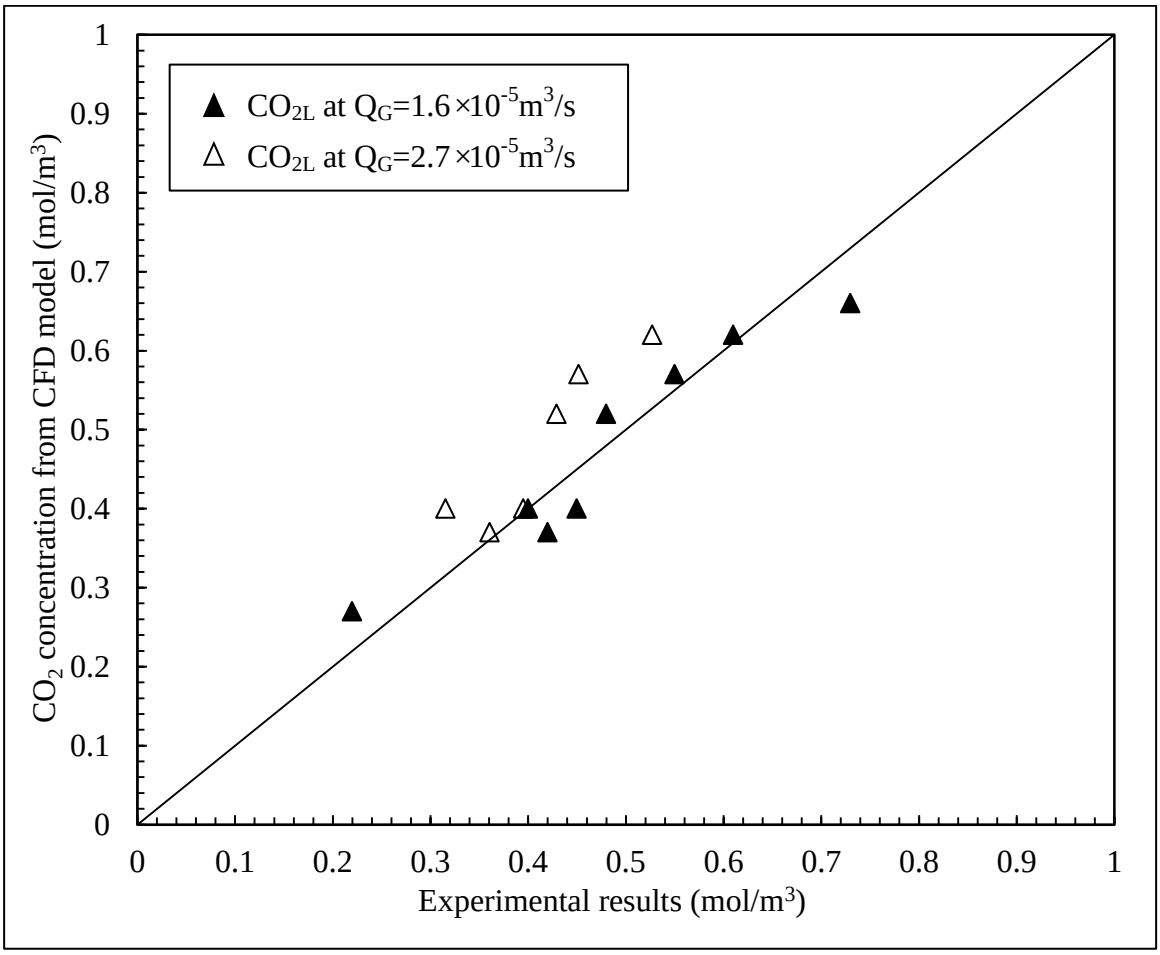

Figure 6.9: Comparison of CO_2 at liquid outlet between experiment and CFD model.

CO_{2in}%=5%, Q_L was varied from 10^{-6}m^3/s to 8.33×10^{-6}m^3/s)

The distribution of velocity and concentration is important with respect to scale up and optimization. A cross sectional view of CO_2 concentration distribution predicted by the CFD model through the fibre bundle along the centreline is shown in Figure 6.10 for a liquid flow rate of 6.6 $\times10^{-6}$m^3/s. The concentration profile is not uniform as the concentration in the center is lower than at the module boundary, which is mainly caused by the entrance effect. This is not unexpected however, the question is does this effect

module performance, as these effects would only be enhanced with scale-up. The following sections investigate these effects.

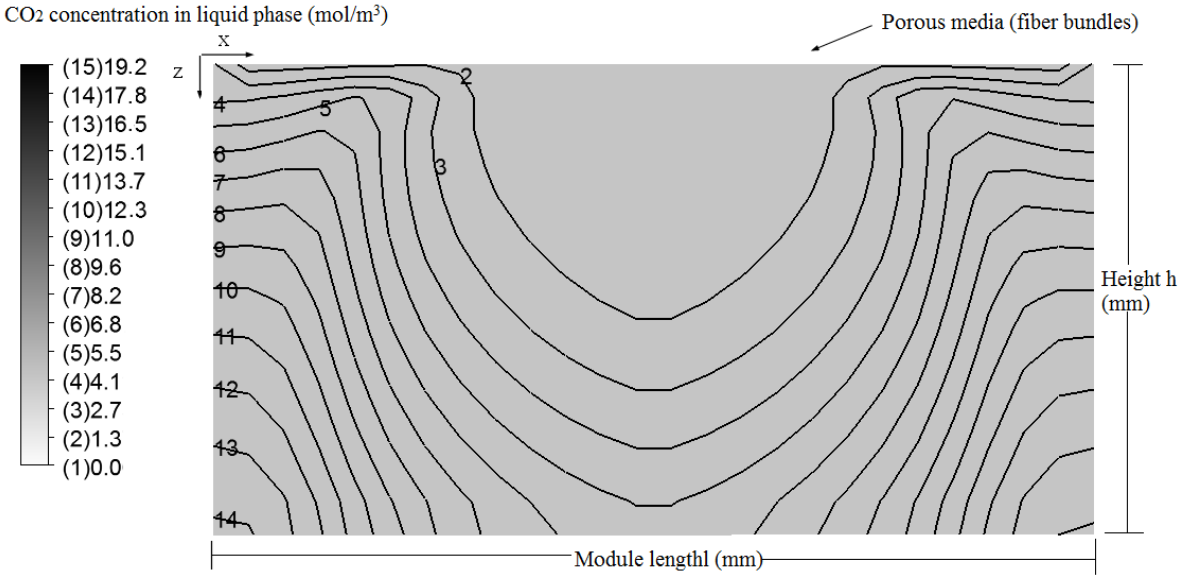

Figure 6.10 : CO_2 concentration distribution (mol/m^3) in porous media (fibre bundles)

(CO_{2in}%=30%, Q_L=6.6 ×$10^{-6}$$m^3$/s, Q_G=5.6×$10^{-6}$$m^3$/s)

6.5.2 Performance comparison of dual membrane contactor and absorption column

Performance comparisons between packed columns and membrane contactor have been reported in the literature by several authors, however most of these work mainly focused on the gas absorption whereas the solvent regeneraton was not inlcuded in the scope. To demonstrate the advantage of dual membrane contactor in terms of its capability in size reduction and reducing solvent consumptionf, the performance of the proposed dual membrane contactor was compared with that of a lab scale packed column for CO_2 absorption. The lab scale packed column (CE-400) used in this study was manufactured

by GUNT®. The system was composed two packed absorption column and desorption column as present in Figure 6.11 with the basic specifications of the absorption column are listed in Table 6.4.

Table 6.4: Specifications of CE-400 absorption column and operation conditions

Height (absorption column)	2×750 (mm)
Height (desorption column)	750 (mm)
Inner diameter (absorption column)	80 (mm)
Inner diameter (desorption column)	80 (mm)
Packing material	Glass raschig rings
Size of raschig rings (Diameter×Length)	10×10(mm)
Interficial area/Volume	0.014
Gas flow rate	7.5(L/min)
CO_2 concentration	10.5%
Temperature	293K

CO_2 absorption was carried out in CE-400 absorption column using water as solvent. The feed stream is a mixed gas of CO_2 and air where the concentration of CO_2 was kept constant at 10.5%. The liquid flow rate was varied from 100 L/hr to 500L/hr. CO_2 concentration at gas inlet and out were measured using Oxybaby® CO_2 analyzer.

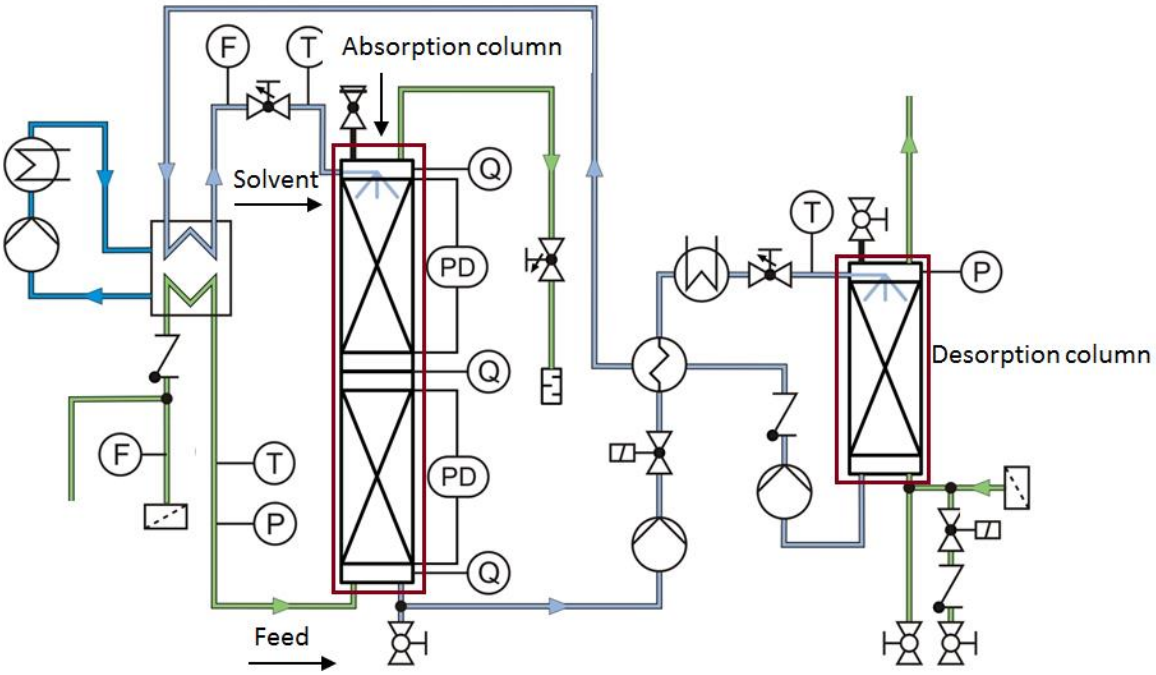

Figure 6.11: Experimental set-up of lab scale packed column for gas absorption (CE-400 Gas absorption column, manufactured by G.U.N.T, Germany)

To compare to the packed column in terms of the size and the consumption of solvent, the performance of dual membrane contactor containing the equivalent amount of interficial area were examined through modelling approach. Figure 6.12 compares the liquid flow rates required to achieve the same CO_2 removal rate in packed column and dual membrane contactor, respectively.

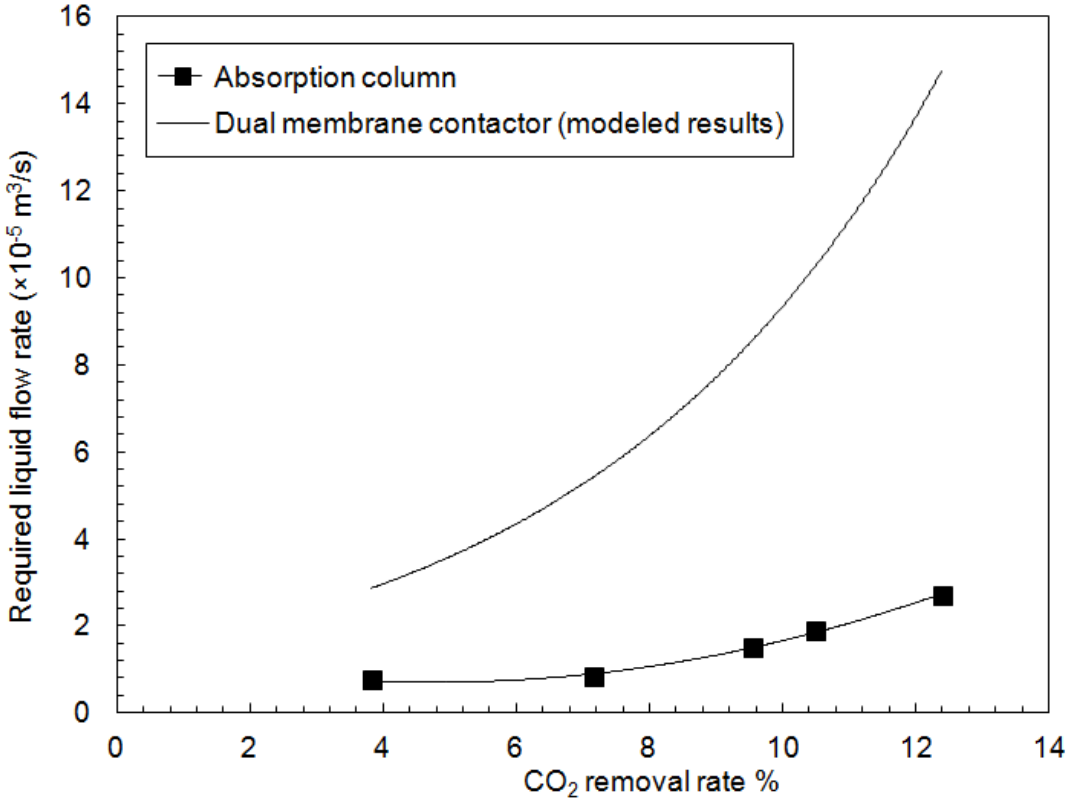

Figure 6.12: Performance of packed column compared to dual membrane contactor for CO_2 absorption

For CO_2 removal rate of 4%, the required liquid flow rate in packed column is 3.8 times of that in dual membrane contactor and it increases as removal rate increases. This result was based on the assumption that the packing fraction of dual membrane contactor is 15%, which was meant to keep consistant with the module fabricated in this study. In this case, the volume of the dual membrane contactor is much smaller, which only takes up to 23.6% of that of packed column. The difference however can be enlarged by increasing the packing density of fiber membrane in the contactor. As shown in Figure 6.13, the volume required for the dual membrane contactor is continuesly reduced as the packing

density increases from 15% to 75%. It further confirms its compatability and the advantage in terms of reduced solvent ,compared to the traditional packed column.

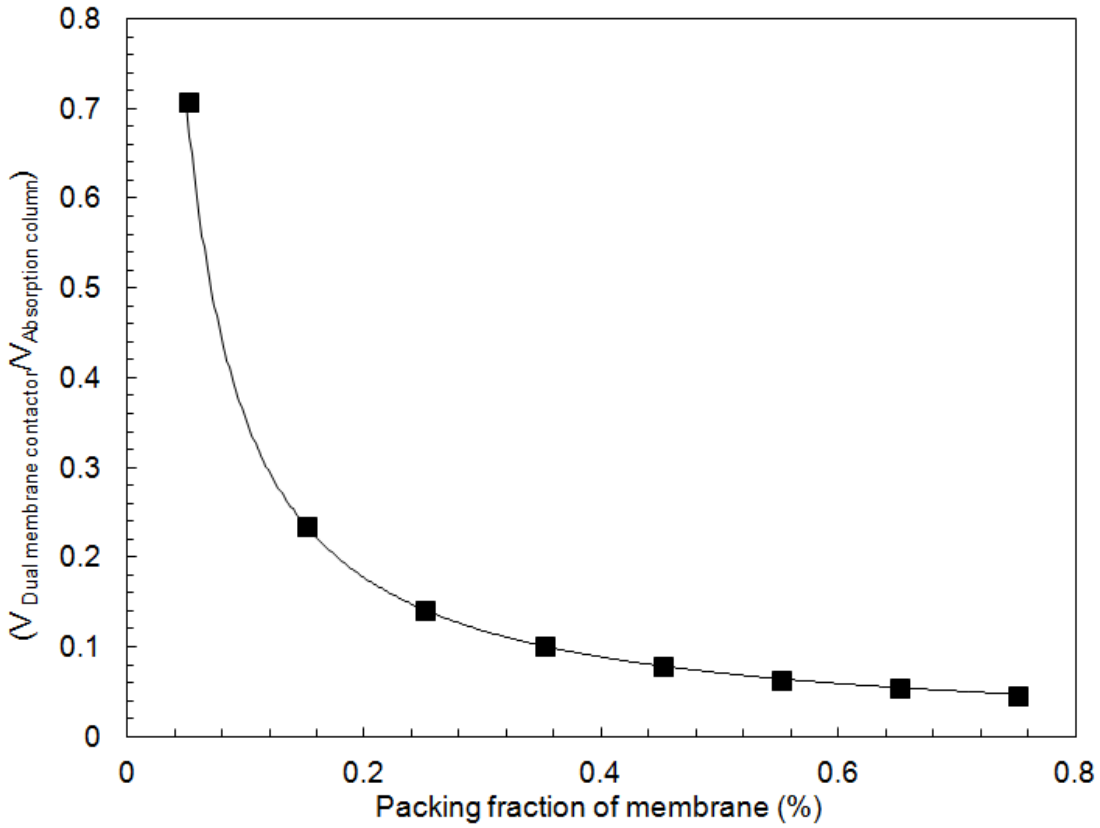

Figure 6.13: The volume of dual membrane contactor with various packing density compared to that of packed column

6.5.3 CFD application to design

The validated CFD model was applied to determine the impacts of various design parameters. One commonly used approach to improve shell side distribution and hence improve module performance is to add baffles into the shell side (Wang et al., 1993). Wang et al. (Wang et al., 2003) constructed a series of baffled modules and examined

their performance in toluene stripping from water. It was found that the baffled modules offer significant improvement in absorption performance over most conventional module geometries. However, the effect of baffles on the shell side flow and concentration distribution has not been studied extensively.

Modules with different numbers of baffle were modeled (Figure 6.14). These models have the same specification as the un-baffled lab scale module. The thickness of the fibre is 1mm.

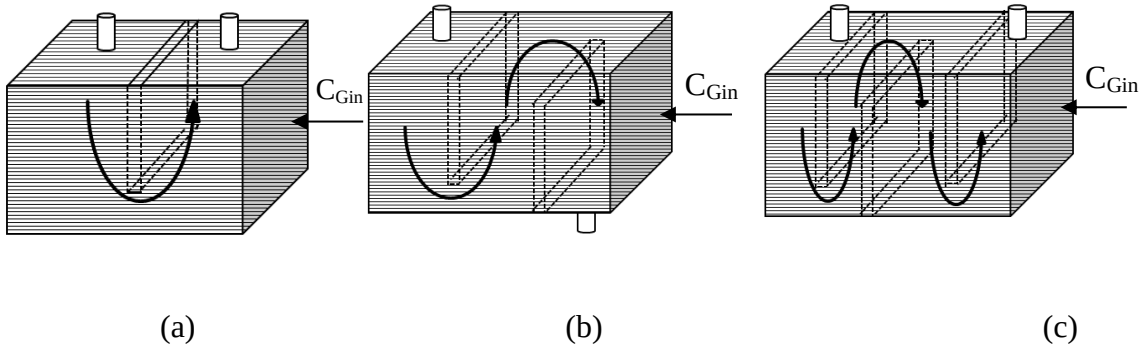

Figure 6.14: Schematic of baffled modules (a) module with 1 baffle; (b) module with 2 baffles; (c) module with 3 baffles

The CFD model was used to simulate the baffled modules with CO_2-N_2 mixed gas containing 30% CO_2 using water as solvent. The gas flow rate was kept constant at 1.8×10^{-5} m^3/s while the solvent flow rate was varied from 1.4×10^{-6} m^3/s to 2.8×10^{-5} m^3/s. The effect of baffles on module performance is shown in Figure 6.15 by varying the numbers of baffles in the module. In general, the absorption flux is improved as the number of baffles increases in the shell side. At high flow rates, the enhancement of performance due to the baffles is more pronounced than that at lower flow rates.

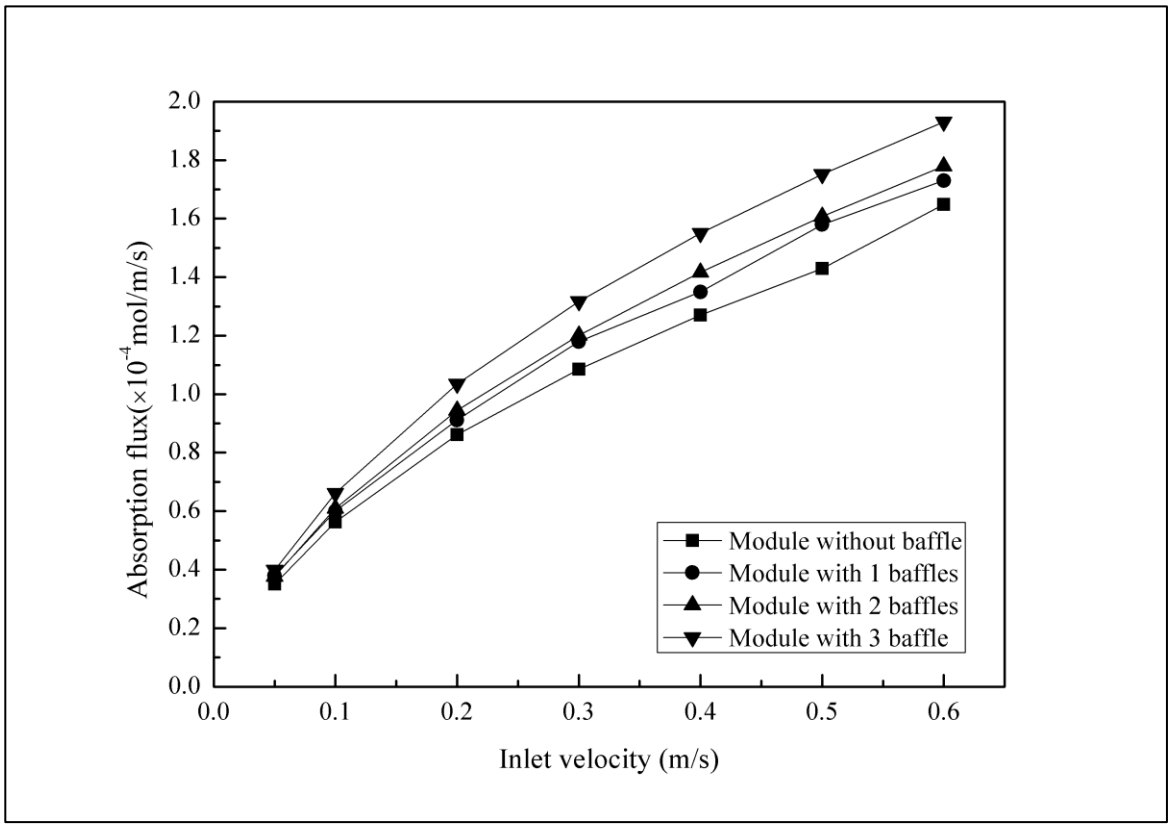

Figure 6.15: Effect of baffle numbers on absorption flux (CO_{2in}%=30%, Q_G=5.6×10^{-6}m^3/s)

Adding more baffles adds cost to modules; therefore there is a balance between enhanced performance and expense. Figure 6.16 summarizes the impact of number of baffles on performance for a feed gas containing 30% and 100% CO_2 respectively while the gas flow rate and liquid flow rate was kept at 5.6×10^{-6}m^3/s and 5.6×10^{-6}m^3/s respectively. Overall, the absorption flux for absorption of concentrated gas (100% CO_2) is higher than absorption of dilute gas (30% CO_2), due to the higher concentration gradient. However, the effect of baffles on module performance is less significant for dilute gas systems.

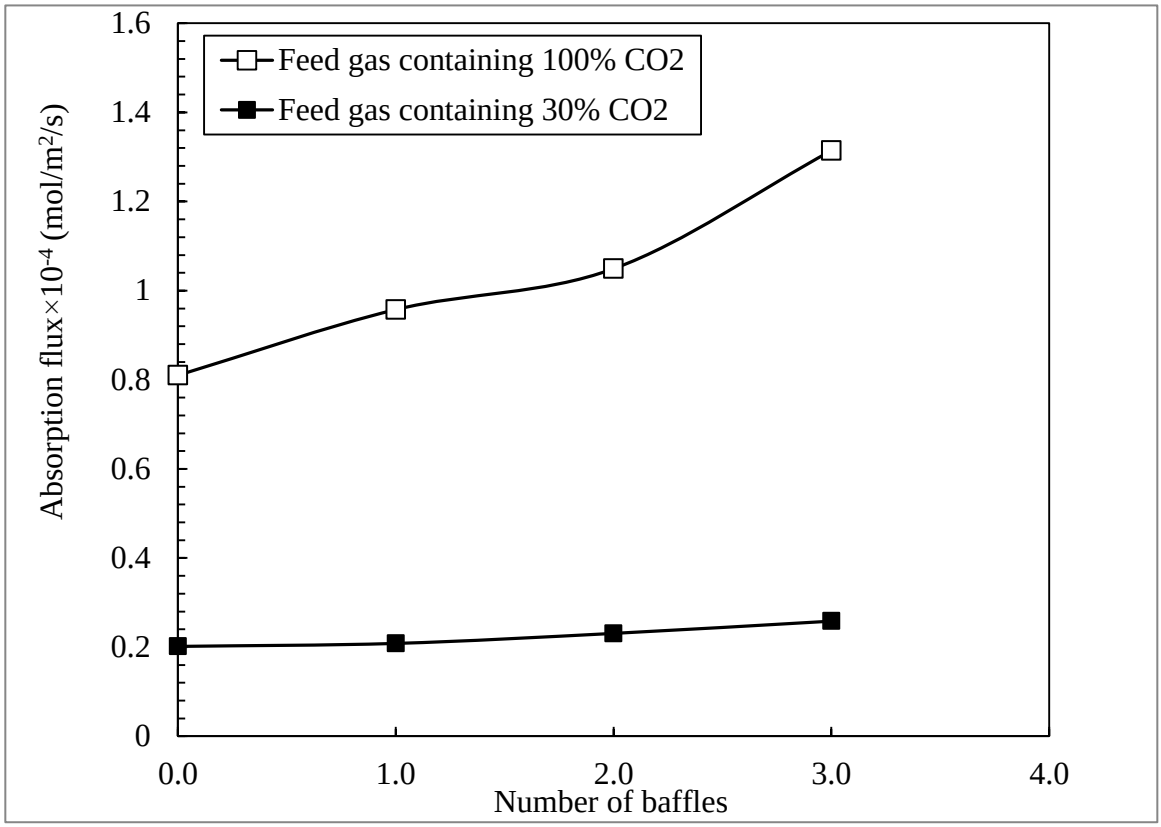

Figure 6. 16: Effect of solute concentration on the performance of baffled module for CO_2 absorption ($Q_G=5.6\times10^{-6}m^3/s$, $Q_L=5.6\times10^{-6}m^3/s$)

6.5.4 The effect of fibre arrangement on mass transfer

One critical design parameter in HFMC is the distance between fibres and the fibre arrangement. For loosely packed modules, fibres can be potted one by one and therefore achieve uniform fibre distribution (i.e. equal distance between each fibre). However, fibres are usually non-uniformly distributed in tightly packed modules. Wang et al. (Wang et al., 2003) studied the shell side flow in a parallel flow module through residence time distribution (RTD) tests and found that the flow was approximated by plug

flow in loosely packed modules. Deviation from plug flow increased as the packing density increased until it reached 50% at which point the flow regime began to once again approximate plug flow (Wang et al., 2003). The proposed cause for the deviation from plug flow was the non-uniform fibre distribution. To study the effect of fibre distribution, a constant local (and overall) packing density was compared with the module with varied local packing density. To achieve variable local packing density the CFD model membrane core was divided into three sections with different local packing densities (8%, 13%, and 20%). The overall packing density was 15% for both cases. The feed gas flow rate was kept constant at $5.6\times10^{-6}m^3/s$ and liquid flow rate varied from 1.33×10^{-5} to 1.6×10^{-4} m^3/s. Figure 6.17 outlines the results. Similar to the observations from Wang et al. (Wang et al., 2003), the cross flow module with variable local packing densities did not perform as well compared to a module with uniform packing density.

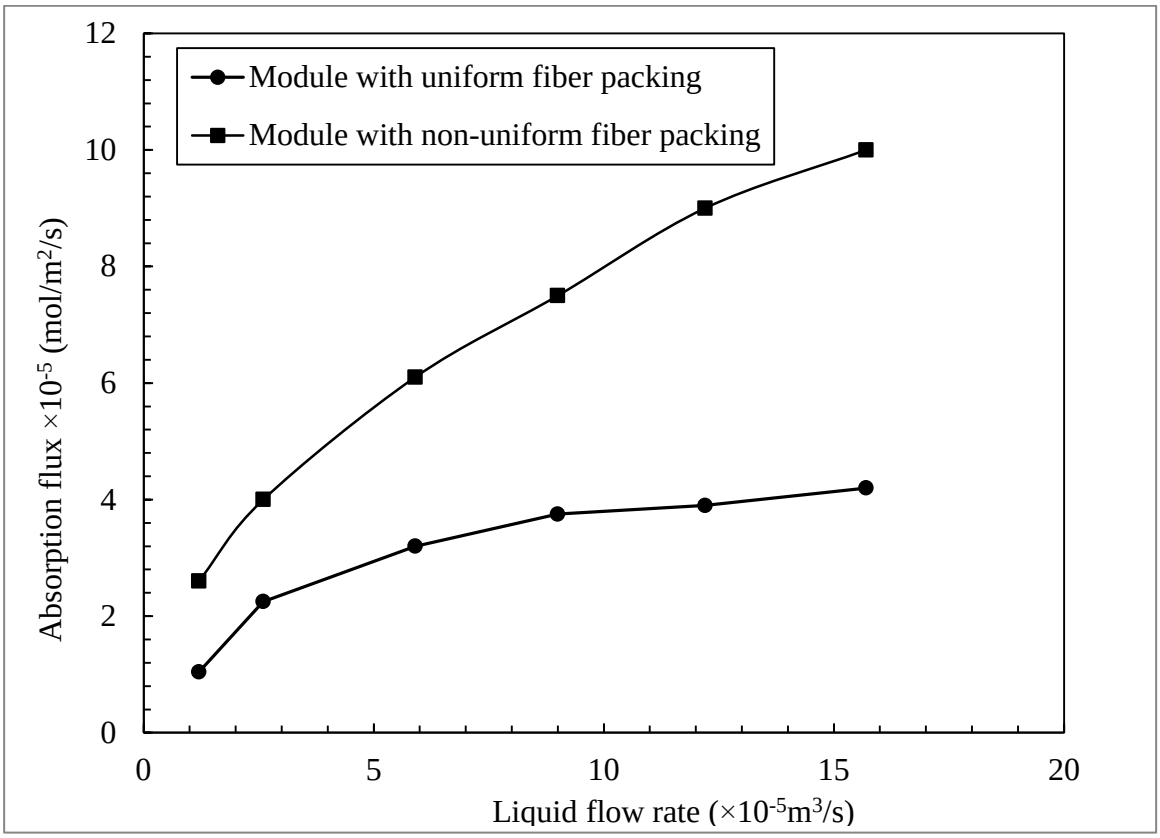

Figure 6. 17 : Effect of non-uniform fibre distribution on CO_2 absorption flux in cross flow module (CO_2% in feed gas=30%, $Q_G=5.6\times10^{-6}m^3/s$)

6.6 Conclusions

In this work, a CFD model was proposed as a design tool in lab scale module design. Although numerous 2D models have been proposed (Wang et al., 1993Dindore et al., 2005; Liao et al., 2003), these models assume a simplified shell side flow. This resulted in difficulties with respect to application in scale-up (Chabanon et al., 2014). In this chapter a CFD model was developed to incorporate the shell side flow distribution into the overall model. In the shell side, the fibre bundles were treated as porous medium to avoid the discretization of computational geometry for each single fibre. As a result, the flow field

and shell side mixing which are a strong function of module design and flow dynamics can be reflected. In the fibre side, the fibres are modelled using the data from the shell model. The proposed CFD model was validated through experiments using a dual membrane contactor of bench scale size. It was then used to study various design parameters for HFMC. The velocity and concentration distribution in cross flow module shows that the velocity in the centre of the fibre bundle is much higher than the boundary. This is not unexpected however, the CFD model gives one a tool to determine the extent of the impact and vary design accordingly. An analysis of adding baffles showed that baffles not only enhance mass transfer but also this impact varies with dilute versus concentrated gases. The impact of fibre arrangement on module performance was also studied through CFD analysis. The result confirms that mass transfer is a strong function of shell side flow distribution. Modules with more evenly distributed fibre bundles tend to results in better performance. The analysis here is a subset of possible analyses that could be done using this CFD model approach. This type of design tool was proven effective in design optimization, operations, and scale up.

Reference

Yang, M.C., Cussler, E. L., Designing hollow-fibre contactors, AIChE Journal, 32 (11) (1986), 1910-1916

Cai, J.J., Howboldt, K., Abdi, M.A., Improving gas absorption efficiency using a novel dual membrane contactor, Journal of Membrane Science, 510 (2016), 249-258

Cai, J.J., Hawboldt, K., Abdi, M.A., Contaminant removal from natural gas using dual hollow fibre membrane contactors, Journal of Membrane Science, 397-398 (2012), 9-16 Darcovich, K., Dal-Cin, M.M., Ballèvre, S., Wavelet, J.P., CFD-assisted thin channel membrane characterization module design, Journal of Membrane Science, 124 (2) (1997), 181-193

Chabanon, E., Kimball, E., Favre, E., Lorain, O., Goetheer, E., Ferre, D., Gomez, A., Broutin, P., Hollow Fibre Membrane Contactors for Post-Combustion CO_2 Capture: A Scale-Up Study from Laboratory to Pilot Plant, Oil Gas Science Technology, 69 (2014),1035-1045

Dindore, V.Y., Brilman, G. F.,Versteeg, D. W. F., Modelling of cross-flow membrane contactors: physical mass transfer processes, Journal of Membrane Science, 251 (2005), 209-222

Dindore, V.Y., Cents, A.H.G., Brilman, D.W.F.,Versteeg, G.F., Shell-side dispersion coefficients in a rectangular cross-flow hollow fibre membrane module, Chemical

Engineering Research and Design, 83(A3) (2005), 317-325

Ergun, S., Fluid flow through packed columns, Chemical Engineering Progress 48 (1952), 89-94

Fluent Inc. Fluent 6.2 UDF Manual, Lebanon, NH: Fluent Inc., Feb. 2005

Gabelman, A., Hwang, S., Hollow fibre membrane contactors, Journal of Membrane Science, 159 (1999), 61-106

Liao, Z., Poh, C.K., Huang, Z., Hardy, P.A. , Clark, W.R., Gao, D., A numerical and experimental study of mass transfer in the artificial kidney, Journal of Biomedical Engineering, 125 (2003), 472-480

Rezakazemi, M., Niazi, Z., Mirfendereski, M., Shirazian, S., Mohammadi, T., Pak, A., CFD simulation of natural gas sweetening in a gas-liquid hollow-fibre membrane contactor, Chemical Engineering Journal, 168 (2011), 1217-1226

Taskin, M. E., Fraser, K.H., Zhang, T., Griffith, B.P., Wu, Z. J., Micro-scale modeling of flow and oxygen transfer in Hollow Fibre Membrane Bundle, Journal of Membrane Science, 362(1-2) (2010), 172-183

Vargaftik, N. B., Handbook of Physical Properties of Liquids and Gases: Pure Substances and Mixtures, Hemisphere Publishing Corporation, 1987

Wang, L.K., Cussler, E.L., Baffled membrane modules made with hollow fibre fabric, Journal of Membrane Science, 85(3) (1993), 265-278

Wang, Y., Chen, F., Wang, Y., Luo, G. and Dai, Y., Effect of random packing on shell-side flow and mass transfer in hollow fibre module described by normal distribution function, Journal of Membrane Science, 216(2003),81-93

Zhang, J., Nolan, T.D.C., Zhang, T., Griffith, B.P., Wu, Z.J., Characterization of membrane blood oxygenation devices using computational fluid dynamics, Journal of Membrane Science, 288(2007),268-279

Chapter 7

CONCLUSIONS AND FUTURE WORKS

This chapter summarizes the work being completed and contributions made to the membrane technology for offshore gas treatment. An outline of future work derived from this dissertation is also discussed.

7.1 Summary

The last decade has seen an increase in exploitation of unconventional resources of petroleum in places, such as deep offshore. There are various challenges with both treating (for re-injection to maintain reservoir pressure to meet flaring regulations etc.) and/or monetizing these gas reservoirs, principally due to gas quality. The key contaminants in the gas must be removed depending on the application (for transport vs. re-injection). Pipelines have a set of specifications need to be met; the liquefied natural gas requires water, acid gases and heavier hydrocarbons removed, while compressed natural gas requires water and possibly heavier hydrocarbons removal. The re-injected gases must be treated to remove sulfur compounds and other contaminants. Space on

offshore platforms is limited and therefore large treatment systems are typically not feasible. Further the performance of contacting equipment can be susceptible to motion effects. Removal of acid gases, CO_2 and H_2S is particularly problematic due to energy and space requirements of typical treatment methods (absorption columns). An alternative to the conventional gas processing equipment for offshore gas processing is membrane contactor. The membrane contactor combines the benefits of the membrane separation and conventional absorption through membrane gas absorption. The primary objective of this dissertation was to develop a novel membrane contactor with more compact design to enhance gas absorption efficiency. Experimental study and numerical simulations were carried out to investigate the performance of the proposed membrane contactor.

7.2 Research Contributions

- A novel design of dual membrane contactor module with more compact structure, smaller footprint and higher performance was proposed and fabricated. The proposed dual membrane contactor was composed of two types of membranes. The purpose of the dual membrane approach is to simultaneously absorb the target gas and partially regenerate the solvent in one unit. The module operates in cross-flow mode and uses hollow fibre membranes.
- A lab scale flow loop was constructed to study the performance of dual membrane contactor. CO_2 absorption using water and propylene carbonate as absorbent were carried out in lab scale membrane contactor, by varying operational conditions. A new empirical correlation was developed to describe mass transfer performance in the proposed dual membrane contactor.

- Initially a two dimensional mathematical model was proposed to describe the mass transfer process in the proposed dual HFMC. The concentration of the target gas component in both gas phase and liquid phase at any position of the module can be predicted via the numerical model. The numerical model was validated through lab scale module experiments. In this initial simplified model, the shell side flow velocity was assumed constant in the module;
- A CFD model was developed as a design tool to facilitate and improve the design of cross flow modules used for gas absorption. To gain an understanding of the effect of module design on the shell side flow dynamics, the impact of variables on the overall performance of the membrane module was investigated. These variables included: the shell side velocity, flow distribution and the concentration of the target component at the liquid outlet of cross flow modules with various designs. The impact of a series of module design factors such as shell configurations, inlet geometry, header geometry, fibre bed height and packing density were also examined.
- To better represent the variable flow in the shell side and tube side of membrane modules with complex geometries, a two stage CFD model was developed. The fibre bundle was treated as a porous medium in the CFD simulation for the shell-side flow. The overall mass transfer coefficient correlation developed in the above work was incorporated into the CFD model. Flow through the fibre was simulated in a separate CFD model. The two CFD models were solved using an iterative process to simulate mass transfer in the whole module. The combined CFD model was validated using experiment results from a lab scale HFMC. The model was

then used to predict the performance of modules with complex structures such as uneven fibre arrangement and baffles.

The major findings and conclusions of the current research are summarized as follows:

- By combining two types of membrane (porous polypropylene membrane and nonporous silicone rubber membrane) into one unit, simultaneous gas absorption and partial solvent regeneration can be achieved at the same time in the proposed dual membrane contactor. As the dissolved gas component is continuously stripped out of the solvent, the driving force responsible for mass transfer remains at a high level, which further results in higher absorption flux in the proposed dual membrane contactor than conventional membrane contactors.
- The absorption performance of dual membrane contactor can be enhanced by adding turbulence promoters such as baffles into shell side. The impact of baffles on performance enhancement is more pronounced when modules are operated under low flow.
- In cross flow membrane contactors, the concentrations of both fluids vary in both directions. To describe mass transfer process of gas absorption, a numerical mathematical model based on mass balance was developed. The numerical simulation was verified with experimental results. The simulation results showed that the ratio of porous membrane area and nonporous membrane area was an influential factor in determining the absorption performance of dual membrane contactor. The highest gas removal rate was obtained when porous membrane took up 55% of the total membrane area.

- To correlate shell-side flow dynamics and mass transfer performance of the proposed dual membrane contactor, an empirical correlation was developed in this work based on experimental results of CO_2 absorption. The proposed empirical correlation is a function of liquid flow rate which further confirms that the mass transfer resistance in the dual membrane system mainly lies in the liquid phase.
- To gain a better understanding on the mass transfer process of gas absorption, a resistance-in-series model was applied to examine the mass transfer resistance contributed by gas phase, liquid phase and membrane, respectively. The result from Wilson plot showed that mass transfer resistance from gas phase and porous membrane could be neglected, comparing to that from liquid phase and nonporous membrane. Specifically, the nonporous silicone rubber membrane contributes to 7% of the total mass transfer resistance while the major mass transfer resistance lied in the liquid phase. Therefore, the module performance of dual membrane contactor can be further enhanced by increasing liquid flow rate and choosing nonporous membrane with higher permeability to the target gas component.
- The selection of proper absorbent is critical for the development of novel dual membrane contactors. Two of the most commonly used physical solvents for CO_2 absorption (water and propylene carbonate) were compared and examined in terms of their efficiency for CO_2 removal and compatibility with the proposed dual membrane contactor. The experimental findings suggested that both solvents could be successfully used in combination with membrane material of the dual membrane contactor. Mass transfer coefficient in CO_2-propylene carbonate system was lower than that in CO_2-water system. Furthermore, the effect of sweep

gas stripping on overall absorption in CO_2-propylene carbonate system was not as pronounced as in CO_2-water system. This is mainly due to the higher affinity of propylene carbonate for CO_2, which makes it difficult for CO_2 to be stripped out of the liquid phase.

- The experimental study of CO_2 absorption using the proposed dual membrane contactor showed that high liquid flow rate, high solute concentration and low pressure on permeate side promoted high absorption flux whereas gas flow rate has a limited impact on absorption flux.
- The proposed two dimensional numerical model was developed by taking into consideration of the change of gas flow rate during the absorption process which was proven to be a critical factor that needs to be accounted for in the simulation. The simulation results were in good agreement with experimental results for CO_2 removal by varying operation conditions.
- For cross flow modules operated with liquid solvent flowing through the shell-side, the overall mass transfer coefficient strongly depends on shell-side flow behavior and the shell geometries. To address the transport between gas phase and liquid phase in dual membrane contactor with various geometries, a CFD model including mass transfer calculation routines was developed. Coupled with the Navier-Stokes equations, the CFD model was solved and used to study the shell side hydrodynamics and mass transfer in the proposed dual membrane contactor. Hollow fibre membrane bundle was treated as a porous medium in the CFD model whereas the assumption was verified through experimental results.

- The CFD modeling was used as a design tool to investigate the impact of shell geometry on the shell side fluid dynamics and the consequent mass transfer. Compared to fluid distribution, the average shell-side velocity was found to be the key factor in determining the mass transfer rate. The impact of flow distribution was found to be less significant. With the local flow fields and concentration profiles visualized in CFD simulations, it was confirmed that by varying the design of shell geometry, the shell-side hydrodynamics and mass transfer could be improved
- When operated under the same operational conditions, absorption flux in rectangular module was found at least 28% higher than cylindrical modules. Compared to modules with large inlet, modules with narrower inlets resulted in higher shell-side velocity and absorption and the shell side flow distribution was less uniform. A cone shaped header improved shell-side flow dynamics and better absorption performance when compared to modules without, Compared to those with deep membrane beds, modules with shallow membrane beds performed better. Modules with higher packing densities had lower absorption fluxes compared to less densely packed modules. The result indicated that a balance between gas removal efficiency and absorption flux needs to be taken into consideration for practical application.
- The prediction of localized mass transfer performance of cross flow membrane modules is challenging. A two stage CFD modeling approach was developed to simulate mass transfer process in both fiber side and shell side. The proposed modelling approach included two integrated models to capture concentration

change in gas phase and liquid phase. The proposed model was validated against experimental measurements and was proven to be effective in predicting concentration change of solute in gas phase and liquid phases. This model is more accurate but is computationally more expensive in time and effort and therefore more useful for very detailed analysis. The model used in Chapter 5 of this thesis is less computationally demanding and could be used as a screening design tool.

- Mass transfer in modules with non-uniform fibre distribution and baffled modules was investigated using the proposed two-stage CFD modeling approach. The baffles promote shell-side mixing, which resulted in better performance. This was particularly significant for absorption of gas flows with high levels of the target gas.

7.3 Publications

- **Cai**, **J.J.,** Hawboldt, K., Abdi, M.A, Contaminant Removal from Natural Gas using Dual Hollow Fiber Membrane Contactors. *Journal of membrane science*, 397-398 (2012), 9-16
- **Cai**, **J.J.,** Hawboldt, K., Majid, A., Improving gas absorption efficiency using a novel dual membrane contactor. *Journal of membrane science*, 510(2016), 249-258
- **Cai**, **J.J.,** Hawboldt, K., Majid, A., Analysis of the effect of module design on gas absorption in cross flow hollow membrane contactors via Computational Fluid Dynamics (CFD) analysis. *Journal of membrane science*, 520 (2016) 415-424

- **Cai**, **J.J.,** Hawboldt, K., Abdi, M.A, Numerical Study of Gas Absorption-Desorption with Dual Membrane Contactors Using CFD Modeling, *Chemical Engineering Journal*, under-review
- **Cai**, **J.J.,** Hawboldt, K., Abdi, M.A, Investigation and Improvement of Flow Distribution in Hollow Fiber Membrane Contactor, 63rd CSCHE conference, Fredericton, Newbrunswick, Canada,2013
- Haghighi, M., **Cai,J.J,** Hawboldt, K. , Abdi, M. A, Sundgaard, C., Hydrate Prevention in Subsea Oil Production Dead-Legs, Offshore technology conference, Houston, USA,2013
- Kenny, S., Hawboltd, K., Lesley, J. Pan. Y, **Cai, J.J.**, Pipeline transportation systems for CCS strategies: observations and technology issues, The third international forum on Transportation of CO2 by pipeline, Newcastle, UK, 2012
- **Cai,J.J**, Hawboldt, K., Abdi, M.A., Contaminant Removal from Natural Gas using Dual Hollow FiberMembrane Contactors, The 88th Gas Processors Association Annual Convention, San Antonio, Texas, 2009
- **Cai,J.J**, Hawboldt, K., Abdi, M.A., CO_2 Removal from Flue Gas Using Hollow Fiber Membrane Contactors. The 4th Annual Atlantic Sustainable Campuses conference, St. John's, Canada, 2010

7.4 Recommendations for Future work

The most important points of improvement, both in terms of experiments and general understanding of membrane gas absorbers are summarized below:

- The effect of operating temperature. The operating pressure and temperature conditions for offshore gas processing vary widely. The reliability of polypropylene porous membrane to withstand membrane fouling in high temperature has not been confirmed yet. More rigorous membrane material such as ceramic membranes which are able to withstand high temperatures can be considered.
- More complex gas mixtures. For offshore gas processing, the feed stream often contain more than one targeted gas components needs to be removed such as removal of CO_2 and H_2S from sour gas. The gas mixture also impacts membrane and solvent selection. The current study focused mainly on the principles of gas absorption at a concept level and therefore single component removal from gas mixture was selected. Numerical model to describe mass transport in a gas mixture combined with experiments needs to be further explored and the model should be further improved and validated through more experimental investigations.
- The effect of membrane wetting over long term operation. Membrane wetting has a detrimental effect on the performance of membrane module which often occurs over long term operations. All experiments carried out in the current study were completed within four hours. The module performance needs to be further explored over long term operation period.
- The effect of mass transfer resistance contributed by gas phase. The mass transfer resistance contributed by gas phase was found negligible in the lab scale membrane module for the conditions studied in this work. The mass transfer

coefficient in the scaled up parallel module was reported (Chabanon et al., 2013) smaller than that obtained from lab scale module due to mass transfer resistance caused by gas maldistribution. This phenomenon needs to be further studied for the future scaling of the dual membrane module.

Reference

Chabanon, E., Kimball, E., Favre, E., Lorain, O., Goetheer, E., Ferre, D., Gomez, A., Broutin, P., Hollow Fibre Membrane Contactors for Post-Combustion CO_2 Capture: A Scale-Up Study from Laboratory to Pilot Plant, Oil Gas Science Technology, 69 (2014),1035-1045